nagra.

Arbeitsbericht NAB 13-13

Hydraulic conductivity and head distributions in the host rock formations of the proposed siting regions

March 2013

R. L. Beauheim

**Nationale Genossenschaft
für die Lagerung
radioaktiver Abfälle**

Hardstrasse 73
CH-5430 Wettingen
Telefon 056-437 11 11

www.nagra.ch

nagra.

Arbeitsbericht NAB 13-13

Hydraulic conductivity and head distributions in the host rock formations of the proposed siting regions

March 2013

R. L. Beauheim

415 Saddle Ct.
Grand Junction, CO 81507, USA

KEYWORDS

regional scale, SGT2, hydrogeology, Northern Switzerland, siting regions, host rock, Opalinus Clay, Effingen Member, 'Brown Dogger', Helvetic Marls, packer testing, quality assurance, QA/QC

**Nationale Genossenschaft
für die Lagerung
radioaktiver Abfälle**

Hardstrasse 73
CH-5430 Wettingen
Telefon 056-437 11 11

www.nagra.ch

Nagra Working Reports concern work in progress that may have had limited review. They are intended to provide rapid dissemination of information. The viewpoints presented and conclusions reached are those of the author and do not necessarily represent those of Nagra.

Zusammenfassung

In der Etappe 1 des Sachplans geologische Tiefenlager hat die Nagra, basierend auf Kriterien zur Sicherheit und technischen Machbarkeit, sechs geologische Standortgebiete für das Tiefenlager für schwach- und mittelaktiven Abfälle (SMA-Lager) sowie drei mögliche Gebiete für das entsprechende Lager für die hochaktiven Abfälle (HAA-Lager) vorgeschlagen. Vier geologische Formationen wurden als geeignete Wirtgesteine für das SMA-Lager identifiziert: Opalinuston, Effinger Schichten, 'Brauner Dogger' und Mergel-Formationen des Helvetikums (Helvetische Mergel). Für das HAA-Lager wurde der Opalinuston als Wirtgestein vorgeschlagen. Ziel der Etappe 2 des Sachplanverfahrens ist die Einengung auf mindestens zwei Standortgebiete pro Lagertyp. In Etappe 3 sind dann die vorgeschlagenen Standorte vertieft zu untersuchen, so dass für die beiden Lagertypen eine gut begründete Wahl der Standorte für die Rahmenbewilligungsgesuche möglich ist.

Um die Ziele der Etappe 2 zu erreichen, muss der Kenntnisstand über die geologischen Verhältnisse in den Standortgebieten für die Durchführung der provisorischen Sicherheitsanalysen ausreichend sein. Die hydraulischen Eigenschaften der Wirtgesteine und die hydraulischen Verhältnisse in den Standortgebieten sind für die Beurteilung der Langzeitsicherheit von zentraler Bedeutung. Hierzu wird eine umfassende, qualitätsgesicherte und nachvollziehbare hydrogeologische Datenbasis zu den verschiedenen Wirtgtesteinen im lokalen und regionalen Maßstab benötigt. Der vorliegende Bericht fasst die hydrogeologischen Datengrundlagen, die wirtgesteinsspezifischen Datenanalysen und die aus den Analysen abgeleiteten Schlussfolgerungen zu den hydraulischen Barriereneigenschaften der Wirtgesteine zusammen. Hierzu zählen:

- eine umfassende Übersicht über die hydrogeologische Datenbasis pro Wirtsgestein (Opalinuston, Effinger Schichten, 'Brauner Dogger', Helvetische Mergel) und die hydrogeologischen Verhältnisse in den Standortregionen (WLB , JSF, JO , NL , ZNO und SR). Die berücksichtigten Felddaten umfassen Packertests, Langzeitbeobachtungen und hydrochemische Analysen der Porenwässer;
- die Bewertung der Datenqualität und der Qualität der Packertest-Interpretationen im Rahmen eines nachvollziehbaren Qualitätssicherungsverfahrens;
- die Analyse der Porenwasserdrücke in den Wirtgesteinen und insbesondere die Interpretation anomaler Porenwasserdrücke im Hinblick auf die lokalen und regionalen hydrogeologischen Verhältnisse;
- Konsistenz der hydraulischen Eigenschaften der betrachteten Wirtgesteine mit Befunden aus anderen Tonformationen;
- eine Zusammenfassung der vorhandenen Datenbasis und eine Bewertung des hydrogeologischen Kenntnisstands in Bezug auf die hydraulische Barrierefunktion der unterschiedlichen Wirtsgesteine.

Table of Contents

List of Tables

List of Figures

1 Introduction

1.1 Background and Scope

The Swiss waste management concept foresees separate repositories for low- and intermediate-level waste (L/ILW) and for high-level waste (HLW). In response to Stage 1 of the Swiss site selection plan, the so-called Sectoral Plan for Deep Geological Repositories ("SGT"), Nagra proposed six siting regions for the L/ILW repository and three siting regions for the HLW repository (Fig. 1-1). Four geologic formations were proposed as host rock formations for the L/ILW repository (Opalinus Clay, Effingen Member, 'Brown Dogger', and Helvetic Marls) and one geologic formation (Opalinus Clay) for the HLW repository (Fig. 1-1). It is the objective of Stage 2 to select at least two siting regions for each repository type, followed by the selection of a single site for each repository type in Stage 3.

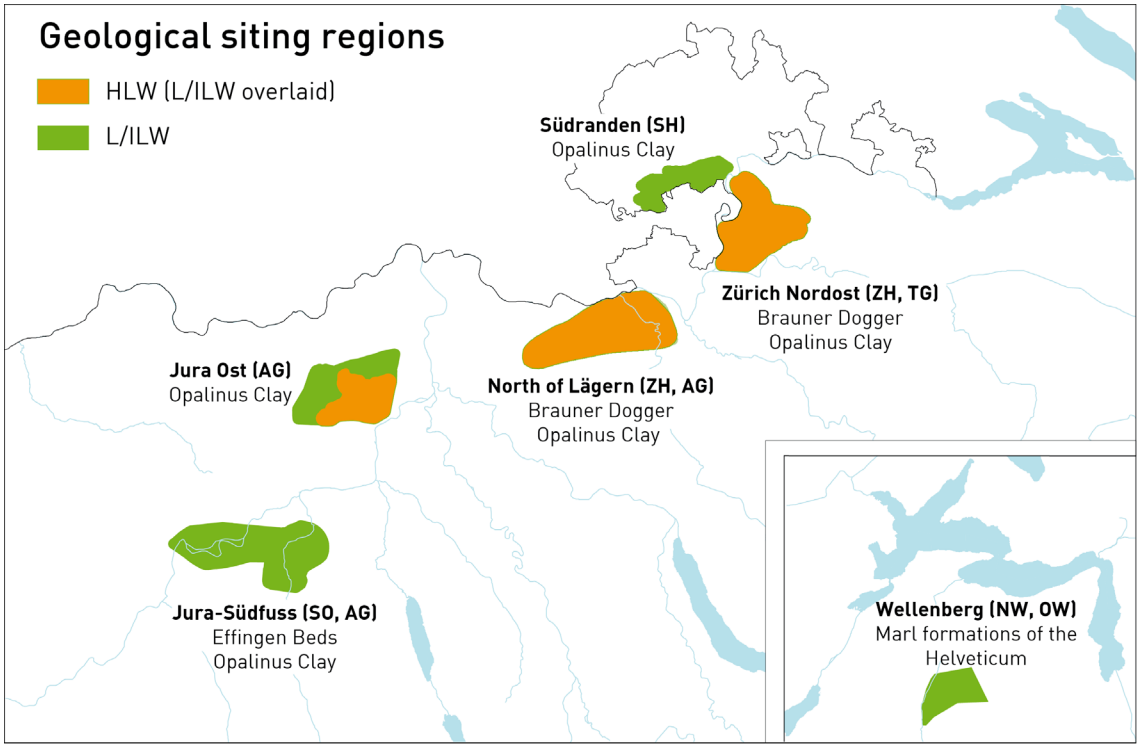

Fig. 1-1: Potential siting areas and host rocks for geological disposal of low- and intermediate-level (L/ILW) and high-level (HLW) radioactive waste in Switzerland (after Nagra 2008a and b).

As a decision basis for the second stage of the site-selection process, geological documents are to be elaborated for the authorities describing the proposed host rock formations in the six siting regions: Jura-Südfuss (JS), Jura Ost (JO), North of Lägern (NL), Zürich Nordost (ZNO), Südranden (SR), and Wellenberg (WLB). This includes, among other aspects, a compilation and assessment of the existing hydrogeological data base and its interpretation in the context of the regional geological setting.

In this context, of special interest are the Federal Nuclear Safety Inspectorate's (ENSI) requirements for complementary hydrogeological interpretations (ENSI 2011). ENSI requirement 14 says: *"Nagra shall provide complementary investigations (chloride profiles on existing core material, integration of hydrogeological and hydrochemical data for evidencing the groundwater flow conditions in the deep aquifer system; integrated interpretation of head measurements in the aquifers) as a contribution to the comparison of the different siting regions ..."*.

This report summarises and integrates all the lines of evidence supporting the existence of low permeability for the four host rock formations (including the adjacent rock formations). In addition to direct testing, evidence for low permeability is provided by pore pressure measurements/estimates and by hydrochemical profiles through the potential host rocks and overlying and underlying rocks. Special emphasis is given to the assessment of the data bases from recent field campaigns that have been collected after completion of the earlier geosynthesis projects WLB and OPA (e.g., boreholes Gösgen, Küttigen, Oftringen, Schlattingen-1). The results of the report will feed into the SGT/Stage 2 geological evaluations.

1.2 Objectives and Deliverables

The evaluations of the hydrogeological conditions on the regional and local scale are driven by the requirements of both the Safety Assessment and the Construction & Operations teams as input for the provisional safety analyses and the site-specific repository layouts (see above). For this, a comprehensive and traceable hydrogeological data base is needed, providing a complete and quality assured compilation of the available field data. The quality assured field data are feeding in an integrated interpretation of the hydrogeological conditions in the siting areas, and in particular, in the local- and regional-scale groundwater flow models. This study contributes to the hydrogeological synthesis procedure by providing:

- A complete survey of the hydrogeological data base per host rock (Opalinus Clay, Effingen Member, 'Brown Dogger', Helvetic Marls) and siting region (WLB, JSF, JO, NL, ZNO, and SR) according to the different categories of field data (packer tests, long-term monitoring, hydrochemical data, …). The hydrogeological data compilation will serve as a reference report to be passed in as part of the general geological documentation for SGT – Stage 2.
- A careful review of the data quality (reliability of measurements, test approaches applied, general uncertainties, etc.) and of the quality of interpretations. The assessment of the data quality is based on a clear specification of the assessment criteria. The review of the data quality shall concentrate mainly on the newly acquired data bases, which have not yet been subjected to detailed QC procedures as part of former geosynthesis projects (WLB, OPA). Those data which have passed successfully the QA process will feed in Nagra's field data bases.

- An evaluation of pore pressures by host rock (spectrum of phenomena, possible explanations of the origin of abnormal pressures) and hydrogeological interpretation in the context of the geological setting. The interpretations form an important input to the numerical groundwater flow simulations on the regional scale (report in preparation) and on the local scale (four reports in preparation, representing the siting regions ZNO&SR, NL, JO, and JS).
- Comparison of the hydrogeological conditions in the host rocks and the adjacent rock with evidence from other geoscientific disciplines (oil&gas exploration, natural gas storage, CO_2 sequestration…). The information on the sealing efficiency of clay-rich cap rock formations in the context of other geological applications will complement the Geodata Set "Safety" as independent evidence.
- Summary of results and conclusions regarding the hydraulic barrier function of the different host rocks.

1.3 Data Base Review and Assessment Criteria

The data bases for the Benken borehole in ZNO and for the Helvetic Marls at WLB have previously been subjected to full QA review and synthesis (Nagra 2002 and Nagra 1997; see also references therein). Those data bases are, therefore, simply summarized herein with no further evaluation. The hydrogeological data bases for the Effingen Member and 'Brown Dogger', however, have not yet been fully reviewed. Therefore, those data bases are reviewed in detail herein. The hydraulic testing that has been performed in the Effingen Member and 'Brown Dogger', as well as the analyses completed to date of those tests, is assessed in relation to the following criteria:

- Reliability of measurements (e.g., quality and calibration of gauges);
- Testing methodology (e.g., appropriate tests of appropriate duration performed);
- Test execution (e.g., test performance followed test design, equipment performed properly);
- Analysis approach (e.g., appropriate methods used to analyze tests);
- Analysis execution (e.g., appropriate selection of fitting parameters, appropriate parameter ranges investigated, appropriate test phases optimized); and
- Parameter estimation (e.g., parameter estimation reliable, sensitivity and uncertainty appropriately defined).

Where possible, the hydraulic head estimates inferred from the hydraulic test analysis are compared to the results of long-term monitoring as an additional check on their reliability. Hydrochemical data from the Effingen Member and 'Brown Dogger' are also summarized herein, but assessment of data quality is left to the analysis reports specifically focused on those data (e.g., Mazurek et al. 2013).

1.4 Report outline

Chapter 2 gives an overview of the geological and hydrogeological conditions in the siting areas of Northern Switzerland. Chapters 3, 4, 5, and 6 of this report present information on the Effingen Member, 'Brown Dogger', Opalinus Clay, and Helvetic Marls, respectively. For each potential host rock, the geologic setting at the relevant siting area(s) is presented, followed by discussion of the hydraulic testing that has been performed in that host rock. As described above, the testing performed in the Effingen Member and 'Brown Dogger' is evaluated in detail, while the testing performed in the Opalinus Clay and Helvetic Marls is simply summarized because it has been previously reviewed. Hydraulic head information derived from both hydraulic test interpretation and long-term monitoring is summarized and related to local geologic conditions. Hydrochemical information relevant to demonstration of low permeability is discussed for each host rock, and a summary is provided of results and conclusions regarding the hydraulic barrier function of each host rock.

Chapter 7 provides an integration of the data for the four potential host rocks in the context of comparisons between Nagra's recent hydraulic testing programmes and those conducted for other radioactive waste disposal programmes, and between the properties of the host rocks in the various siting regions and the host rocks and sites proposed by other radioactive waste programmes. Information relevant to the understanding of low-permeability systems from other types of projects and scientific investigations is also discussed. An overall summary and conclusions are given in Chapter 7.

2 Regional geological and hydrogeological setting

Five of the six candidate siting regions, namely Jura Südfuss (JS), Jura Ost (JO), Nördlich Lägern (NL), Zürich Nordost (ZNO) and Südranden (SR), are situated in the Molasse Basin and the Tabular Jura of Northern Switzerland, respectively (Fig. 1-1). The local hydrogeological conditions in these regions are controlled by the general regional geological and tectonic setting of the Alpine foreland, consisting of a thick and flat lying sequence of Mesozoic and Teriary sediments in the Molasse Basin and an extended regional fault and thrust belt along the Jura arc. Chapter 2 gives a brief introduction in the main lithostratigraphic and tectonic features of the Alpine foreland and refers to the geological and hydrogeological modeling activities on the regional and local scale, which have been initiated in Stage 2 of the Sectoral Plan. An in-depth discussion of the local geological and hydrogeological conditions follows in the subsequent chapters for the individual siting regions. For the Wellenberg site, a complementary paragraph is included (Chapter 6.1), summarizing the geological conditions in the Helvetic zone of the central Swiss Alps.

2.1 Regional geological setting

A comprehensive survey of the existing state of knowledge of the geology of Switzerland has been given in Nagra (2002) and Nagra (2008b). The appraisal includes classic textbook references and key papers on structural geology and tectonic evolution of Switzerland, the results from seismic field campaigns and deep drilling programs initiated by the oil&gas industry, geological information from underground constructions such as railway and road tunnels and last, but not least, the achievements of Nagra's site investigation programmes during the last 40 years. In recent years, new investigations have been initiated in the field of geo-thermal energy exploration. The reader is referred to the various references in Nagra (2008b) for further general information on the geology of Switzerland.

In Stage 2 of the Sectoral Plan, Nagra initiated complementary field investigations, aimed at broadening the data base on brittle deformation structures across a large area of Northern Switzerland with special focus on the five potential siting regions JS, JO, NL, ZNO and SR (Madritsch & Hammer 2012). The gathered data, mostly stemming from outcrops in Upper Jurassic limestone, enabled an enhanced structural geological characterisation of the region of interest. The subsequent synopsis of the regional geology is based on the summary in Madritsch & Hammer (2012) and provides complementary evidence from the recent investigations on brittle deformation structures as far as they are of potential relevance for the hydrogeological conditions in the candidate host rock formations on the regional and local scale.

Tectonic evolution

The five siting regions in Northern Switzerland are located within the northern Alpine foreland (Fig. 2-1 and Fig. 2-3). The main structural units identified in this region result from its Cenozoic tectonic evolution (0 – 66 Mio years ago). The most important stages of this evolution are the formation of the European Cenozoic Rift System and the Alpine orogeny.

The formation of the European Cenozoic Rift System in early Tertiary (54 – 25 Mio years ago) led to the opening of the Upper Rhine Graben. Uplift of the Upper Rhine Graben flanks (the Blackforest representing the right-side flank) most likely took place during Late Oligocene to Early Miocene time (~ 25 Mio years ago). The formation of the NW-SE striking Hegau-Bodensee Graben is considered to be related to this event. Numerous studies have shown that

the structural configuration of the various rift system elements is largely controlled by the geometry of pre-existing Paleozoic basement structures. These structures had been formed in the course of the Variscian and Hercynian orogenies (380 – 280 Mio years ago) and are typically oriented N-S, NW-SE and ENE-WSW. Several authors suggest multiple reactivations of these structures during Mesozoic and Cenozoic times. The most important structure for the area of interest is the Permo-Carboniferous Trough of Northwestern Switzerland. The trough is completely buried by Mesozoic strata, but its geometry is quite well constrained from wells, seismic reflection and gravity data.

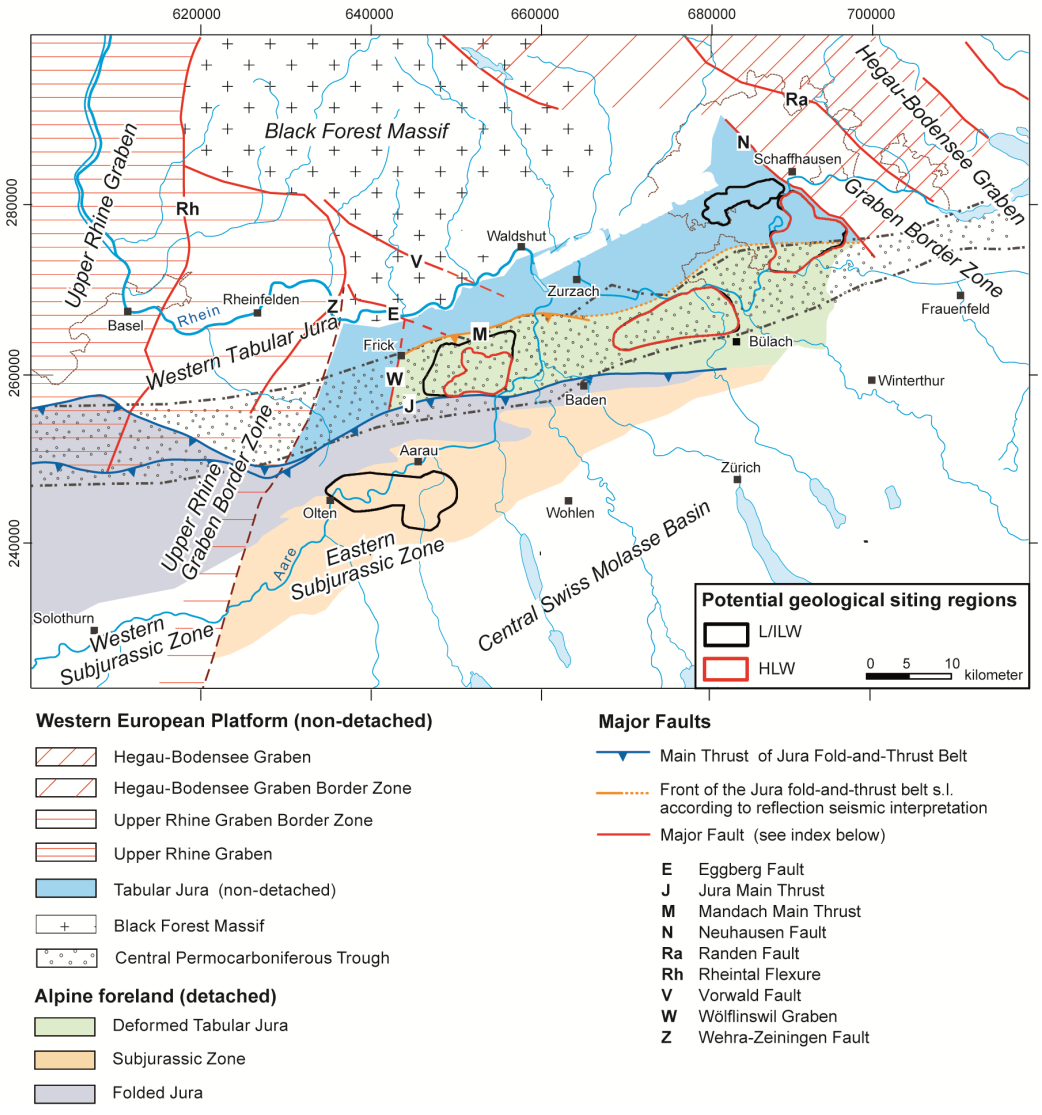

Fig. 2-1: Schematical sketch illustrating the main tectonic units of the region and the major fault structures (modified from Madritsch & Hammer 2012).

In the course of the Alpine orogeny, continental collision in the Central Alps of Switzerland is inferred to have onset in early Tertiary (56 – 34 Mio years ago). The northward adjacent Molasse Basin of Switzerland developed in response to syn- and post-collisional thrusting and erosion processes. The basin fill is marked by two coarsening-, thickening-, and shallowing-upward mega-sequences. The youngest sediments of the basin are preserved in its northernmost parts and are of Late Miocene age (~ 10 Mio years ago). In Late Miocene times, the Alpine deformation front jumped far into the northern foreland which led to the formation of the Jura Fold-and-Thrust Belt. This foreland propagation of the deformation front was enabled by a décollement horizon in the Middle to Upper Triassic evaporites. The Central Swiss Molasse Basin was turned into a piggy-back basin (i.e., deposition center forming on top of the moving thrust sheets). The Tabular Jura north of the Jura Fold-and-Thrust Belt is considered to rest autochthonously on the crystalline basement and not to be detached along the Triassic décollement horizon.

Many authors argue that the main deformation phase of the Jura Fold-and-Thrust Belt was a short-lived event and only lasted until the Early Pliocene (5.3 – 2.6 Mio years ago). However, several geomorphological investigations at the front of the belt have revealed mild Post-Pliocene activity, thus raising the question to what extent and by what kind of mode the compressional deformation in the Alpine foreland is still active. There are also geomorphological indications that the Southern Upper Rhine Graben area is still subsiding, suggesting recent tectonic activity along the European Cenozoic Rift System as well.

Regional structural setting

The major tectonic units in the area of interest and its surroundings are illustrated in Figures. 2-1 – 2-3. All of these units developed during the poly-phase tectonic evolution of the Alpine foreland. From internal (south) to external (north) foreland, these units are:

- Central Swiss Molasse Basin - this part of the Swiss Molasse is a piggy-back basin located in between the Central Alps and the Jura Fold-and-Thrust Belt
- Jura Fold-and-Thrust Belt s.l. – this unit dissects the study area from east to west and largely defines its structural configuration (Figs. 2-1 and 2-3). From south (internal) to north (external), the belt can be divided into three zones:

  The *Subjurassic Zone* marks the belt's southern boundary towards the Central Swiss Molasse Basin. It is marked by gentle ENE-WSW to E-W striking flexures (e.g., the Eppenberg Flexure) and folds, most notable the isolated Born-Engelberg Anticline that features a clear topographic expression. The kinematics of this anticline in relation to the neighbouring Fold-and-Thrust Belt structures is poorly understood.

  The *Folded Jura*, representing the Jura Fold-and-Thrust Belt s.str., is characterised by closely spaced thrust sheet stacks and tight thrust-related folds. The dominantly ENE-WSW striking folds and thrusts are occasionally cut by N-S striking faults. The frequency of these structures increases towards the Upper Rhine Graben with which they are presumably related. Moreover, NW-SE striking faults, such as the Olten Fault, occur. Both of these fault sets are most often sub-vertical and commonly interpreted as transfer faults. The roughly E-W striking Jura Main Thrust forms the transition to the Folded Tabular Jura.

The *Folded Tabular Jura* further north is apparently less intensively deformed. The lower Aare Valley (Figs. 2-1 and 2-3) separates this tectonic unit into a western and eastern part. While the western part comprising the Jura Ost siting region features a clear boundary towards the northward adjacent Tabular Jura formed by the ENE-WSW striking Mandach Thrust, the eastern part of the Folded Tabular Jura including the siting region Nördlich Lägern, has no clear northern boundary and the transition towards the Tabular Jura is ill-defined.

- Tabular Jura – this tectonic unit is located to the north of the Jura Fold-and-Thrust Belt. The study area comprises the eastern and central part of the Swiss portion of this tectonic unit. It is characterised by horizontally layered to slightly SSE dipping Mesozoic sediments that form the southeastern edge of the Black Forest Massif. Here, the sedimentary cover presumably lies autochthonously upon the Paleozoic basement and is not affected by the thin-skinned décollement tectonics that characterises the Jura Fold-and-Thrust Belt. Compared to the latter, the Tabular Jura is apparently less deformed and does not feature regional scale compression structures with the exception of the Mettau Fault. The influence of the graben system bordering this tectonic unit to the east and west is poorly constrained.
- Northern Swiss Molasse Basin – the Northern Swiss Molasse Basin is located north of the Jura Fold-and-Thrust Belt and its theoretical eastward prolongation. To the E and NE, it is bordered by the Tabular Jura. It is presumably not affected by the décollement tectonics that caused the formation of the Jura Fold-and-Thrust Belt. This part of the Molasse Basin is apparently affected by the tectonic processes related to the formation of the Hegau-Bodensee Graben.
- Upper Rhine Graben – one of the major segments of the Cenozoic European Rift System, which was formed under E-W to WNW-ESE directed extension. Its eastern border zone is inferred to reach into the western part of the Swiss Tabular Jura (*cf.* Nagra 2008b). The small N-S striking Wölflinswil Graben apparently forms the easternmost well-defined extension structure that is presumably related to the Upper Rhine Graben rift system and as such marks the boundary to the central part of the Swiss Tabular Jura.
- Hegau-Bodensee Graben – this unit dissects the easternmost part of the Tabular Jura and the Northern Swiss Molasse Basin in a NW-SE direction. Presumably it formed in consequence with the uplift of the Black Forest Massif but detailed information on the formation kinematics is so far not available. The Randen Fault (Fig. 2-1) is considered as the western border fault of this graben system and marks the eastern boundary of the study area. The area between the Randen and the Neuhausen Faults further west is considered as the Hegau-Bodensee Graben Border Zone (*cf.* Nagra 2008b).
- Black Forest Massif – this tectonic unit borders the Tabular Jura to the north and is comprised of Paleozoic to Early Triassic rocks. The processes which led to the formation of this basement high are still under discussion.

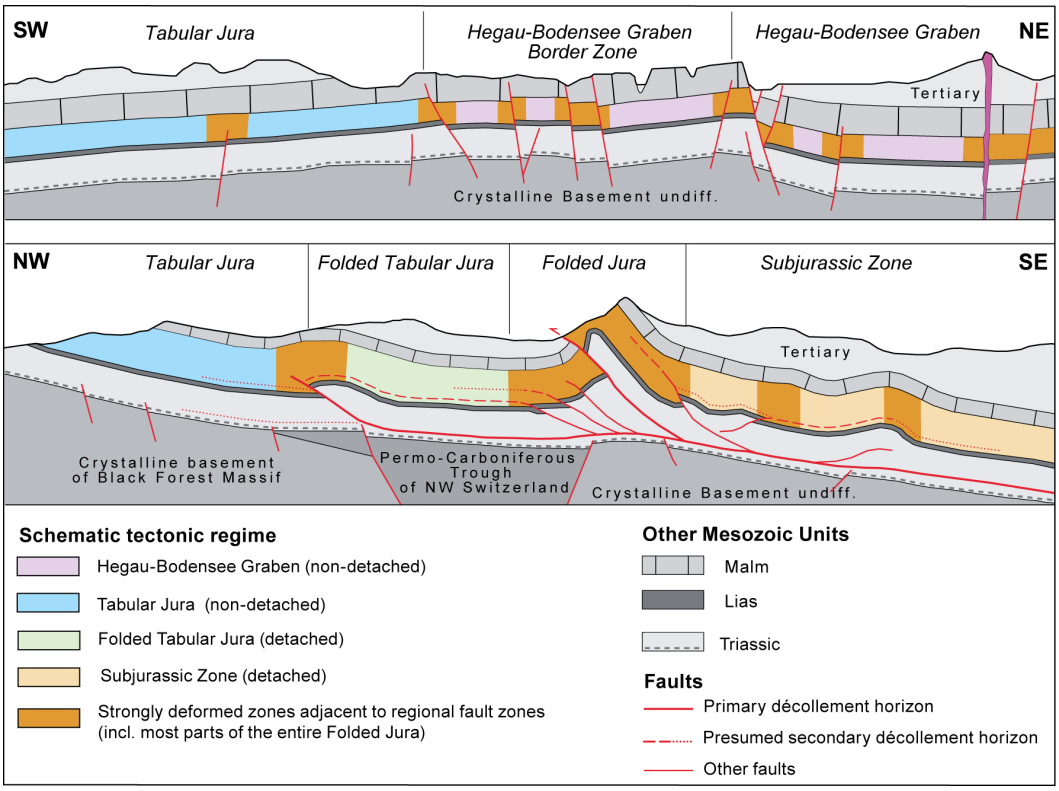

Fig. 2-2: Two schematic cross-sections through the tectonic sketch of Fig. 2-1.

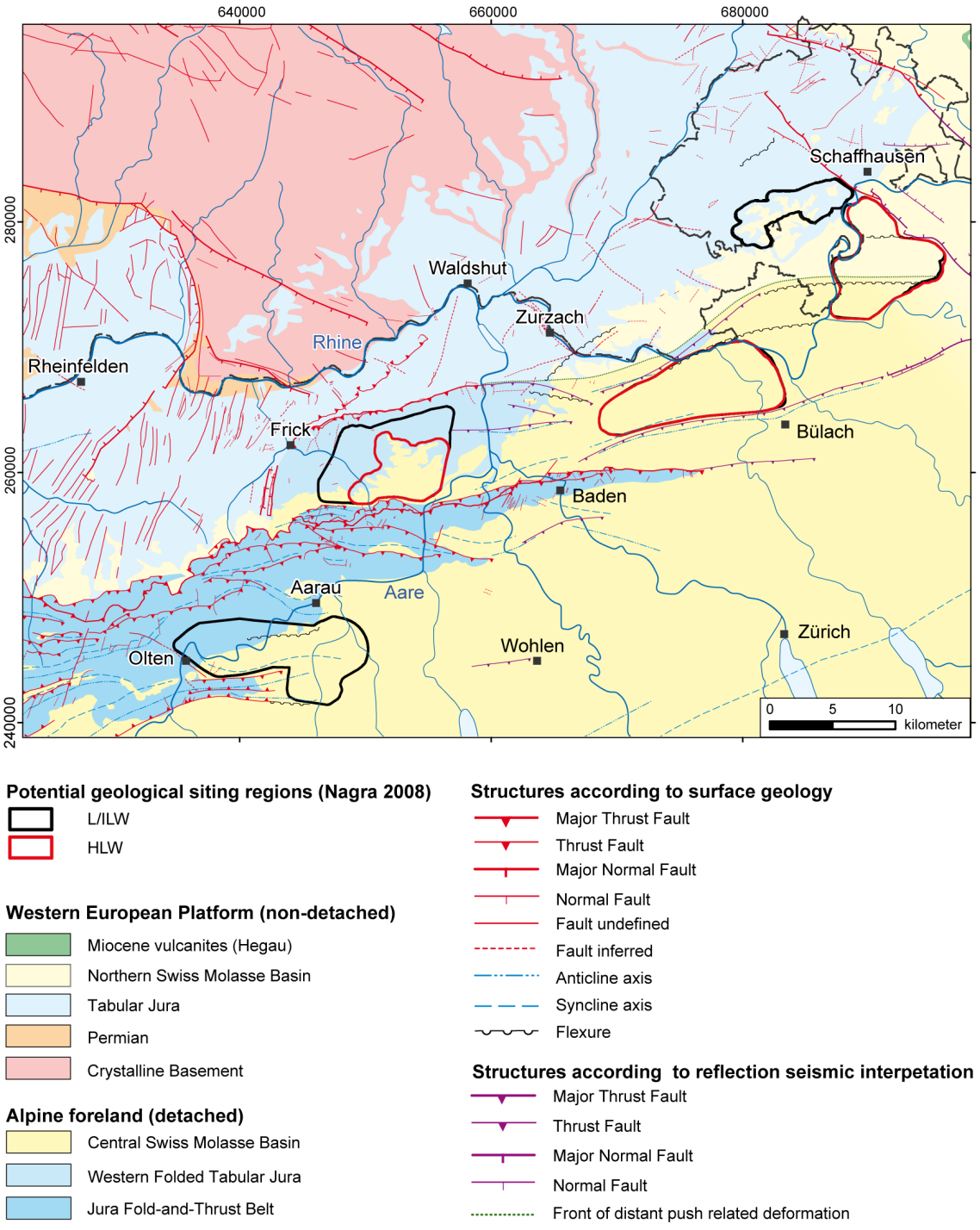

Fig. 2-3: Tectonic map of the proposed siting regions in Northern Switzerland showing major tectonic units and the fault pattern of the area in more detail (from Madritsch & Hammer 2012).

Results of complementary analyses of brittle deformation structures

Madritsch & Hammer (2012) conducted complementary field investigations as a contribution to SGT/Stage 2, aimed at broadening the data base on brittle deformation structures across a large area of Northern Switzerland. Over 80 field outcrops were mapped in detail resulting in more than 2300 fracture measurements and representing the most extensive data set of this kind available for the region to date. Eventually, the data were subjected to an extensive analysis and integrated interpretation in the regional tectonic context.

The gathered data, mostly stemming from outcrops in Upper Jurassic limestone, enabled an enhanced structural geological characterisation of the five geological siting regions in terms of fracture orientation. The most common fracture orientations are NE-SW, NW-SE and N-S. Relative overprint and cross-cutting criteria of different fracture types allowed establishing a regional chronology of Cenozoic brittle deformation. Moreover the kinematic analysis of fault-slip sets yielded paleostress-tensors.

The formation of bedding orthogonal fracture sets that are observable across the entire study area is only weakly defined. At the latest, these structures formed in conjunction with Early Cenozoic tectonic events. Indications for Paleogene or earlier extension are given by the occurrence of extensional flexures and normal faults in the Tabular Jura that pre-date strike-slip faults associated with Neogene Alpine shortening. Kinematic data related to these extensional events remained scarce and no reliable paleostress tensor could be established. Strike-slip faults are the most commonly observed brittle deformation structures in the investigation area. In the Tabular Jura, these strike-slip faults were often found to overprint pre-existing normal faults. In the region of the Jura Fold-and-Thrust Belt, strike-slips faults were frequently found to be rotated with the folded sedimentary stack. This indicates that strike-slip faulting initiated pre- or syn-kinematically with the main contractional deformation phase. At some locations, strike-slip faulting also appears to post-date folding. Based on the kinematic analysis of strike-slip faults, it was possible to constrain a robust paleostress tensor across the entire region indicating NNW-SSE shortening. Occurrence of reverse faults was mostly limited to high strain areas affected by the tectonics of the Jura Fold-and-Thrust Belt. In most cases these reverse faults were found to be kinematically compatible with the strike-slip faults and yielded roughly the same paleostress orientation (e.g NNW-SSE shortening).

The recent investigations on brittle deformation structures indicate a comparatively simple Cenozoic deformation history of the region (e.g., little influence of the Rhine Graben tectonics). Issues of ongoing studies are the definition of the Jura Fold-and-Thrust Belt front which seems to reach farther to the north than expected (e.g., beyond north of the Rhine River at some locations) and the surprisingly complex extension tectonics in the border zone of the Hegau-Bodensee Graben (in the area of Schaffhausen).

2.2 Geological and hydrogeological modelling studies

A 3-D geological model of Northern Switzerland has been elaborated in the context of SGT Stage 2, forming the basic structural framework for quantitative analyses and integrated geoscientific evaluations on the regional and local scale (Gmünder et al. 2013a). The quantitative analyses included groundwater modelling on the regional scale and on the scale of the siting regions, respectively simulations of regional/local heat flow, and last, but not least, numerical analyses of the regional/local stress conditions (Gmünder et al. 2013b, Luo et al. 2013a-d, Papafotiou and Senger 2013, Heidbach et al. 2013). In the present report, many of the geological maps and cross sections of the siting regions were derived from the 3-D geological model (Chapter 2.2.1) and the 3-D hydrogeological model (Chapter 2.2.2) of Northern Switzerland.

2.2.1 Regional geological model of Northern Switzerland

The Nagra 3D geological model of Northeastern Switzerland 2012.1 (abbreviated in the following to 3D GeoMod 2012.1) was established for setting up a regional hydrogeological model; it is decribed in detail in Gmünder et al. (2013a). Here, the main features of GeoMod 2012.1 are shortly summarized, as it will serve as the reference model in Chapter 3 for the discussion of the hydrogeological conditions on the regional scale.

The delineation of the model boundaries and the definition of the layer horizons were motivated by geological and hydrogeological considerations (geological / hydrogeological units, outcropping of regional aquifers specifiying the local recharge/discharge conditions in the North, Alpine recharge areas to the South, etc.). Besides the layer horizons, the most important known regional faults zones were implemented in a simplified manner as they are expected to have a significant effect on regional groundwater flow.

The GeoMod 2012.1 is based on pre-existing 3D geological models from different sources (Gmünder et al. 2013a and references therein; see Fig. 2-4). These models were combined and necessary adjustments (due to overlapping of the model domains, different resolution and/or slightly different depth of layers) had to be performed. Information for volumes that were not covered by these three models has been compiled from additional sources such as GIS-layers, thickness models, seismic data, etc. (see Gmünder et al. 2013a and references therein).

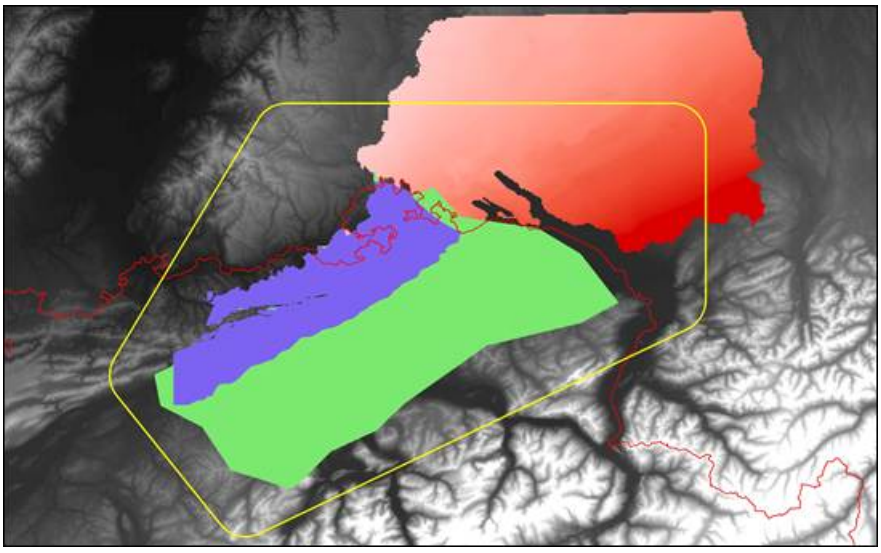

Fig. 2-4: Extend of the three combined models using the example of the base Opalinus Clay horizon.

Blue: Nagra (2008b), green: "Interoil model" and red: "LGRB model" (see Gmünder et al. 2013a and references therein. The red line traces the Swiss border, the yellow polygon traces the maximum extend of the model.

The regional fault systems as derived from geological surface mapping and the interpretation of seismic profiles (see Fig. 2-3; Madritsch & Hammer 2012) were implemented in the 3-D geological model in a simplified manner. Some of the fault surfaces have been constructed based on horizon-specific structural maps while others have been constructed on a series of faults sticks digitized from the existing models which refer to the published structural maps. Especially the fault zones had to be simplified to some extent as for some of them no precise

information about strike, dip or even exact location is known (see Gmünder et al. 2013b for further details).

In total, the model consists of 17 horizons (from top to bottom: topography, base of the Quaternary, base of the Obere Süsswasser Molasse (OSM), base of the Obere Meeresmolasse (OMM), base of the Tertiary, Base of the Kimmeridgian-Tithonian, top of the Effingen Member, base of the Malm, base of the upper Dogger, top/base of the Hauptrogenstein Formation, base and top of the Klingnau Formation, top of the Passwang Formation, top/base of the Opalinus Clay, top/base of the upper Muschelkalk, base of the mesozoic) and 13 fault zones (BIH, Born Anticline, Haeggenschwil, Homburg, Jura Main thrust, Mandach, Neuhausen, Randen, Ruemi, Singen, Stahringen, Trimbach-Olten and Wölflinswil), some of which include several fault planes (see Fig. 2-5). Note that the Mettau fault was not implemented in the 3-D model, because the fault system is shallow and therefore of limited significance.

2.2.2 Groundwater flow modelling in the Molasse Basin of Northern Switzerland

Based on the GeoMod 2012.1, a regional hydrogeological model has been established. For this purpose, some of the stratigraphic horizons had to be extended to cover the whole model domain (see Fig. 2-4; bottom horizon of the Opalinus Clay). In addition, two hydrogeological units were added to the stratigraphic column to allow for a better representation of the hydrogeological situation (the Hauptrogenstein aquifer and the Keuper aquifer). The layers included in the regional hydrogeological model are (from top to bottom): the Quaternary, OSM, OMM, USM, the Malm aquifer, the Effingen Member, the "upper" Dogger, the Hauptrogenstein aquifer (sub-unit of the Hauptrogenstein Formation), the "lower" Dogger, the Opalinus Clay, the clay-rich Lias and Keuper, the Keuper aquifer, the Gipskeuper, the Muschelkalk aquifer and the basal Anhydritgruppe. Since a facies change between the eastern and western model domain occurs roughly in the middle of the model domain, layers in the eastern and western parts are not necessarily the same. This affects mainly the Hauptrogenstein aquifer which was only mapped in the western part of the model domain but not in the eastern part.

The regional faults were taken over from the geological model. A simplified representation of the fault zones was sought in the regional hydrogeological model to limit the complexity of the mesh generation process. For this purpose, the faults were rotated vertically with the center of rotation at top surface.

Four local-scale hydrogeological models were established for the simulation of groundwater flow in the siting regions JS, JO, NL and ZNO/SR. Fig. 2-5 displays the footprints of the 4 local scale models together with the lateral model boundaries of the regional hydrogeological model. The traces of the regional fault systems are represented as red lines. In order to construct the local-scale hydrogeological models, the model domain of the different local models was cut out of the regional model. Since the spatial resolution of the local model is much higher, it was possible to represent the faults in greater detail with the actual dip as specified in the geological model. Furthermore, several hydrogeological units were added to ensure an adequate representation of the local groundwater flow conditions. Thus, local aquifer systems were implemented within the Dogger, Lias and Keuper units. As an example, the highly complex local-scale hydrogeological model of the Jura Ost siting region is shown in Fig. 2-6.

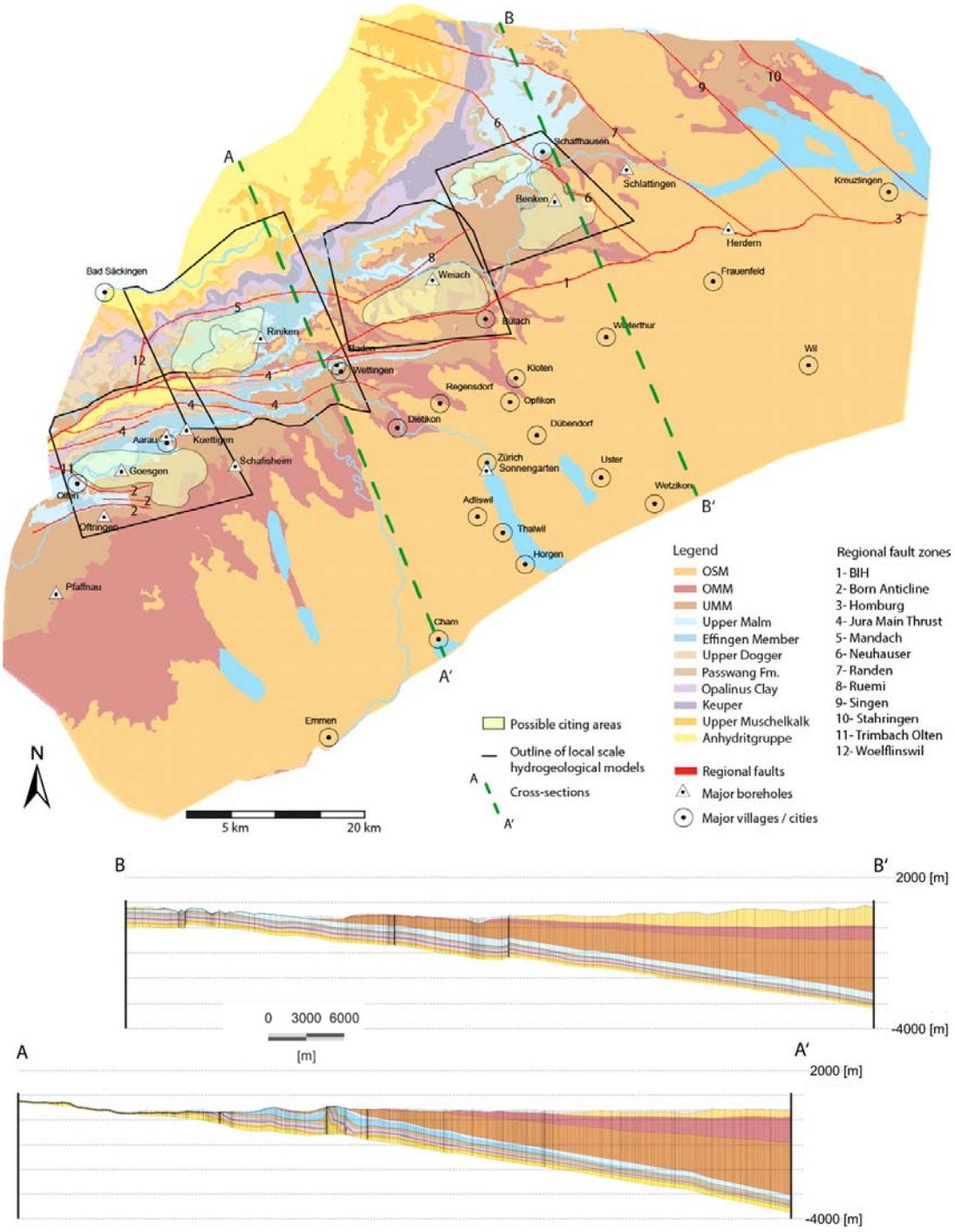

Fig. 2-5: Delineation of the regional hydrogeological model of Northern Switzerland (Gmünder et al. 2013a,b) with cross sections through the whole model domain.

The black frames display the footprints of the local hydrogeological models.

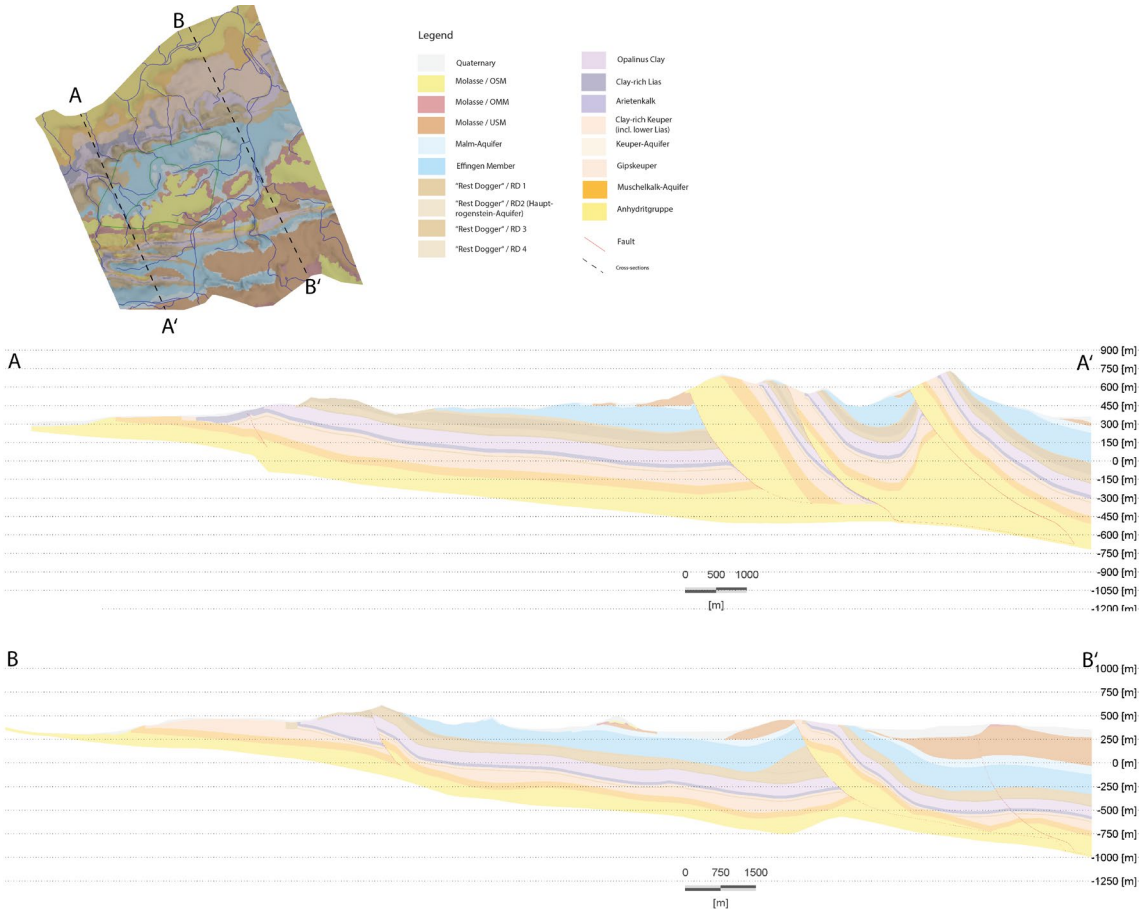

Fig. 2-6: Vertical view of the local-scale hydrogeological model Jura Ost with two cross sections through the model domain.

Note that cross sections are exaggerated twice in the z-direction (Luo et al. 2013c).

3 Effingen Member

The rocks of the Effingen Member are considered as potential host rocks for the geological disposal of L/ILW in the Jura-Südfuss siting area (see Fig. 1-1). The Effingen Member of the Wildegg Formation (sometimes referred to as Effingen Beds) comprises the majority of the Oxfordian strata (Malm, Upper Jurassic) in the Jura-Südfuss area. In the area of interest, the Effingen Member is 170 to 260 m thick at depths of 410 to 720 m below the surface (according to Nagra 2010, Appendix A3) and consists of interlayered calcareous marls to limestones. The Effingen Member has been described sedimentologically by Gygi (1969, 2000a, b). First investigations of the Effingen Member by Nagra date back to the Sediment Study performed by Nagra in the 1980s (Nagra 1988).

Site investigation boreholes (KB5a and SB 2) at the Gösgen nuclear power plant site and geothermal boreholes at Küttigen (Küttigen-1 and 2) and Oftringen (NOK-EWS) (referred to hereinafter as simply the Gösgen, Küttigen, and Oftringen boreholes) provided the opportunity to investigate the hydrogeological, mineralogical, chemical, and physical properties of the Effingen Member and its pore water at relevant depths in and near the Jura-Südfuss siting area (Fig. 3-1).

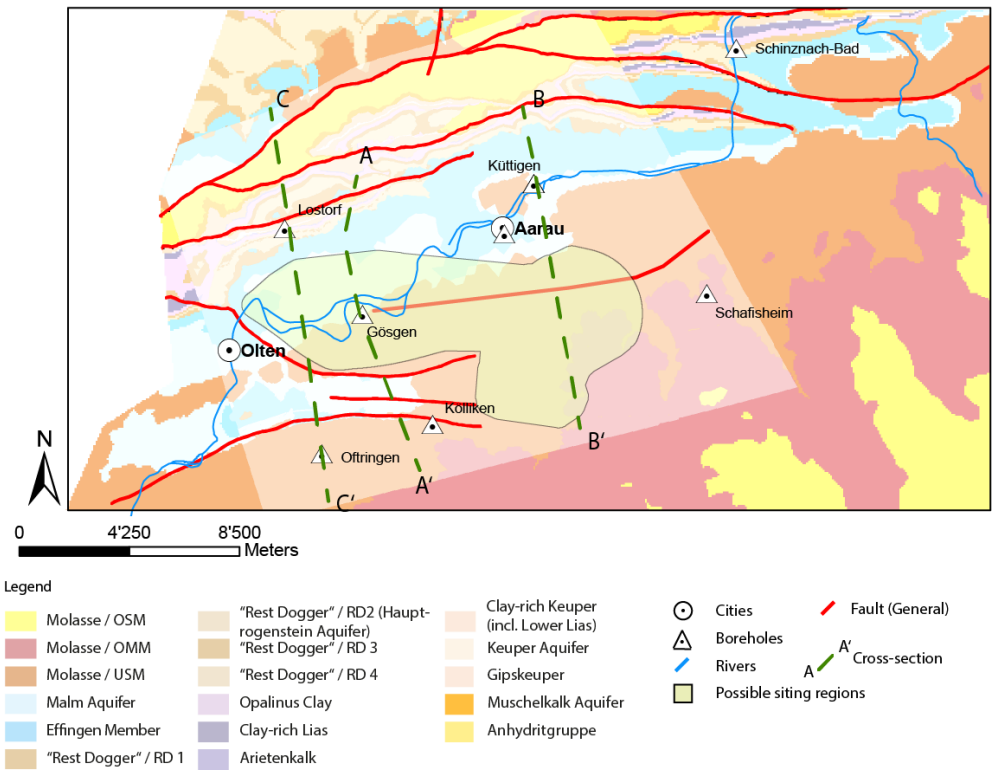

Fig. 3-1: Location of the Jura-Südfuss, proposed siting area for geological disposal of L/ILW in Switzerland, modified from Nagra (2008b).

3.1 Geologic Setting

The candidate siting area Jura-Südfuss features two different host rock formations at suitable depth range, namely the Effingen Member and the Opalinus Clay. Overall, the JS region extends over 65 km^2, with the Effingen Member being considered within a subarea within the eastern portion of the overall siting area (Fig. 3-1). In the eastern part of JS, the Effingen Member was considered as a potential host rock due to the absence of known tectonic features and the presence of a suitable lithology with adequate thickness at a suitable depth range (Nagra 2008a).

Understanding of the spatial conditions in the area is based on 2D seismic investigations and partly on the results from the deep borehole at Schafisheim, as well as the shallower boreholes at Gösgen, Küttigen, and Oftringen (Fig. 3-1). The siting area lies close to the Folded Jura at the northern boundary of the Molasse Basin and is, therefore, partly subject to strong tectonic stress, which is expressed visibly in some of the regional structures (Jura Main Thrust, Born Anticline, Trimbach-Olten; see also Fig. 2-5). There are also indications of tectonic structures on the sub-regional scale; zones of undisturbed bedding are rare (Madritsch & Hammer 2012; Fig. 2-3).

The Gösgen, Küttigen, and Oftringen boreholes are located in the eastern Subjurassic zone of the Molasse basin (Fig. 3-1). The Subjurassic zone lies along the southern boundary of the Folded Jura. This zone is characterised by compressional features such as anticlines and thrust faults, which affect both the Tertiary and Mesozoic units. These structures are clearly visible in the profile shown in Fig. 3-2. The most prominent compressional feature in the area of interest is the Born-Engelberg anticline (Fig. 3-1, Fig. 3-2), which separates the Oftringen borehole from the Jura-Südfuss siting area.

In the area of interest, the Effingen Member is 220 to 240 m thick and consists of interlayered mostly calcareousmarls and argillaceous limestones. It is part of the Wildegg Formation (Malm, Oxfordian), which includes the underlying limestone of the Birmenstorf Member. This limestone, together with the limestones of the Hauptrogenstein Formation, constitutes the regional aquifer underlying the low-permeability Effingen Member. Some limestones of the Passwang-Formation below the Hauptrogenstein Formation may also contain local aquifers. The limestone of the Geissberg Member constitutes the overlying aquifer.

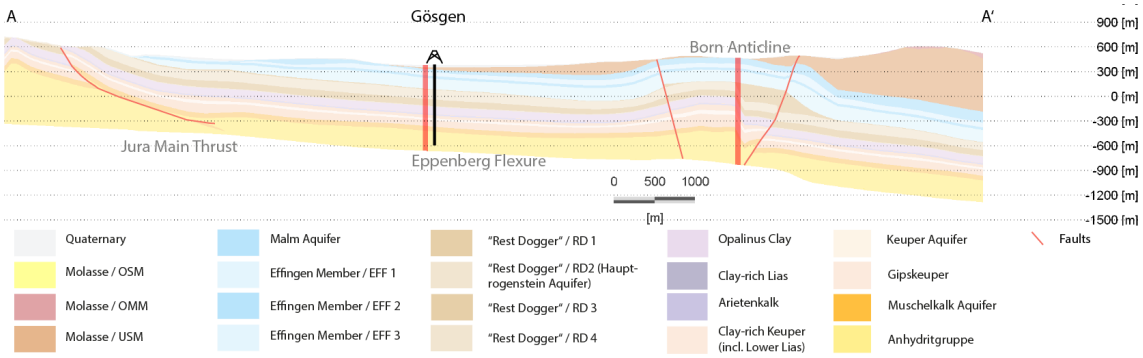

Fig. 3-2: Geological profile across the area of interest.

The profile trace is shown in Fig. 3-1 (profile A – A').

The Effingen Member is divided in 3 sub-units, representing the upper sequence of limestone layers and clay-rich marls (EFF 1), the Gerstenhübel Beds sequence (EFF 2) and the alternating sequence of limestone layers and marls at the bottom (EFF 3).

Deplazes et al. (2013) have proposed, based on the clay content from geophysical logs the following mineralogical facies inventory for the Effingen Member (EFF), from top to bottom (Fig. 3-3):

- Three alternating sequences of (argillaceous) limestones and thinner (calcareous) marls (Kalkbankabfolgen, KBA 1 – 3): The three strata with variable thicknesses of 4 – 12 m are observed in all boreholes. The similar pattern in the clay content suggests that these sequences are continuous.
- Gerstenhübel Beds sequence (GER): An alternating sequence of limestone layers and thin, clay-rich marls. Based on the proposed clay content correlation (Fig. 3-3), the GER sequence has a regional extension with a thickness of 10 – 30 m in the eastern part of the siting region and not more than a few meters in the western part.
- Local alternating sequences of (argillaceous) limestones and thinner (calcareous) marls (KBA4 – 5, KBAx): There are several minor limestone sequences in the lower part of the EFF below the GER. The thickness is in the m range, the extension is quite uncertain.
- Sequences which are dominated by (calcareous) marls (Kalkmergelabfolgen) can be found between the KBAs. The KMAs above the GER show more similarities in the clay content pattern than the KMAs below the GER.

The thicknesses of the different facies in the stratigraphic profiles are defined visually using the clay content from geophysical logs (see also Traber & Blaser 2013). This resulted in the identification (and possible horizontal correlation) in the different boreholes as shown in Tab. 3-1 and Fig. 3-3.

Tab. 3-1: Estimated facies thicknesses in [m] in Effingen Member boreholes after Deplazes et al. 2013.

	OES	**KBA1**	**KBA2**	**KBA3**	**GER**	**KBA4**	**KBA5**	**KBAx**
Pfaffnau-1	n/a	11 934.5-945	7 962.5-969	11 983.5-994.5	7 1031.5-1038	n/a	n/a	n/a
EWS Oftringen	28 420-447.5	9 485.5-494.5	8 514-521.5	8 537-545	2 584.5-587	4 612-616	5 623.5-628	6 632.5-638.5
Gösgen-SB2	15 66-80.5	11 109.5-120	9 140-148.5	9 164-173	2 216.5-218	6 253-259	7 277.5-284.5	10 288.5-298.5
EWS Schönenwerd	n/a	8 21-29.5	8 52.5-60.5	8 76-84	2 194-196	n/a	n/a	n/a
EWS Aarau	11 44-55.5	12 92-104	6 120-126.5	8 140.5-148.5	23 192.5-216	3 231.5-234	4 244.5-248.5	4 251.5-255
EWS Küttigen-2	n/a	10 65.5-75.5	7 90-97.5	7 112.5-119.5	27 166-193	3 211-214	5 224.5-229	5 234.5-239.5
EWS Biberstein	4 38.5-42.5	10 77.5-87	8 103-111	7 127-133.5	31 178-209.5	3 229.5-233	3 239.5-242	3 245-248
SB Schafisheim	n/a	4 702.5-707	4 711.5-715.5	6 724-730		n/a	n/a	n/a
SB Riniken	n/a	n/a	n/a	6 41-47	30 94-124	7 153.5-160	9 174.5-183.5	n/a

The Gösgen boreholes are located in the northwestern Molasse basin, close to the thrust of the Folded Jura (Fig. 3-2). Borehole SB2 penetrated directly into the Oxfordian sediment sequence (Malm) below an about 30-m-thick Quaternary overburden (Fig. 3-4). The Oxfordian sediments include coral-reef type limestone from the Olten Member (Balsthal Formation) down to 57 m, micritic limestone from the Geissberg Member (Villigen Formation) down to 66 m, followed by silty to sandy marls with intercalated limestone layers of the Effingen Member (Wildegg Formation) down to 307 m, and finally limestone of the Birmenstorf Member down to 323 m (Albert et al. 2009). The borehole then penetrated 24 m of Dogger sediments, including 3 m of oolitic limestone and marl of the Herznach Member, 10 m of biodetritic limestone of the Varians Beds and Spatkalk, and the upper 11 m of the oolitic limestone of the Hauptrogenstein Formation.

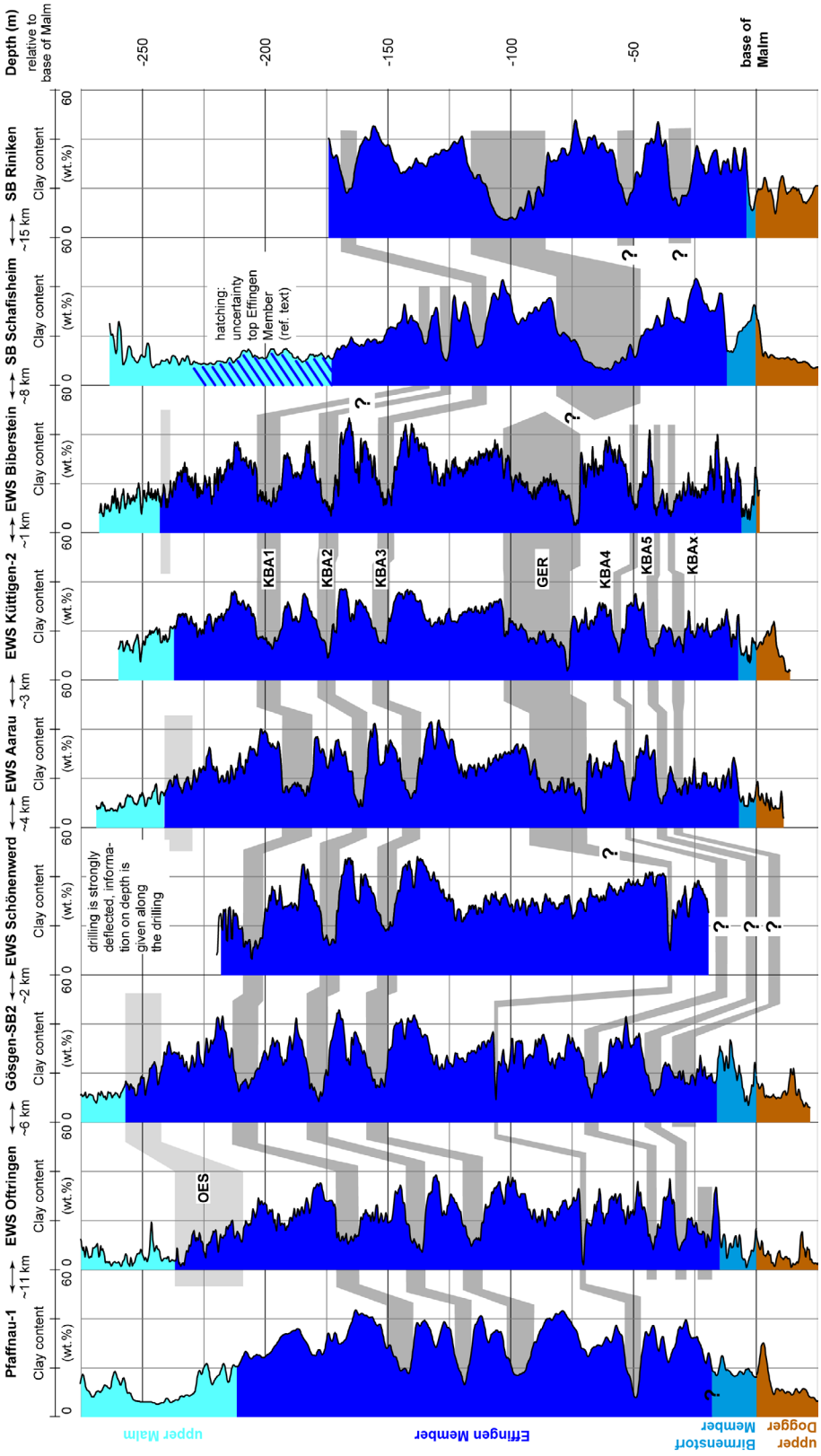

Fig. 3-3: Clay contents of the Wildegg-Formation based on geophysical logs (Albert & Schwab 2012, Deplazes et al. 2013) between Pfaffnau and Riniken.

The grey shadings indicate suggested correlations between the coring sites.

Fig. 3-4: Lithostratigraphical profile in Gösgen borehole SB2 (from Enachescu et al. 2010).

The Küttigen boreholes intersected Quaternary deposits and Upper Jurassic sedimentary rocks comprising the Malm (Oxfordian) and the top of the Dogger (Fig. 3-5). The Malm sequence comprises the Geissberg Member (28 m) at the top, the entire thickness of the Effingen Member (230 m), and the Birmenstorf Member (7 m) at the base. As at the other locations, the Effingen Member includes a number of sections rich in limestone beds. The most significant of these occurs at 166 – 194 m (Fig. 3-5) and probably corresponds to the Gerstenhübel Beds as defined by Gygi (1969, 2000a, b) in the Jakobsberg quarry. The bottoms of the boreholes are located in the Hauptrogenstein unit of the uppermost Dogger.

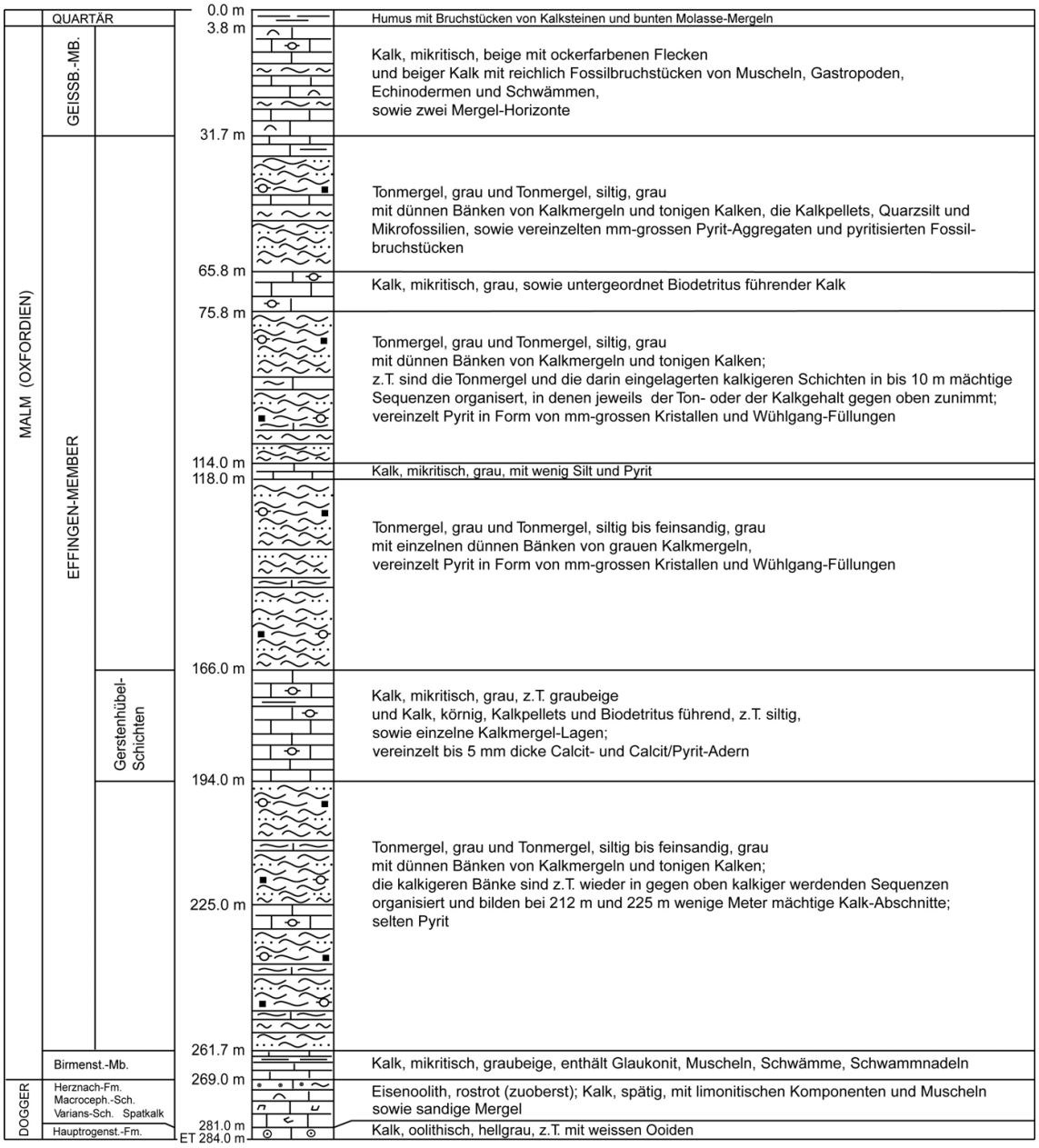

Fig. 3-5: Lithostratigraphical profile of borehole Küttigen-1 (from Albert et al. 2007).

A north-south cross section through the Küttigen site is shown in Fig. 3-6, illustrating how all the strata penetrated by the Küttigen boreholes crop out less than 2 km to the north.

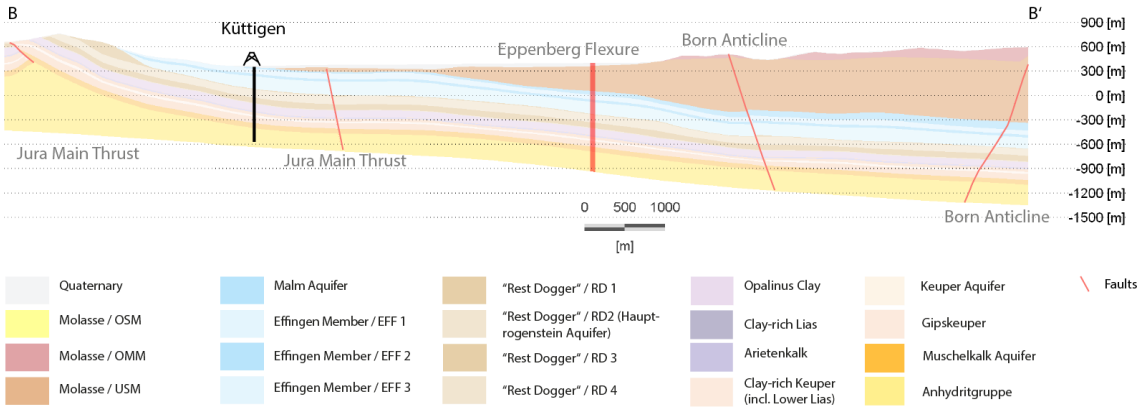

Fig. 3-6: North-south geological profile through the geothermal borehole Küttigen.
Profile location is given in Fig. 3.1 profile B – B'.

The sequence drilled at Oftringen (Fig. 3-7) includes the Lower Freshwater Molasse (Oligocene – Miocene basinal deposits), underlain by a thin Eocene shale layer (Boluston). An unconformity separates the Tertiary deposits from the underlying Malm and upper Dogger units. In the lower part of the Malm (Upper Jurassic, Oxfordian) is the Wildegg Formation which includes the low-permeability Effingen Member and the underlying Birmenstorf Member.

The Effingen Member at Oftringen is 220 m thick (420 – 642 m depth) and is overlain by three Malm limestone units, 57 m thick (from top, Letzi and Wangen, Geissberg, and Crenularis Members). The Effingen Member comprises bedded calcareous marls with about eight sections rich in limestone beds (5 to 20 m thick) that subdivide the marl-rich sections (Albert & Bläsi 2008). It is underlain by alternating marl/limestone beds of the Birmenstorf Member (642 - 657 m), which in turn are underlain by oolitic limestones of the Dogger.

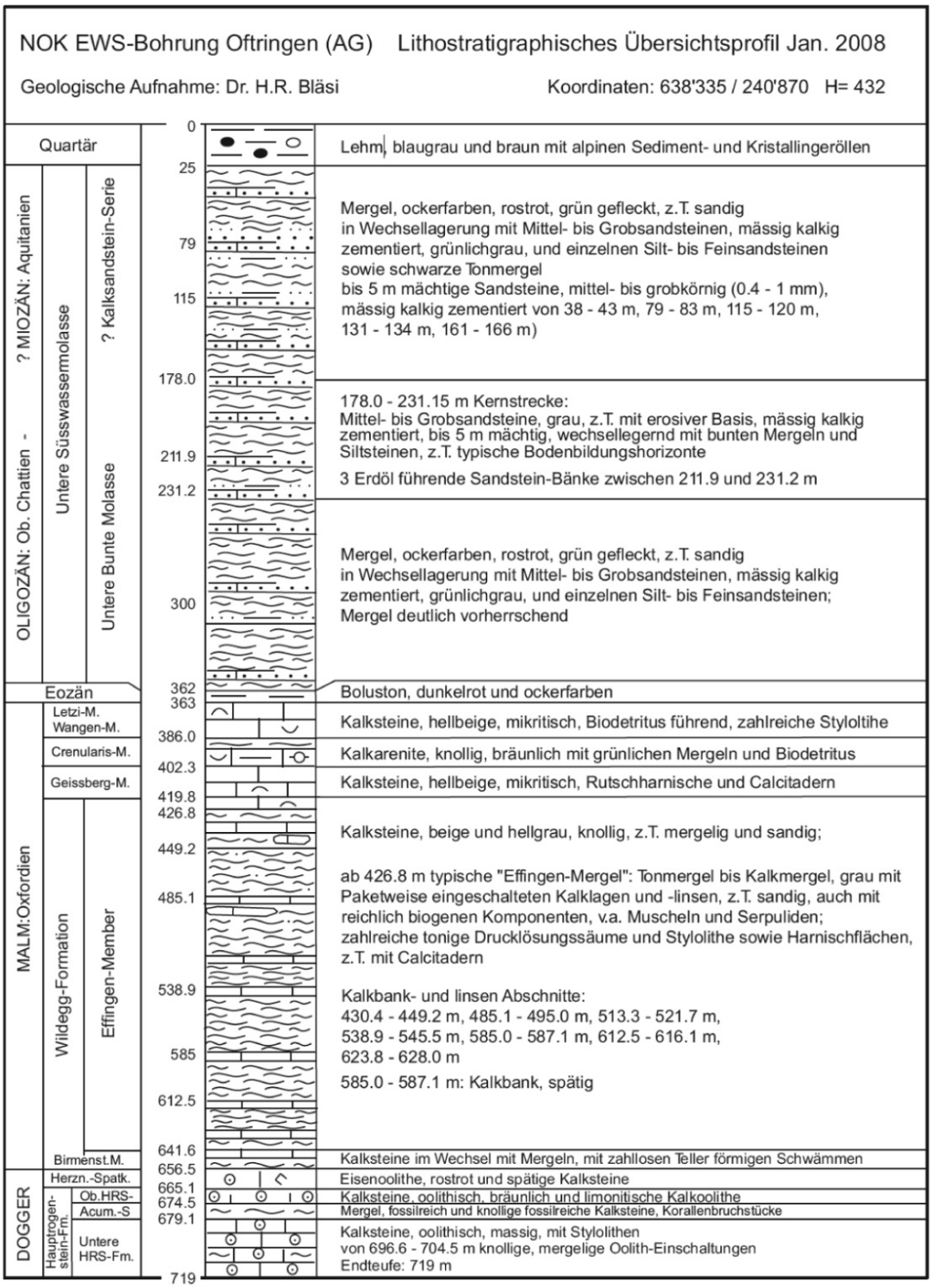

Fig. 3-7: Lithostratigraphical profile of the Oftringen borehole (Albert & Bläsi 2008).

A north-south cross section through the Oftringen site is shown in Fig. 3-8, illustrating the faulting and deformation associated with the Born-Engelberg anticline a few km to the north.

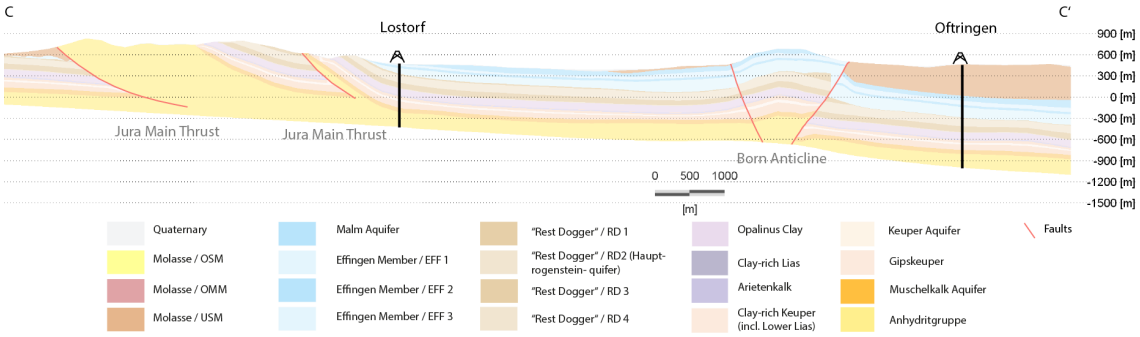

Fig. 3-8: North-south geological profile (no vertical exaggeration) through the Oftringen borehole.

Exact location is given in Fig. 3-1, profile C-C'.

3.2 Hydraulic Tests

The low permeability of the Effingen Member is demonstrated most directly by the hydraulic tests that have been conducted. Nagra has tested the Effingen Member in the Gösgen, Küttigen, and Oftringen boreholes. Because these boreholes were not purpose-drilled and owned by Nagra, Nagra did not have the opportunity to test them as comprehensively as might have been desired. Instead, as much testing as possible was performed in the limited time periods available, with the primary emphasis being on the estimation of hydraulic conductivity. Information on formation pressure (hydraulic head) was desired, but the time available for testing was insufficient to allow more than a rough bracketing of the range of possible pressures, at best. The hydraulic tests conducted in the Effingen Member in the Gösgen, Küttigen, and Oftringen boreholes are evaluated below in terms of: (1) test performance – suitability of test phases, adequacy of test phase durations, performance of equipment, reliability of data; (2) test analysis – suitability of analysis methods applied, adequacy of analysis method implementation, treatment of uncertain parameters, estimation of uncertainty, reliability of results; and (3) potential for improving parameter estimation by reanalysis of tests.

3.2.1 Gösgen Tests

Hydraulic tests were conducted over six intervals in the Gösgen SB2 borehole, five of which spanned portions of the Effingen Member. The sixth interval (denoted Test 1) was below the Effingen Member, and extended from the Callovian (Dogger) Hauptrogenstein Formation to the Oxfordian (Malm) Birmenstorf Member. Testing began at the bottom of the hole and progressed upward through the calcareous marls of the Effingen Member. The first test utilized a single packer to test a 30.1-m interval at the bottom of the hole. The next four tests utilized a double-packer tool to test sequential 62.7-m intervals. For the final test, the straddle-packer interval was shortened to 17.66 m to retest a subsection of the Test 3 interval containing limestone. Tests 1 through 5 were conducted between December 17 and 23, 2008, and Test 6 was conducted from December 23, 2008 through January 5, 2009. Baechler et al. (2009) report a water table in the Quaternary deposits at Gösgen at an elevation of about 375 m (~ 5 m below ground level [bGL]).

The tests are described in Enachescu et al. (2010), along with preliminary analyses of the tests. The analysis results, consisting of the best estimates and global uncertainty ranges for hydraulic conductivity and freshwater head, are presented in Tab. 3-2.

Tab. 3-2: Gösgen Preliminary Analysis Results from Enachescu et al. (2010).

Test #	**Interval Top**	**Interval Bottom**	**K [m/s]**			**Freshwater Head [m asl]**		
	[m bGL]*	[m bGL]	Min.	Best est.	Max.	Min.	Best est.	Max.
1	316.90	347.00	3.3E-10	5.3E-10	1.7E-9	450.1	454.9	461.3
2	253.89	316.61	4.8E-15	1.5E-14	6.4E-14	120.5	199 – 250	253.0
3	191.17	253.89	4.8E-15	1.4E-13	3.2E-13	189.5	260 – 331	352.6
4	128.98	191.69	4.8E-15	2.1E-14	8.0E-14	251.7	262 – 380	394.4
5	75.79	138.50	1.6E-14	1.9E-13	8.0E-13	366.0	371 – 381	417.0
6	212.32	229.98	2.8E-13	4.8E-13	1.7E-12	260.1	260 – 331	351.8

* Ground level (GL) at Gösgen borehole is 380.75 m above sea level (asl).

The sequence of test phases applied during Test 1 was reasonable given the hydraulic conductivity encountered in that interval, but longer recovery phases (slug-withdrawal shut-in (SWS) and constant-head withdrawal shut-in (HWS)) would have been beneficial. The data appear to be reliable and suitable for analysis. Although the methods used to analyze Test 1 are not as rigorous and comprehensive as they could be, the analysis results given for Test 1 in Tab. 3-2 appear to be generally reliable. The reliability of the analysis is in large part due to the relatively high hydraulic conductivity of the interval, which allowed well-developed test responses to be observed. The analysis could be improved by including specific storage as a fitting parameter (rather than fixing it at an estimated value as was done by Enachescu et al. 2010), by simultaneous fitting to the data from multiple sequences expressed in different formats (e.g., derivatives, Cartesian), and by performing a more extensive perturbation analysis to estimate parameter uncertainty. In any case, the interval is clearly overpressured with respect to the water table.

The test-zone compressibility (C_{tz}) calculated for the Test 1 interval is approximately 1E-7 Pa^{-1}, which is approximately 2.4 orders of magnitude higher than the compressibility of water. Either the test-zone volume used by Enachescu et al. (2010) is significantly incorrect (too low), gas was present in the test interval during the slug-withdrawal shut-in (SWS) recovery and constant-head withdrawal shut-in (HWS) recovery phases of the test, or the shut-in tool (SIT) was not completely closed during these recovery phases. The possible presence of gas, and its effects on the test analysis, should be investigated further.

Test 2 was appropriately focused on a single pulse-withdrawal (PW) phase, followed by a slug-withdrawal (SW) phase that was intentionally only long enough to confirm qualitatively the low hydraulic conductivity (K) indicated by the PW phase. The Test 2 interval clearly has a lower K than the Test 1 interval, as evidenced by the low amount of pressure recovery observed during the PW test. With a duration of less than 8 hr, the test was too short to allow precise determination of hydraulic properties. The estimated K shown in Tab. 3-2 is probably within an order of magnitude of the true value, but the uncertainty on freshwater head is, if anything, understated. An uncertainty range of 140 to 330 m asl might be more appropriate. In any case, the interval appears to be underpressured with respect to the water table. As was the case with Test 1, the

analysis could be improved by including specific storage as a fitting parameter, by simultaneous fitting to the data expressed in different formats (e.g., derivatives, Cartesian), and by performing a more extensive perturbation analysis to estimate parameter uncertainty.

Test 3 followed the same appropriate design as Test 2, but the PW initiation did not appear to be quite as clean as was the case in Test 2. As was the case for Test 2, Test 3 was too short to allow precise determination of hydraulic parameters. The nSIGHTS analysis of the test shows some minor implementation errors with uncertain impacts. The analysis indicates a best estimate for hydraulic conductivity an order of magnitude greater than that for Test 2, but this difference is doubtful considering the qualitative similarity of the two test responses. The uncertainty range of nearly two orders of magnitude provides a better indication of how well hydraulic conductivity is known for this interval. The freshwater head uncertainty range given in Tab. 3-2 for Test 3 is actually derived from Test 6; based solely on the data from Test 3, the range would be much wider. The large uncertainty notwithstanding, the interval appears to be underpressured with respect to the water table. The analysis could be improved by including specific storage as a fitting parameter, by simultaneous fitting to the data expressed in different formats (e.g., derivatives, Cartesian), and by performing a more extensive perturbation analysis to estimate parameter uncertainty.

Test 4 followed the same appropriate design as Tests 2 and 3. Test 4 was qualitatively very similar to Test 2, and the resulting estimates of hydraulic conductivity are also very similar. Based on the analysis presented in Enachescu et al. (2010), however, the range of uncertainty on hydraulic conductivity would seem to extend an order of magnitude higher than they indicate in their summary tables (which provide the basis for Tab. 3-2). Their relatively crude sensitivity analysis shows the results have very little sensitivity to freshwater head, so no reliable estimate of head can be made. Qualitatively, the interval appears to be underpressured relative to the water table. The analysis could be improved by simultaneous fitting to the data expressed in different formats (e.g., derivatives, Cartesian) and by performing a more extensive perturbation analysis to estimate parameter uncertainty.

Test 5 represented the third attempt to test an interval near the top of the Effingen Member – previous attempts to test the intervals from 67.97 to 130.69 m bGL (Test 5a) and from 69.98 to 132.69 m bGL (Test 5b) were abandoned because of anomalous responses at the start of each attempted PW test. The same type of anomalous, irregular, rapid initial recovery was observed during the PW portion of Test 5. In all cases, the test-interval pressure rose irregularly by 55 - 110 kPa in approximately five minutes, after which a sustained rise in pressure at a much lower rate occurred. A short time after the anomalous pressure rise, the temperature gauge in the test interval also showed an anomalous rise and fall in temperature that was not accompanied by the expected change in pressure (assuming the test-zone compressibility remained as measured when the PW was initiated). The lack of correspondence between temperature change and pressure change suggests that the temperature gauge, which was positioned directly below the upper packer, was not measuring the temperature of the water in the interval (or test-zone compressibility had increased significantly). An influx of slightly warmer gas into the interval could have resulted in formation of a gas pocket at the top of the interval where the gauge was located that gradually approached temperature equilibrium with the water. The presence of a gas pocket might have been detected had a measurement of the test-zone compressibility been made when the PI was initiated, but the method used to initiate the pulse did not allow such a calculation. We also note that the tubing that had been pressurized with gas to create the elevated pressure for the PI appeared to slowly lose its residual gas charge over the course of the PI test after the shut-in tool had been closed. As the tubing pressure was lower than the test-interval pressure, leakage of gas from the tubing should not have affected the test results. Overall confidence in the entire Test 5 sequence, however, is low. The PI test response was

qualitatively similar to the Test 2 PW response, raising doubts that the hydraulic conductivity of the interval is an order of magnitude higher than that of the Test 2 interval as indicated by Enachescu et al. (2010) and shown in Tab. 3-2. The crude sensitivity analysis performed showed that the results have very little sensitivity to freshwater head, so no reliable estimate of head can be made – the range given in Tab. 3-2 is unrealistically narrow, particularly on the low end, but includes the elevation of the water table reported by Baechler et al. (2009) at 375 m. No conclusions can be drawn about whether the interval is overpressured, normally pressured, or underpressured relative to the water table.

Test 6 was conducted over a 13-day period from December 28, 2009 to January 5, 2010. For this test, the straddle interval was shortened to 17.66 m to allow targeted testing of a subsection of the Test 3 interval containing limestone beds. Unfortunately, the responses observed during testing are inconsistent and unexplainable. The testing sequence began with a slug-withdrawal (SW) phase, even though nothing in Test 3 indicated that a slug test would be appropriate for this interval – pulse tests should clearly have been favored. The SW response was predictably slow, but appeared to proceed normally for approximately 100 hr, as the test-interval and tubing pressures rose in unison. When the SIT was closed to initiate a slug-withdrawal shut-in (SWS) phase, however, the test-interval pressure did not rise more rapidly as was expected, but instead changed very little over 39 hr. When the SIT then opened inadvertently, initiating another slug sequence, the test-interval pressure rose very little, not at all as it did during the initial SW phase. After approximately 100 hr, the SIT was closed again, and this time the test-interval pressure began to rise at the most rapid rate yet observed. After 41 hr, the SIT again opened inadvertently, and very little response was observed over the following ~25-hr SW phase. Only the initial SW phase and the final SWS phase showed the expected behavior; no explanation is apparent for the behavior observed during the other test phases. The test-interval and tubing pressures were consistently lower than the bottomhole and annulus pressures, so could not have been leaking to either of those locations.

Enachescu et al. (2010) chose to analyze only the second SWS test and the following SW test, even though the initial SW test appeared to show the best slug response. This choice completely controlled the analysis results. Without an independent measurement of test-zone compressibility (C_{tz}), the SWS test analysis can provide only highly correlated estimates of hydraulic conductivity (K) and C_{tz}. A slug test is unaffected by the shut-in C_{tz} and provides an uncorrelated estimate of K. Therefore, the slug-test portion of the sequence provided the only constraint on K, and C_{tz} during the SWS phase was calculated based on that K. Had the initial SW phase, which showed much more recovery, been used for the analysis rather than the final SW phase, the estimated K would have been higher and the associated C_{tz} calculated for the SWS phase would also have been higher. Considering that the C_{tz} calculated using the K from the final SW phase is already 2.2E-7 Pa^{-1}, 2.7 orders of magnitude higher than the compressibility of water, the still higher C_{tz} calculated from the K from the initial SW phase would be approaching the compressibility of gas (1.25E-6 Pa^{-1} at 800 kPa). In either case, either gas was present in the test zone or the SIT was not completely closed. Considering that the C_{tz} for Test 3, which included the Test 6 interval, was only 1.6E-9 Pa^{-1}, it is most likely that the SIT was not completely closed during the SWS phase. Because of the inconsistencies and unexplained behavior observed during Test 6, no defensible conclusions can be drawn about K, C_{tz}, or freshwater head.

In conclusion, the hydraulic testing in the Gösgen borehole and the analyses completed to date provide largely qualitative information about the hydraulic properties of the strata tested. A summary of defensible K and freshwater head ranges is given in Tab. 3-3. Parameter values are best known for the lowermost interval that extended from the Hauptrogenstein Formation up into the Birmenstorf Member because of its relatively high K. The interval is clearly

overpressured relative to a hydrostatic freshwater condition to ground surface. The possibility of gas in this interval needs to be investigated further, as it would affect the estimates of K. Tests 2 through 5, all of the Effingen Member, show clear evidence of low K, but the range of uncertainty spans at least two orders of magnitude based on the current analyses. Tests 2 through 4 also show evidence of underpressurization relative to the water table, but reliable estimates, if possible at all, will require more detailed analyses. The inferred freshwater head in Test 2 interval is lower than the regional discharge level, implying that the cause of underpressures is not related to gravity-driven groundwater flow. More detailed analysis may allow a determination of the head in the Test 5 interval, but this is not certain. Inconsistent and unexplained responses during Test 6 leave no possibility of defensible parameter estimates. Based on this evaluation, Tests 2, 3, and 4 are the best candidates for reanalysis if reduction of the uncertainty associated with the interpreted results is deemed warranted.

Tab. 3-3: Defensible parameter estimates from Gösgen hydraulic tests: parameter ranges and best estimates [BE].

Test #	**Interval Top** [m bGL*]	**Interval Bottom** [m bGL*]	**Probable K** [m/s] Range, [BE]	**Probable Freshwater Head** [m asl] Range, [BE]	**Comments**
1	316.90	347.00	3E-10 to 2E-9 [5E-10]	450 to 461 [455]	Hauptrogenstein Formation – Birmenstorf Member; Interval may contain gas
2	253.89	316.61	1E-15 to 1E-13 [1E-14]	140 to 330 [200]	Need more detailed analysis; inferred head below regional discharge level
3	191.17	253.89	1E-15 to 3E-13 [2E-14]	undetermined	Head probably below ground surface, but need more detailed analysis; includes 2-m-thick limestone of Gerstenhübel Beds
4	128.98	191.69	1E-15 to 3E-13 [2E-14]	undetermined	Head probably below ground surface, but need more detailed analysis
5	75.79	138.50	1E-15 to 8E-13 [3E-14]	undetermined	Anomalous PW response; no conclusion possible on head
6	212.32	229.98	undetermined	undetermined	No defensible analysis possible; interval may contain gas; includes 2-m-thick limestone of Gerstenhübel Beds

* Ground level (GL) at Gösgen borehole is 380.75 m above sea level (asl).

3.2.2 Küttigen Tests

Hydraulic tests were conducted over six intervals of the Effingen Member in the Küttigen 2 borehole. Testing began near the bottom of the Effingen Member with a 40.15-m straddle interval and progressed upward for the first five tests. Test 3 was conducted over an interval containing only Effingen marl. Tests 1, 4 and 5 included at least one limestone sequence identified in Deplazes et al. (2013) (Tab. 3-1).Test 2 included the entire 27.2-m thickness of the Gerstenhübel Beds (166.0 to 193.2 m bGL) in addition to overlying and underlying marl. For the final Test 6, the straddle-packer interval was shortened to 6.12 m to retest and collect

groundwater samples from a subsection of the Test 2 interval containing the contact between the Effingen marl and the upper portion of the Gerstenhübel Beds.

The tests were conducted between March 9 and 13, 2007. The tests are described in Enachescu et al. (2007), along with preliminary analyses of the tests. The analysis results, consisting of the best estimates and global uncertainty ranges for hydraulic conductivity and freshwater head, are presented in Tab. 3-4.

Tab. 3-4: Küttigen Preliminary Analysis Results from Enachescu et al. (2007).

Test #	**Interval Top** [m bGL]*	**Interval Bottom** [m bGL]	**K** [m/s]			**Freshwater Head** [m asl]		
			Min.	Best est.	Max.	Min.	Best est.	Max.
1	209.84	249.99	5.0E-14	7.3E-13	1.0E-11	420.2	611.7	726.0
2	162.00	202.15	1.5E-10	6.7E-10	1.7E-9	409.0	418.3	423.2
3	121.93	162.08	1.0E-13	1.8E-12	5.0E-11	268.6	287.8	314.5
4	62.00	102.15	7.5E-16	1.2E-15	1.0E-14	undetermined		
5	37.00	77.15	1.2E-15	5.0E-15	7.5E-14	undetermined		
6	163.00	169.12	4.9E-10	1.3E-9	8.2E-9	394.3	397.2	409.6

* Ground level (GL) at Küttigen borehole is 374.20 m above sea level (asl).

Test 1 in the Küttigen borehole was disturbed by shut-in tool (SIT) problems. The SIT was first shown to be leaking when the tubing was pressurized during the PSR (Pseudo Static Recovery phase) in preparation for a pulse-injection test. The leak could not be fixed without removing the test tool from the borehole, so an SW phase, which was the only kind of test that could be performed that did not rely on a properly functioning SIT, was initiated. The SW phase was inexplicably ended after 1.87 hr and only 1 kPa of recovery by closing the SIT which had already been demonstrated to be malfunctioning. During the subsequent 8.7-hr SWS phase, the test-interval pressure rose at a much slower rate than had been observed during the initial PSR. When the tubing was then pressurized again to test the SIT, the SIT was found to still be leaking. Despite this clear evidence that the SWS was not reliable, Enachescu et al. (2007) chose to base their test interpretation on the SW and SWS phases. Their results are not defensible. A better choice would have been to attempt to analyze the PSR before the tubing was pressurized along with the SW, but even in that case, the assumption that the SIT was not leaking during the early portion of the PSR could not be proved. Based on the initial PSR response, the test interval appears to be overpressured relative to a hydrostatic freshwater condition, with a head of perhaps 390 m asl or greater; no estimates of hydraulic conductivity can be made.

Test 2 was a successful test with no equipment problems and well-defined pressure responses. The analysis presented by Enachescu et al. (2007) is reasonable as far as it goes, but could be improved by simultaneous fitting to derivatives calculated for the SW, SWS, and PW phases in combination with the overall Cartesian pressure record. Based on that fit, a perturbation analysis could be performed to estimate parameter uncertainty. Such an analysis would probably show that T was within the 6E-9 to 7E-8 m^2/s range of uncertainty shown in Enachescu et al. (2007), while narrowing that range. Freshwater head would probably be shown to have a value somewhat lower than the range shown in Tab. 3-4, perhaps 407 to 417 m asl. The Test 2 interval comprised the entire 27.2-m thickness of the Gerstenhübel Beds along with 12.95 m of Effingen

marl. If all of the T was provided by the Gerstenhübel Beds, the corresponding K range would be 2E-10 to 3E-9 m/s.

Test 3 represented an incorrect choice of test phases, as well as inadequate time for testing. Rather than beginning with an SW phase, the testing might better have begun (and ended) with a PW phase that, given the limited time available for testing, would have given more of a response that could be analyzed. The 0.8-hr SW phase and following 3.1-hr SWS phase provided little data for analysis. The lack of a recovery response during the SW provides a maximum bound on K, but identifying a unique value of K below this maximum from the SWS response requires knowledge of C_{tz}. A C_{tz} of 4.9E-10 Pa^{-1} was calculated from the initial SW response, and should have then been a specified parameter in the analysis. Enachescu et al. (2007), however, ignored this necessary constraint, and instead fitted on both C_{tz} and K, an approach that can only yield correlated estimates of both parameters. From their fitting, they derived "best fit" estimates of K of 1.8E-12 m/s and C_{tz} of 2.9E-9 Pa^{-1}. Because C_{tz} is known to be 4.9E-10 Pa^{-1}, K must actually be on the order of 3E-13 m/s. Given these errors in the analysis, the reliability of the static formation pressure estimates cannot be evaluated. Other minor errors are apparent in the implementation of nSIGHTS for the test analysis, but should have had no significant effect on the results. Considering the short duration of the test, the range of uncertainty must be wide. Reanalysis of the test is advised.

Test 4 made the most of the time available for testing, focusing on a single PW test. In the analysis by Enachescu et al. (2007), however, static formation pressure was fixed at a near-hydrostatic condition rather than being included as a fitting parameter. While sensitivity to static formation pressure was assessed at a late stage in the analysis, fitting to it might have allowed determination of an uncertainty range. Specific storage could also have been included as a fitting parameter, rather than given a specified value. The range of uncertainty given in Tab. 3-4 for K appears to extend to too high a value because of an unnecessary evaluation of the sensitivity of K to C_{tz}. C_{tz} was measured and should not, therefore, be subject to factors of two and three uncertainty. Minor, likely insignificant, errors are again noted in the implementation of nSIGHTS for test analysis.

Test 5 was similar to Test 4, although considerably shorter. The short duration of the test, in fact, leaves it with very little value. The analysis of Enachescu et al. (2007), while (intentionally) not as comprehensive as it might have been, shows that the test provides little information beyond the skin zone around the borehole. The Cartesian plot of the best-fit nSIGHTS simulation shows obvious implementation errors, as well as inconsistencies with the reported borehole history and parameter information. The 95.4% joint-confidence region plot for inner and outer zone K shows that the outer zone K could be as much as three orders of magnitude greater than the inner zone K, or more than seven orders of magnitude lower than the inner zone K. In other words, there is no evidence an outer zone exists and no justification for use of a composite model in the analysis. The sensitivity analysis with respect to static formation pressure is of little value because no information on goodness of fit is provided for the 200 simulations performed, and the analysis was clearly limited by the lower bound specified for the outer zone K. A best-fit simulation could have been performed including static formation pressure and specific storage as fitting parameters, followed by a perturbation analysis to determine parameter sensitivity. Overlooking the question about an outer zone even existing, the analysis presented provides no justification for the relatively narrow range of uncertainty for outer zone K given in Tab. 3-4, and in fact supports an uncertainty range spanning in excess of ten orders of magnitude. The analysis provides no defensible parameter values, although experience from other tests shows that the low recovery observed during the PW indicates a K of less than 1E-13 m/s.

The primary purpose of Test 6 was to collect groundwater samples from the upper Gerstenhübel Beds limestone. Pumping was erratic because transmissivity was too low to support continuous pumping. Periodic measurements of pH and electrical conductivity were made that should have been supplemented by measurements of specific gravity. Specific gravity is important because vertical hydraulic gradients are not defined using freshwater heads, but with environmental heads (Lusczynski 1961) that require knowledge of the vertical distribution of specific gravity. Enachescu et al. (2007) do not provide enough information to determine the effective tubing radius during the SW test. Their analysis may be adequate to determine K within an order of magnitude, but could be improved by using the SW test to estimate K, and then using that K to estimate C_{tz} from the PSR (Pseudo Static Recovery phase). Static formation pressure could also be included as a fitting parameter. The T range estimated by Enachescu et al. (2007) of 3E-9 to 5E-8 m^2/s is probably approximately right, but the question arises as to how that T is distributed over the 3.0 m of Effingen marl and 3.12 m of Gerstenhübel Beds within the test interval. Based on the low K values seen in the other tests for the Effingen Member marl, the Gerstenhübel Beds limestone probably provides virtually all of the T, with a corresponding K of 1E-9 to 2E-8 m/s. This K range partially overlaps, but extends higher, than the range estimated for the Gerstenhübel Beds limestone from Test 2.

In conclusion, the hydraulic testing in the Küttigen borehole and the analyses completed to date provide largely qualitative information about the hydraulic properties of the strata tested. The testing was severely limited by restrictions beyond Nagra's control, and the qualitative nature of the results is all that was expected given those constraints. A summary of defensible K ranges is given in Tab. 3-5. The Gerstenhübel Beds limestone appears to have a K several orders of magnitude higher than that of the Effingen marl, somewhere between 2E-10 and 2E-8 m/s. Reanalysis of the Gerstenhübel Beds tests should allow better determination of its head and better definition of the K range. The Effingen Member marls clearly have low K, probably no higher than approximately 3E-13 m/s, but better estimates would require reanalysis. SIT problems during Test 1 rule out any defensible estimation of hydraulic properties. Little can be concluded about the hydraulic head of the Effingen Member in the Küttigen borehole other than that the lower Effingen and the Gerstenhübel Beds appear to be overpressured relative to a hydrostatic freshwater condition. If less qualitative analysis results are desired, tests 2, 3, 4, and 5 should be given the highest priority for reanalysis, but the restrictive conditions imposed on the testing will limit the gains that can be achieved.

Tab. 3-5: Defensible parameter estimates from Küttigen hydraulic tests: parameter ranges and best estimates [BE].

Test #	**Interval Top** [m bGL*]	**Interval Bottom** [m bGL*]	**Probable K** [m/s] Range, [BE]	**Probable Freshwater Head** [m asl] Range, [BE]	**Comments**
1	209.84	249.99	undetermined	> 390	SIT problems
2	162.00	202.15	2E-10 to 3E-9 [8E-10]	407 to 417 [412]	limestone of Gerstenhübel Beds
3	121.93	162.08	~ 3E-13	undetermined	Reanalysis needed with C_{tz} fixed at known value; head uncertain
4	62.00	102.15	1E-15 to 1E-13 [1E-14]	undetermined	Head unknown
5	37.00	77.15	< 1E-13	undetermined	K estimated from similar responses in other test intervals; no conclusion possible on head
6	163.00	169.12	1E-9 to 2E-8 [4E-9]	undetermined	Gerstenhübel Beds limestone; no head estimate from test without reanalysis

* Ground level (GL) at Küttigen borehole is 374.20 m above sea level (asl).

3.2.3 Oftringen Tests

Hydraulic tests were conducted over ten intervals in the Oftringen borehole. Testing began near the bottom of the hole and progressed upward for the first five tests, which were all performed with a 50.04-m straddle interval. The Test 1 interval included the upper 34.94 m of the Callovian Hauptrogenstein Formation, the 8.6 m of the Herznach and Spatkalk Formations, and the lower 6.5 m of the Oxfordian Birmenstorf Member. Tests 2 through 5 covered different parts of the Effingen Member. Tests 6 through 10 were conducted using a 9.09-m straddle interval. Tests 6 and 10 straddled the same portion of the Geissberg Member, with the primary purpose of Test 10 being to collect water samples. Tests 7 and 8 retested subsections of the Test 2 interval, and Test 9 retested a subsection of the Test 3 interval. The tests were conducted between October 19 and November 5, 2007.

The tests are described in Fisch et al. (2008), along with preliminary nSIGHTS analyses of the tests. The analysis results, consisting of the best estimates and global uncertainty ranges for hydraulic conductivity and freshwater head, are presented in Tab. 3-6. In general, the analysis strategy and implementation were not as efficient as they might have been.

Tab. 3-6: Oftringen Preliminary Analysis Results from Fisch et al. (2008).

Test #	Interval Top	Interval Bottom	K [m/s]			Freshwater Head [m asl]		
	[m bGL*]	[m bGL]	Min.	Best est.	Max.	Min.	Best est.	Max.
1	650.00	700.04	3.3E-12	7.0E-12	1.4E-11	442	456.1	457
2	590.00	640.04	3.6E-13	4.7E-13	5.6E-12	428	433.8	457
3	550.00	600.04	8.0E-13	2.0E-12	4.0E-12	396	410.6	447
4	500.00	550.04	1.8E-14	4.1E-14	2.2E-13	303	390.1	393
5	449.85	499.89	1.9E-14	3.0E-14	3.8E-14	282	383.2	403
6	408.50	417.59	2.4E-8	4.0E-8	2.0E-6	417	432.4	476
7	632.50	641.59	3.3E-14	6.2E-14	8.0E-14	279	383	445
8	621.50	630.59	3.7E-14	6.3E-14	1.4E-13	182	382.5	392
9	583.00	592.09	7.8E-12	1.3E-11	1.3E-11	352	383	414
10	408.50	417.59	7.4E-7	2.5E-6	4.9E-6	382	430.7	454

* Ground level (GL) at Oftringen borehole is 433.0 m above sea level (asl).

Test 1 of the upper Hauptrogenstein Formation, the Herznach and Spatkalk Formations, and the lower Birmenstorf Member comprised six distinct test phases (after the PSR / [Pseudo Static Recovery phase]) over a period of less than 23 hr, which is an inappropriate approach to the determination of transmissivity and hydraulic head in a low-permeability formation. With such a limited time available for testing, no more than two complementary test phases (such as an SW and SWS (in other words, a DST)) should have been conducted to allow time for significant recoveries that might allow definitive determination of hydraulic properties. For this test, the first and last test phases (PW and HIS), which occupied 7 of the 23 test hours, were discarded in the analysis by Fisch et al. (2008) because they couldn't be reconciled with the other test phases. From the plots of the test data, it appears that the pulse tests, and perhaps the SW, were not initiated cleanly, but instead were subject to oscillations, and these procedure-induced early-time transients were not represented properly in the analysis model. The range of K values inferred from the analysis appears reasonable, although the analysis could be improved in many ways. The pulse responses show little evidence that a composite model is appropriate, and specifying, rather than optimizing on, an inner zone radius is ill-advised. A composite fit optimizing on individual sequence derivatives in addition to the Cartesian pressure trace should have been performed. Pulse and slug phases should be presented and matched using a log-log Ramey B plot (Ramey et al. 1975), which is more sensitive to early-time data than the semilog Ramey A plot that was used. Equipment and/or procedure-induced transients should have been treated as history periods rather than included in the simulation periods. Given the limitations of the analysis performed thus far, the range of uncertainty on head is probably greater than that given in Tab. 3-6, perhaps more like 430 to 470 m. Consequently, while the interval is likely to be slightly overpressured, it is not a certainty. Interestingly, the bottomhole interval below the Test 1 lower packer, which consisted of approximately 17.7 m of Hauptrogenstein Formation limestone, showed a stabilized head of approximately 420 m (~ 13 m bGL) by the end of Test 1 (Fisch et al. 2008). One would not expect the bottomhole head to be lower than the head in the Test 1 interval, and yet such a difference is clearly indicated by the responses of the two intervals during Test 1.

Tests 2, 3, and 4 followed a similar pattern of an initial PSR, followed by a PI, an SW, an SWS, and a short concluding PI over total testing times of only 20 to 30 hr. In general, an initial PW would have been preferable over a PI because it would have drawn water into the hole rather than injected residual drilling fines into the formation. Had the PW recovery then been rapid, a second test, such as another PW with a different starting pressure differential, might have been initiated. Given the responses observed during Tests 2, 3, and especially 4, second test phases were not warranted – a single, well-conducted test phase provides more definitive information than a series of short phases largely dominated by wellbore storage and skin.

During Test 2 of the Effingen Member, an SW test was attempted in slim tubing, but the packer isolating the slim tubing from the larger tubing appeared to malfunction. Without knowing the volume in which the water level was rising, no analysis of the SW test can be performed. The SWS test can be analyzed only if C_{tz} is known. The QLR indicates that a C_{tz} of 1.1E-9 Pa^{-1} was estimated from the first PI test and a similar C_{tz} of 1.0E-9 Pa^{-1} was estimated from the second PI test. Therefore, such a value should have been used in the analysis of the SWS test. However, the detailed analysis report makes no mention of the C_{tz} value used, which prevents any evaluation of the accuracy of the K estimates. Difficulties were encountered in simultaneously matching the SWS and PI phases, but there was apparently no attempt to optimize on a composite fit comprising the Cartesian pressure response and the derivatives for the individual phases, which might have been useful. The first PI test was not initiated cleanly, and it is doubtful that procedure-induced transients were treated properly as history. The estimated range of K values is probably reasonable (assuming an appropriate C_{tz} was used), but could be improved through a more comprehensive reanalysis. The reasonableness of the estimated head range is hard to judge without a more concerted effort to optimize on the different test phases. The interval may be normally pressured, or slightly over- or underpressured.

The SW phase in Test 3 of the Effingen Member appeared to proceed appropriately, although the amount of recovery was low. No discussion is given by Fisch et al. (2008) of the critical C_{tz} parameter, although the successful SW phase placed constraints on possible values of K. Difficulties were encountered in simultaneously matching the initial PI and subsequent phases, but there was apparently no attempt to optimize on a composite fit comprising the Cartesian pressure response and the derivatives for the individual phases, which would have been useful. As a result, none of the diagnostic plots for the various phases show particularly good fits. While the estimated K range would likely change little from a more comprehensive analysis, the range of possible heads could be refined. With the current analysis, no conclusion can be drawn about the interval being overpressured, underpressured, or normally pressured. Whatever the head, it is probably less than 25 m from a normally pressured condition.

The initial PI phase during Test 4 of the Effingen Member clearly indicated that an SW would not be an appropriate test phase for this interval; a single PW would have been the best approach to testing. Nevertheless, an SW phase was conducted that could not be analyzed because of too little pressure recovery. In the analysis of Fisch et al. (2008) of the overall test sequence, the measured C_{tz} of 4.3 to 5.0E-10 Pa^{-1} was inexplicably discarded in favor of a "more realistic" value of 8E-10 Pa^{-1}. Even when the fixed parameters, including C_{tz}, were sampled to determine their effects on the analysis, the range of values allowed for C_{tz} excluded the measured values. This decision had the effect of nearly doubling the values of K inferred from the tests. To establish ranges of uncertainty on K and head, Fisch et al. (2008) combined a series of marginally acceptable simulations, all of which fit to only the Cartesian pressure record, sacrificing the better diagnostic and fitting capabilities of the derivatives for each test phase. The test could be reanalyzed using a proper composite fit and an appropriate value of C_{tz}. K is probably on the order of 1E-14 m/s, and the interval appears to be underpressured, but more definitive statements require reanalysis.

Test 5 of the Effingen Member was properly conducted from a conceptual standpoint. The problems with pulse initiation appear to have been properly handled in the analysis. To establish ranges of uncertainty on K and head, Fisch et al. (2008) combined a series of marginally acceptable simulations, all of which fit to only the Cartesian pressure record, sacrificing the better diagnostic and fitting capabilities of the derivatives for each test phase. The test could be reanalyzed using a proper composite fit. K is probably on the order of 1E-14 m/s, and the interval is clearly underpressured (head is less than 400 m asl), but more definitive statements require reanalysis.

Test 6 of the Geissberg Member showed strong evidence of the presence of gas. Calculated C_{tz} values were 1.75E-6 and 1.62E-6 Pa^{-1}, both of which are nearly an order of magnitude higher than the compressibility of gas at the test pressures (2.5E-7 to 2.9E-7 Pa^{-1}). As proposed in the QLR of Fisch et al. (2008), this suggests the presence of gas in the test string during the pulse initiations used to calculate C_{tz}, leading to overestimation of C_{tz}. Gas was apparent in the other test phases as well. Reliable analysis of the test would require measurement of both water and gas flow and use of a two-phase model. The parameter values reported by Fisch et al. (2008) can be given no credence, although it is clear that this interval is several orders of magnitude more conductive than any other interval tested in the borehole.

Test 7 covered a subsection of the Effingen Member tested in Test 2. While the testing procedure followed was appropriate, the equipment designed to maintain the packers at a constant pressure apparently malfunctioned. The observed decrease in packer pressures may have affected the test interval pressure, as well as estimated values of head. As with the other tests, simulations were fit only to the Cartesian pressure record, rather than to a combination of the Cartesian pressure and the Ramey B derivatives for the pulse tests. The reported range for K appears to be reasonable. The reported uncertainty on head is quite large, covering conditions ranging from significantly underpressured to slightly overpressured. Overpressure, however, appears unlikely. The upper uncertainty bound on head is probably more on the order of 425 m asl. Reanalysis could probably provide a more accurate estimate of head.

Test 8 covered another subsection of the Effingen Member tested in Test 2. The testing procedure followed was appropriate, but equipment to maintain the packers at a constant pressure continued to malfunction. No satisfactory fits were obtained from the limited analysis performed by Fisch et al. (2008), which was too concerned with preconceived notions about acceptable ranges of parameter values. The test could be reanalyzed using a proper composite fit including Ramey B derivatives, treating the procedure-induced transients at pulse initiation as history, and not constraining parameter values to preconceived ranges. Ctz, which is discussed only in connection with the QLR and not later analyses, might be allowed to vary within its measured range to improve the overall fit. K is probably on the order of 1E-14 m/s, and the interval appears to be underpressured, but more definitive statements require reanalysis.

Test 9 covered a subsection of the Effingen Member tested in Test 3 that included a limestone bed, identified as the Gerstenhübel Beds limestone in Senger et al (2013), from 585.0 to 587.1 m bGL (Albert and Bläsi 2008) containing a prominent vein filled with calcite, celestite, and pyrite (Waber 2008). The PI phase does not appear to be reconcilable with the following test phases for an unknown reason. While improvements could be made to the analyses presented by Fisch et al. (2008), the uncertainty range on K appears reasonable and defensible. This interval is definitely more conductive than most of the other Effingen intervals tested, and also has a higher C_{tz} (5 to 6E-9 Pa^{-1}), suggestive of either the presence of gas or a compliant vein/fracture. Their estimate of the uncertainty range on head appears to cover values that are too low – a more appropriate range might be 403 to 455 m asl, more similar to the range defined for Test 3. With the current analysis, no conclusion can be drawn about the interval being over-

pressured, underpressured, or normally pressured. Reanalysis should be able to reduce the range of uncertainty on head.

Test 10 covered the same interval as Test 6 and faced the same problems with gas. While the interval is clearly more conductive by several orders of magnitude than any other interval tested in the Oftringen borehole, no credence can be placed in parameter values derived from a single-phase flow model.

In conclusion, the hydraulic testing in the Oftringen borehole and the analyses completed to date provide largely qualitative information about the hydraulic properties of the strata tested. A summary of defensible K and freshwater head ranges is given in Tab. 3-7. Parameter values are best known from Tests 1 and 9 because of the relatively high K (3E-12 to 1E-11 m/s and 8E-12 to 1E-11 m/s, respectively) in those intervals. Test 1 investigated strata from the Hauptrogenstein Formation up into the Birmenstorf Member. The interval is most likely somewhat overpressured relative to a hydrostatic freshwater condition. Test 9 investigated a section of the lower Effingen Member that included the Gerstenhübel Beds limestone layer from 585.0 to 587.1 m bGL[1]. The relatively high K estimated from Test 9 is attributed to the limestone layer rather than to the overlying and underlying marls, and if the estimated T is apportioned only over the 2.1-m limestone interval, the resulting K ranges from 3E-11 to 4E-11 m/s. Tests 2 and 3 appear to have the highest K of the other Effingen test intervals, ranging from 4E-13 to 6E-12 m/s and 8E-13 to 4E-12 m/s, respectively. No determination can be made as to the head in intervals 2, 3, and 9 – they may be normally pressured or slightly under- or overpressured. Tests 4, 5, 7, and 8, show the lowest K values in the Effingen Member, ranging from approximately 1E-14 to 1E-13 m/s, and appear to be underpressured to some degree. Tests 6 and 10 of the Geissberg Member showed it to have much higher K than any other interval tested, but two-phase conditions leave no possibility of defensible parameter estimates, including determination of head. If reduction in the uncertainty associated with the test analyses is deemed warranted, tests 2, 3, 4, 5, 7, 8, and 9 should be given the highest priority for reanalysis.

[1] Depth derived from core documentation (corresponds to 584.5-587.0 m bGL in Tab.3.1).

Tab. 3-7: Defensible parameter estimates from Oftringen hydraulic tests: parameter ranges and best estimates [BE].

Test #	Interval Top	Interval Bottom	Probable K [m/s] Range, [BE]	Probable Fresh-water Head [m asl] Range, [BE]	Comments
	[m bGL*]				
1	650.00	700.04	3E-12 to 1E-11 [7E-12]	430 to 470 [450]	Hauptrogenstein Formation to Birmenstorf Member interval
2	590.00	640.04	4E-13 to 6E-12 [1E-12]	417 to 473 [440]	
3	550.00	600.04	8E-13 to 4E-12 [2E-12]	410 to 457 [430]	Includes 2.1 m of Gersten-hübel Beds limestone
4	500.00	550.04	1E-14 to 1E-13 [4E-14]	undetermined	Probably underpressured
5	449.85	499.89	~ 1E-14	< 400	Underpressured
6	408.50	417.59	High, > 1E-8??	undetermined	Geissberg Member is two-phase system
7	632.50	641.59	3E-14 to 8E-14 [6E-14]	279 to 425 [385]	
8	621.50	630.59	~ 1E-14	< 425	Underpressured
9	583.00	592.09	8E-12 to 1E-11 [9E-12]	403 to 455 [430]	Includes 2.1 m of Gersten-hübel Beds limestone
10	408.50	417.59	High, > 1E-8??	undetermined	Geissberg Member is two-phase system

* Ground level (GL) at Oftringen borehole is 433.0 m above sea level (asl).

3.2.4 Conclusions on Effingen Member Hydraulic Conductivity

The hydraulic tests performed at the Gösgen, Küttigen, and Oftringen boreholes show that the Effingen Member marls have low hydraulic conductivity, less than 1E-12 m/s in most cases, and perhaps as low as 1E-15 m/s. The current test analyses do not indicate that the different depths at which the Effingen Member occurs in the three boreholes affect hydraulic conductivity in any way. All Effingen Member test intervals included at least one limestone sequence identified in Deplazes et al. (2013) (Tab. 3-1). With the exceptions of the intervals containing the Gerstenhübel Beds in the Küttigen (Tests 2 and 6) and Oftringen (Tests 3 and 9) boreholes and KBA4, KBA5 and KBAx in Oftringen Test 2, the current test analyses do not allow any definition of different hydraulic properties between intervals that contained or did not contain limestone sequences. Where a thick Gerstenhübel Beds limestone is present within the Effingen Member (i.e., Küttigen), it has an effective K that may be as high as 2E-8 m/s, indicating that groundwater flow is controlled by fractures. At Oftringen, where the Gerstenhübel Beds are thin, it may have a K of only 3 to 4E-11 m/s. The Gösgen intervals containing the thin Gerstenhübel Beds (Tests 3 and 6) did not show test responses notably different from the other intervals, all of which contained other limestone sequences. The Oftringen Test 2 interval contained approximately 4 m of KBA4, 5 m of KBA5 and 6 m of KBAx, and had an average K over the entire 50.04 m interval of 4E-13 to 6E-12 m/s. If all of the T was attributed to just the 15-m thickness of KBA4, KBA5 and KBAx, the K would be 1E-12 to 2E-11 m/s. If the limestone sequences are consistently more permeable than the marls, the K of the marls is probably less than 1E-13 m/s. Clear evidence for a (unsaturated) two-phase flow system has not been found in the Effingen Member.

The Effingen Member is overlain and underlain by higher conductivity units that, at least locally, contain gas in addition to water. The overlying Geissberg Member at the Oftringen borehole has not been well characterized, but appears to have a two-phase flow system with hydraulic conductivity several orders of magnitude higher than that of the Effingen Member. No testing of the Geissberg Member was performed in either the Gösgen or Küttigen boreholes. No water was observed when drilling through the Geissberg Member at Gösgen, which may indicate that it is much less conductive than it is at Oftringen. The strata below the Effingen Member, from the Birmenstorf Member to the Hauptrogenstein Formation, have not been characterized individually but collectively have higher hydraulic conductivity than the Effingen Member. At the Gösgen borehole, this interval has an average K ranging from 3E-10 to 2E-9 m/s based on single-phase analysis. If, as suggested by the C_{tz} estimate, it is a two-phase system, estimates of K would change. At the Oftringen borehole, the average K is lower, ranging from 3E-12 to 1E-11 m/s, and no gas appears to be present.

3.2.5 Conclusions on Effingen Member Hydraulic Head

The hydraulic head of the Effingen Member has not been well characterized at any location. At the Gösgen borehole, three test intervals covering most of the Effingen Member appeared to be underpressured relative to the water table, while no determination could be made in two other intervals. At the Küttigen borehole, the lower Effingen Member and the Gerstenhübel Beds limestone appear to be overpressured, while no determination can be made for the shallower test intervals. At the Oftringen borehole, three Effingen intervals appeared to be underpressured relative to a hydrostatic freshwater condition to ground surface (no water table has been defined), while no determination could be made in the other intervals. The head in the overlying Geissberg Member cannot be determined from the hydraulic testing performed at the Oftringen borehole, nor can it be determined at the Gösgen borehole where no water was observed in the Geissberg Member during drilling; the absence of observable water may reflect unsaturated conditions and/or low permeability. Water inflow from the Geissberg Member was reported during drilling of the Küttigen-2 borehole (Klump et al. 2008), but because no head measurement was made, the pressure condition at the top of the Effingen Member is not known precisely. The interval from the Birmenstorf Member to the Hauptrogenstein Formation is overpressured in both the Gösgen and (probably) Oftringen boreholes.

Without knowing the pressure/head boundary condition at the top of the Effingen Member at Gösgen and Oftringen, evaluation of head conditions within the Effingen Member is problematic. Several Effingen Member intervals in each borehole appear to be underpressured relative to the water table or a hydrostatic freshwater condition to ground surface. The corresponding heads are below the local and even below the regional discharge level, indicating that the cause of these abnormal heads cannot be attributed to gravity driven groundwater flow. Vinard et al. (2001) showed that stress relief due to mechanical unloading, which may be caused by glacial unloading, denudation, and/or differential erosion, could be the cause of underpressures observed in the low-permeability Helvetic marls at Wellenberg, and Effingen Member underpressures may have a similar explanation. Grauls (1999) discusses a variety of possible causes of abnormal formation pressures such as compaction disequilibrium, lateral strains, dynamic transfers (two-phase flow systems) and thermal or chemical stresses. The compaction disequilibrium (e.g., glacial unloading) and two-phase flow processes may offer plausible explanations for the observed abnormal pressures. A better definition of the head profile from the Hauptrogenstein Formation to the surface, obtained by water-level monitoring in boreholes completed to the units above and below the Effingen Member, as well as improved test analyses that might more precisely define the head in the Effingen test intervals, is needed to investigate this issue more thoroughly.

The overpressured condition of the lower Effingen Member in the Küttigen borehole may be related to the overpressure in the overlying and higher conductivity Gerstenhübel Beds limestone. Although the Birmenstorf Member to Hauptrogenstein Formation interval was not tested at Küttigen, if it is overpressured as it is at Gösgen and Oftringen, the pressure in the lower Effingen may reflect an equilibrium between the underlying units and the Gerstenhübel Beds, which probably derive their high heads from their higher elevation outcrops north of Küttigen (Fig. 3-6). Alternatively, the overpressure may reflect the compressive stress regime of the area, with the low permeability of the Effingen Member preventing the overpressure from dissipating.

Whereas the Hauptrogenstein Formation at Gösgen and Küttigen appears to be directly connected to higher elevation outcrop areas (Fig. 3-2 and Fig. 3-6), which may be the source of the observed overpressures, the Hauptrogenstein Formation at Oftringen appears to be cut off from potential recharge areas by faults (Born anticline; see Fig. 3-7). The observed overpressures may, therefore, be relics from a time before the faulting and/or be related to the compressive stress regime that caused the faulting, with the low permeability of the overlying Effingen Member preventing the overpressures from dissipating.

3.3 Hydrochemical Information

Certain types of hydrochemical information can be interpreted to reach conclusions on the residence time of water in the Effingen Member, as well as on the nature and rate of solute transport through the Effingen Member. In particular, concentrations of the conservative anion chloride (Cl^-), the stable water isotopes ^{18}O and ^{2}H, and the noble gas isotope ^{4}He all provide useful information, as do measurements of diffusion coefficients.

The experimental procedures used to collect hydrochemical information from the Gösgen, Küttigen, and Oftringen boreholes, as well as the analytical results and interpretation, are described thoroughly in Mazurek et al. (2013), from which this report section is adapted.

Chloride data were obtained from analysis of waters collected using multiple techniques:

- aqueous extraction techniques were applied to Effingen Member core samples from the Gösgen KB5a borehole and the Oftringen borehole and to drill cuttings from the Küttigen-1 borehole;
- out-diffusion experiments were performed on four Oftringen core samples;
- advective displacement experiments were performed on single samples from Oftringen and the Gösgen KB5a borehole; and
- groundwater samples were collected from the Hauptrogenstein Formation to Birmenstorf Member interval in the Gösgen SB2 borehole, the Gerstenhübel Beds in the Küttigen-2 borehole, and the Geissberg Member in the Oftringen borehole.

Water isotope (^{18}O and ^{2}H) data were obtained from diffusive exchange experiments performed on core samples from the Oftringen borehole only (water isotope data obtained from the advective displacement experiments on core sample OFT 444.50 are not considered reliable by Mazurek et al. (2013), as well as from the three groundwater samples listed above. ^{4}He data were obtained from outgassing experiments performed on 18 Oftringen core samples, as well as from groundwater sampling of the Geissberg Member in Oftringen.

The *apparent* pore water concentrations of Cl^- obtained from the aqueous extraction and out-diffusion experiments have to be interpreted further to infer representative *in situ* pore water concentrations by adjusting for anion-accessible porosity by applying an adjustment factor to the measured porosity. This takes account of the effect of the so-called 'diffuse layer' in pore water adjacent to the surfaces on the distribution of anionic solutes in the pore water. The resulting *in situ* pore water concentrations and associated uncertainties are highly dependent on porosity data and on assumptions about anion-specific accessible porosity. This anion-accessible (or 'geochemical') porosity effect is particularly marked in low-permeability clay-rich rocks. For example, in the case of the Opalinus Clay at the Mont Terri URL, the factor by which water-loss porosity is reduced to give the anion-accessible porosity factor is x0.5.

The pore water compositions obtained using the advective displacement method are independent of water content and/or porosity, but there is uncertainty as to which portion of the porosity (accessible porosity) is being displaced and sampled, and as to any disturbing effects induced by exerting a high hydraulic gradient to force advective flow through the sample.

Van Loon (2013) conducted two through-diffusion experiments on samples from the Effingen Member at Oftringen (OFT 619.07) and Gösgen (GOS 122.89). Apart from diffusion coefficients (discussed below), porosities specific to the diffusing species (HTO, $^{36}Cl^-$) were obtained from the transient parts of the experiments. On this basis, both samples yielded anion-accessible porosity fractions around 0.5 of the pore space accessible to water.

3.3.1 Gösgen

The Gösgen SB2 borehole in which the hydraulic testing discussed in Section 3.2.1 was performed was percussion drilled and, therefore, no core samples were available for pore water extraction. Ten drillcore samples were collected from the upper 87 m of the Effingen Member in nearby Gösgen borehole KB5a, two of which (GOS 122.89 and GOS 123.71) were conditioned for pore water preservation between core sampling and processing. Because no samples were collected over the lower 154 m of the Effingen Member, samples are not representative of the entire unit. Single drillcore samples were also taken from the Olten (GOS 50.12) and Geissberg (GOS 63.92) Members overlying the Effingen Member in the borehole. A groundwater sample was collected from the lowermost hydraulic testing interval in the Gösgen SB2 borehole, which included Dogger strata (Hauptrogenstein, Varians, Spatkalk, and Herznach Formations) as well as the lower portion of the Malm Birmenstorf Member. The exact groundwater inflow point is unknown. Presumably, it is located in the biodetritic limestone of the Varians Formation and/or the oolitic limestone of the Hauptrogenstein Formation, the latter being known as a heterogeneous, local aquifer in this area.

Aqueous extraction was applied to all of the drillcore samples from Gösgen borehole KB5a using procedures described in Mazurek et al. (2013). Only the preserved samples GOS 122.89 and GOS 123.71 were suitable for determination of *in situ* water- and solute-accessible porosity (ϕ_{WL}); all other samples had been exposed to air for a month before analyses. Therefore, for calculating pore water concentrations from the non-preserved samples, the porosity based on

bulk dry density measurements (ϕ_{phys}) was assumed to be representative of *in situ* physical porosity, increasing the uncertainty associated with the analyses. Only anions were analyzed in the solutions extracted from the samples that had not been fully preserved after sampling because cations might have changed during storage. In addition to the aqueous extraction, an advective displacement experiment was performed on a subsample of the GOS 122.89 sample as described in Mazurek et al. (2013).

Fig. 3-9 shows the estimates of pore water Cl^- concentrations obtained from the aqueou extraction experiments, using an anion-accessible porosity reduction factor of x0.5data, as depth profiles. Extraction data for most of the Gösgen samples have been processed using ϕ_{phys} data, as explained above, and only for the two samples that were preserved, GOS 122.89 and GOS 123.71, are ϕ_{WL} data available. Cl^- concentrations increase markedly with depth, although it must be borne in mind that the data extend only through the upper 36% of the Effingen Member. Two of the samples, GOS 117.38 and GOS 153.31, from the centre and base of the sampled section of the Effingen Member respectively, show the highest pore water Cl^- concentrations, about 15.8 and 15.3 g/L respectively. However, the bulk dry density measurements from which the ϕ_{phys} values have been derived have large uncertainty due to shrinkage of the sample material during drying. This source of uncertainty combined with uncertainty attached to the anion-accessible porosity means that these Cl^- values have to be regarded as only semi-quantitative, though the qualitative trend of increasing Cl^- with depth is probably still valid. Considering, however, that the Cl^- concentration in the strata underlying the Effingen Member is on the order of 5.6 g/L (5600 mg/kg_{H2O}), it is possible that Cl^- concentrations through the entire Effingen Member have an arcuate profile, with concentrations decreasing through the lower, unsampled portion of the unit. Such arcuate profiles are observed in both the Küttigen and Oftringen boreholes (see Sections 3.3.2 and 3.3.3).

The occurrence of high Cl^- concentrations in the middle part of the Effingen Member and lower concentrations in the overlying and underlying strata suggests the Cl^- concentration is controlled by diffusive exchange. Insufficient time has elapsed since the development of the low-salinity conditions currently observed in the aquifers overlying and underlying the Effingen Member for diffusion to create an equilibrated profile. Van Loon (2013) conducted a through-diffusion experiment on sample GOS 122.89, obtaining an effective diffusion coefficient (D_e) value for Cl^- normal to bedding of 3.2E-12 m^2/s.

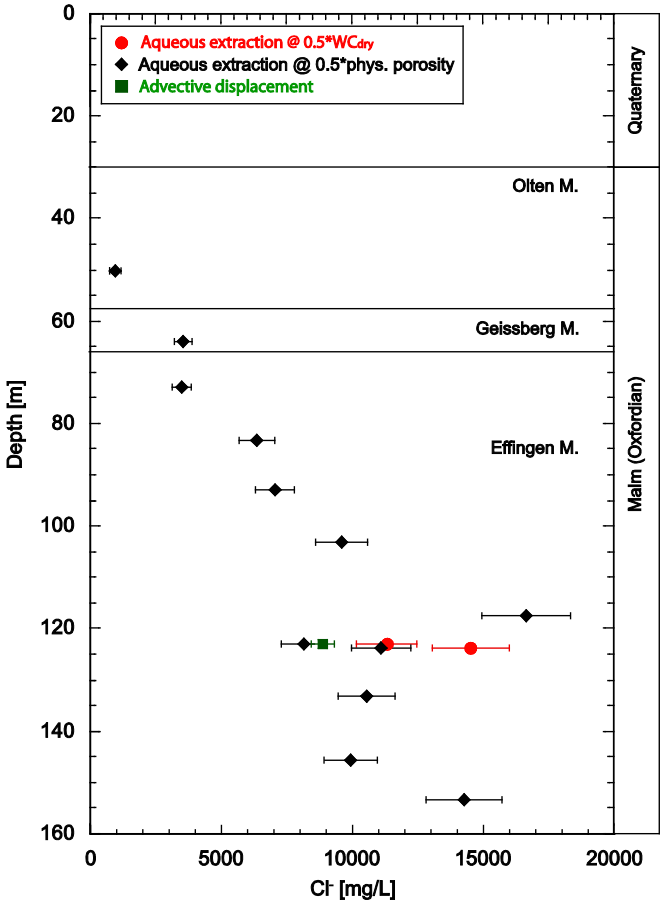

Fig. 3-9: Depth profile for Cl^- in pore waters of borehole KB5a at Gösgen, based on back-calculation of results from aqueous extracts assuming 50% of ϕ_{WL} or ϕ_{phys} is anion-accessible (after Mazurek et al. 2013).

Note that the Effingen Member extends to 307 m, and that Cl^- concentration in underlying Dogger strata is ~ 5600 mg/kg_{H2O}.

3.3.2 Küttigen

Neither of the boreholes drilled at Küttigen was cored, so only drill cuttings from Küttigen-1 are available to provide information on pore water chemistry. Aqueous extractions were also carried out on 9 samples of drill cuttings from the Effingen Member in the Küttigen-1 borehole, but due to uncertain physical and chemical condition and suitability of the samples the reliability of the results is considered to be poor (Mazurek et al. 2013). Reliable porosity measurements were not possible on the drill cuttings and instead porosities could only be estimated from correlations of mineral compositions and inferred lithologies with Effingen Member samples from Oftringen. Only semi-quantitative or qualitative interpretative commentaries are given here so that the indicative information from Küttigen can be taken into account in the general discussion about the Effingen Member.

Isotopic analysis of the Gerstenhübel Beds groundwater from Küttigen-2 gives $\delta^{18}O$ of -7.9 $‰_{SMOW}$ and $\delta^{2}H$ of -60.5 $‰_{SMOW}$ (after extrapolation to uncontaminated conditions (Mazurek et al. 2013)), which place the sample to the right of the global meteoric water line (Fig. 3-10), but significantly different from the position of the pore waters and groundwater sampled in the Oftringen borehole (see Section 3.3.3). It is not possible to distinguish whether

this is due to primary fractionation processes in the source water, to mixing of connate marine water with water with a heavier isotope composition, or to artefacts of the sampling that result in greater uncertainties.

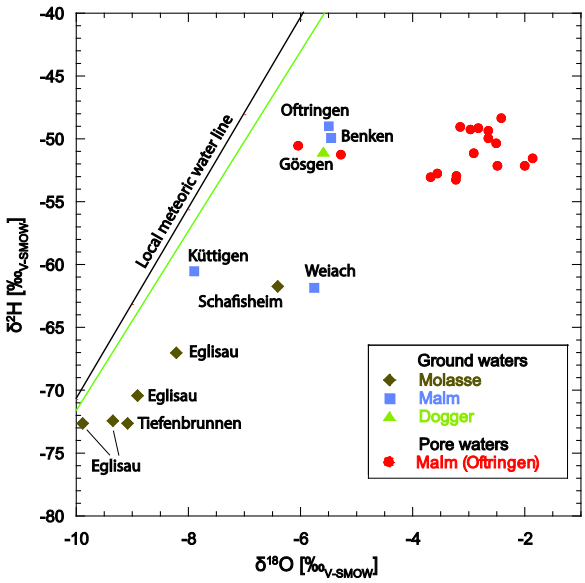

Fig. 3-10: Stable isotopes of water ($\delta^{18}O$, $\delta^{2}H$) in groundwater from the Effingen Member in Küttigen-2 borehole compared with regional pore and groundwater samples from the Dogger, Malm and Tertiary age (from Mazurek et al. 2013).

Overall, the hydrochemical and isotopic data together with the low hydraulic conductivity suggest a long residence time for groundwater in the Gerstenhübel unit of the Effingen Member at Küttigen. As for previous studies of groundwater in the Upper Malm (e.g., Schmassmann 1990; Balderer 1990), the groundwater is interpreted as a mixture of Tertiary brackish to marine water and a component of Tertiary and/or Quaternary meteoric waters. Contributions from brackish water during the Tertiary are also possible. However, there is no evidence of inflow of groundwater from deeper formations such as the Triassic.

3.3.3 Oftringen

Twenty-three intact drillcore samples were obtained and preserved from the Oftringen borehole between the depths of 393 and 648 m: 20 samples from the Effingen Member, 2 samples from the overlying Crenularis Member, and 1 sample from the underlying Birmenstorf Member. Aqueous extraction tests were carried out on all of the preserved drillcore samples. For four of these samples, covering the most important lithologies, aqueous extractions were carried out at four different solid:liquid (S:L) ratios in order to identify the chemically conservative versus reactive behaviour of individual solutes.

Out-diffusion experiments were carried out on four drillcore samples from the Oftringen borehole. The four Oftringen samples tested are distributed across the Effingen Member and include an argillaceous limestone (OFT 438.59) and three sandy-calcareous marls (OFT 501.23; OFT 560.74; OFT 619.07). Pore water concentrations for the reliably conservative anion Cl^- are back-calculated with water-loss porosity and an assumed value for anion-accessible porosity factor, as is done for aqueous extraction results. The out-diffusion experiments also allow

calculation of the Cl^- diffusion coefficient. Using water-loss porosity (4.4 to 9.5%) and an anion-accessible porosity factor of x0.5 in the calculations, the horizontal (parallel to bedding) effective diffusion coefficient, D_e, for Cl^- for the four samples ranges from 1.4E-12 to 5.1E-12 m^2/s, with the lowest value representing the argillaceous limestone sample (OFT 438.59) (Mazurek et al. 2013). Vertical (normal to bedding) diffusion coefficients may be lower still. Van Loon (2013) conducted a through-diffusion experiment on sample OFT 619.07, and obtained a D_e value for Cl^- normal to bedding of 3.1E-12 m^2/s, compared to the value of 4.4E-12 m^2/s parallel to bedding from the out-diffusion experiment.

Fig. 3-11 shows the estimates of pore water Cl^- concentrations obtained from the aqueous extraction and out-diffusion experiments as a depth profile, using the anion-accessible porosity reduction factor of x0.5, and also shows the best estimate of Cl^- from the advective displacement experiment on OFT 444.50. Cl^- concentrations appear to increase slightly with increasing depth in the upper part of the Effingen Member to maximum values at 450 – 500 m depth, below which Cl^- concentrations decrease fairly regularly to minima near and just below the base of the Effingen Member.

Diffusive exchange experiments were performed on 19 drillcore samples from the Oftringen borehole to allow measurement of stable water isotopes. Sixteen of the samples were from the Effingen Member, two were from the Crenularis Member, and one was from the Birmenstorf Member. The $\delta^{18}O$ and δ^2H values of the pore waters are shown in a $\delta^{18}O$-δ^2H diagram in Fig. 3-12 and versus borehole depth in Fig. 3-13. The $\delta^{18}O$ and δ^2H values cluster between about -2 to -4‰ and -45 to -55‰ respectively for all but four samples (Fig. 3-12). All samples plot to the right of the Global Meteoric Water Line (GMWL; Fig. 3-12), and are enriched in the heavy isotopes compared to average Holocene and Pleistocene infiltration. Although the isotope signature of the pore water might have been altered by water-rock interaction and possible other processes (e.g., ion-filtration), the ^{18}O- and ^2H-enriched composition indicate a long residence time for the pore water because all these processes require long time periods or are not known to have occurred during Quaternary times.

The depth distribution of pore water $\delta^{18}O$ values in the Effingen Member is complex and appears to reflect the superposition of several processes (Fig. 3-13). In a 70-m interval below the water-conducting zone in the Geissberg Member, the values fluctuate similarly to Cl^- concentrations (Fig. 3-11). This is followed by a concave profile (relative to ^{18}O-enriched values at top and bottom) between about 480 and 580 m depth before the values become again more negative towards the Birmenstorf Member at about 640 m depth.

The $\delta^{18}O$ and δ^2H values of the pore water show a broadly constant composition versus depth in the Effingen Member with a tendency for slightly lower values at the base of the profile towards the Birmenstorf Member (Fig. 3-13). Isotope compositions of pore water in the Crenularis Formation (samples OFT 393.13 and OFT 399.59) approach that of the Geissberg Member groundwater.

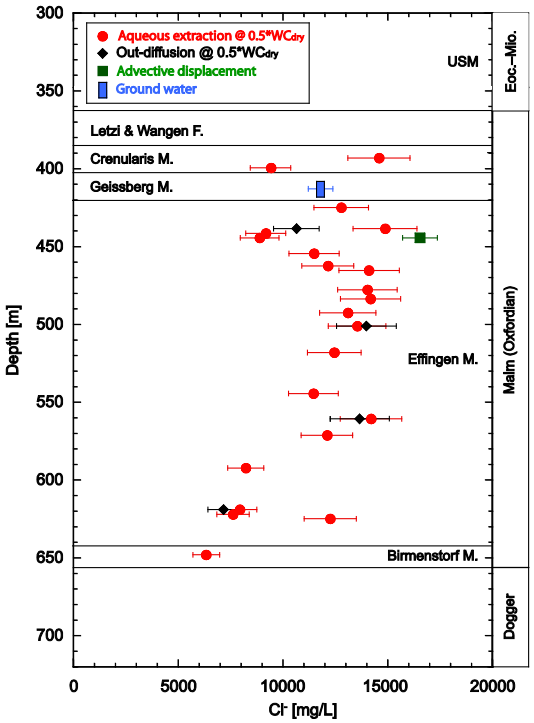

Fig. 3-11: Depth profile for Cl^- in pore waters of the Oftringen borehole, based on back-calculation of results from aqueous extracts and out-diffusion experiments assuming 50% of ϕWL is anion-accessible.

Cl^- concentrations from the advective displacement experiment and from groundwater sampled from the Geissberg Member are also shown (after Mazurek et al. 2013).

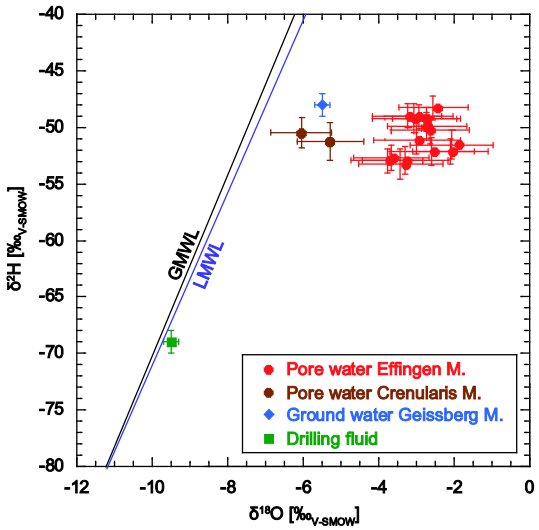

Fig. 3-12: δ^2H – $\delta^{18}O$ diagram of pore-water isotope composition in the Oftringen borehole obtained by the diffusive isotope exchange technique (after Mazurek et al. 2013).

The isotopic composition of the groundwater in the Geissberg Member is corrected for drilling fluid contamination. GMWL: Global Meteoric Water Line; LMWL: Local Meteoric Water Line.

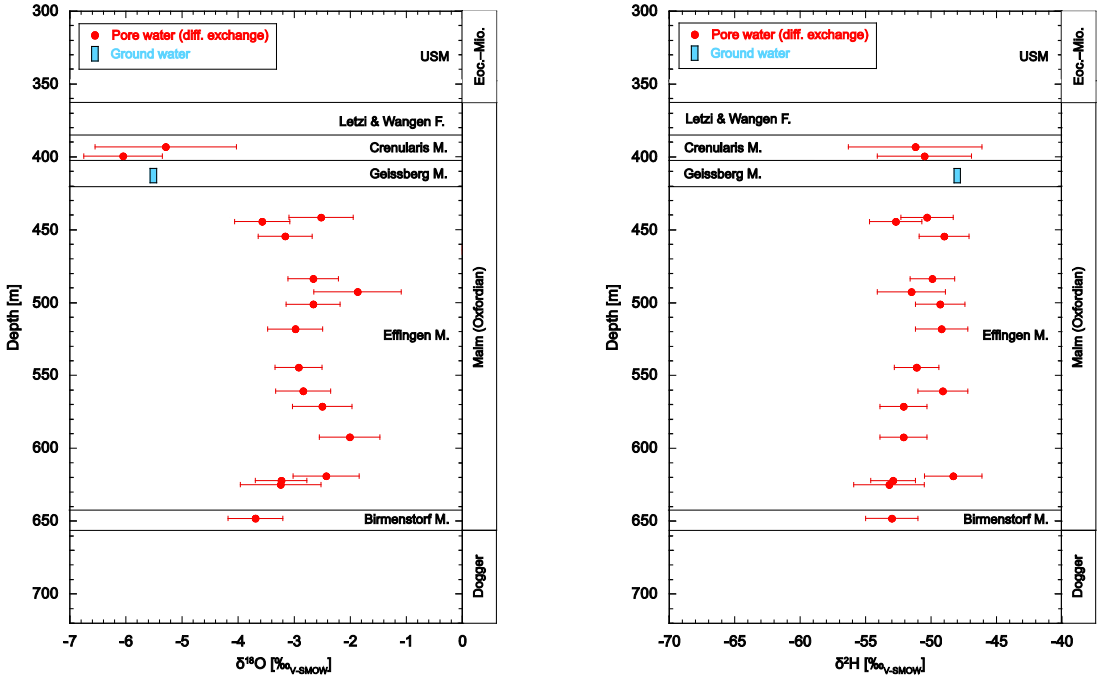

Fig. 3-13: $\delta^{18}O$ and $\delta^{2}H$ of pore water as a function of depth of the Oftringen borehole (after Mazurek et al. 2013).

The isotopic composition of the groundwater in the Geissberg Member is corrected for drilling fluid contamination. Errors are based on linear propagation of analytical uncertainties.

Concentrations of ^{4}He in pore waters of rock samples from the Oftringen borehole vary in a narrow range between 1.0×10^{-4} and 3.3×10^{-4} ccSTP/g_{H2O} (Fig. 3-14). The ^{4}He concentrations in pore water are thus about 4 orders of magnitude above that of air-saturated water (4.65×10^{-8} ccSTP/g_{H2O} at 10 °C).

In general, ^{4}He concentrations measured in pore water from the Effingen Member at Oftringen are similar to or slightly higher than those measured for the Opalinus Clay at Benken (Fig. 3-14). In relation to depth, ^{4}He concentrations show almost no variation within the Effingen Member except for the two uppermost samples, OFT 423.45 and OFT 425.06, which have slightly lower ^{4}He concentrations.

The average ^{4}He concentration in pore water of the Effingen Member rocks is about 2.1×10^{-4} ccSTP $^{4}He/g_{H2O}$. Since the deposition of the rocks about 160 Ma ago the total ^{4}He that was produced and accumulated in the pore water amounts to 2.0×10^{-3} ccSTP $^{4}He/g_{H2O}$, (see also Mazurek et al. 2013). Comparison of this theoretical maximum content of ^{4}He in the Effingen Member pore waters to measured contents indicates that a large proportion (about 96%) of the produced ^{4}He must have been transported out of the rock-water system. This neglects any influx from underlying formations, so the overall flux out of the formation may have been even higher.

The shape of the profile, *i.e.* the essentially straight line, suggests that, in a diffusive system, out-diffusion is fast in comparison to the *in-situ* production rate of He, and that the system is close to or at steady state with respect to loss, influx from below and *in-situ* production of ^{4}He.

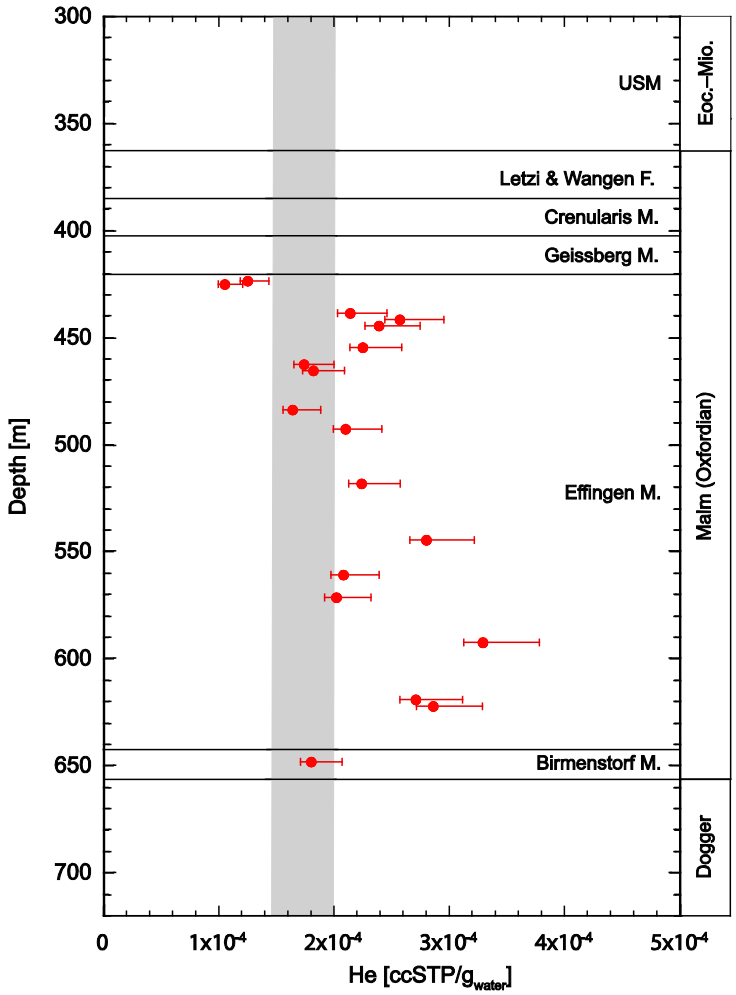

Fig. 3-14: ^{4}He concentrations in pore waters as a function of depth in the Oftringen borehole (after Mazurek et al. 2013).

The grey shaded area indicates ^{4}He concentrations in pore waters of the Keuper–Malm profile in the Benken deep borehole (Nagra 2002). Error bars are -5% and +15%.

3.3.4 Summary and Conclusions of Hydrochemical Information

The Cl^- profiles from the Gösgen and Oftringen boreholes show Cl^- concentrations increasing from the top of the Effingen Member to the middle section, where the Gösgen profile ends. The Oftringen profile shows that Cl^- concentrations decrease from the middle to the bottom of the Effingen Member. Thus, the Oftringen data show, and the Gösgen data are consistent with, an arcuate Cl^- profile from top to bottom. Profiles such as this indicate that diffusion, rather than advection, is the dominant transport mechanism. If significant vertical advection were occurring from the overpressured Hauptrogenstein Formation, the Cl^- in the Effingen Member would be swept upward and a uniform gradient would be established between the Cl^- in the underlying aquifer and the Cl^- in the overlying aquifer. Because the highest Cl^- concentrations are in the middle of the Effingen Member, diffusion must be slowly transporting Cl^- downward into the underlying, low-salinity aquifer and upward into the overlying, low-salinity aquifer.

Pore water $\delta^{18}O$ values from the Oftringen borehole show a nonequilibrium depth profile similar to that for Cl^-, probably reflecting slow diffusional processes rather than advective transport.

The rate of ^4He production within the Effingen Member at the Oftringen borehole and its loss to overlying groundwater appears to have reached a steady-state condition. Development of such a steady-state condition can only occur over a very long (~ Ma) time.

3.4 Summary of Results and Conclusions Regarding the Hydraulic Barrier Function of the Effingen Member

The physical properties of the Effingen Member combine to make it an effective barrier to radionuclide transport. Firstly, the clays in the Effingen Member will sorb most cationic radionuclides, so only transport of nonsorbing radionuclides is of concern. Transport may occur through advection and/or diffusion, but both processes are limited in the Effingen Member by the controlling parameters. Advection is controlled by the hydraulic conductivity, hydraulic gradients, and porosity. Vertical advection is of more concern than horizontal advection, because of the shorter vertical travel distances to release points. In a layered sequence of beds such as the Effingen Member, the average or effective vertical hydraulic conductivity (K_v) is dominated by the layers having the lowest K_v, which appear to be the marls. The higher K limestone layers (KBA and Gerstenhübel Beds) will have little effect on the vertical flow of water. K_v of the marls may be an order of magnitude lower than the horizontal K, or approximately 1E-14 m/s. Hydraulic gradients differ among the three boreholes tested, but are probably irrelevant in any case, as hydraulic conductivities are so low. For K_v of 1E-14 m/s, porosity of 5%, and a unit gradient, a conservative solute would travel only 6.3 m per Ma.

The low hydraulic conductivities, curved Cl^- and $\delta^{18}O$ profiles, and high and uniform ^4He concentrations suggest that diffusion is the dominant solute-transport process in the Effingen Member, and calculated Péclet numbers support this conclusion. Estimated Cl^- D_p values for the Effingen Member are on the order of 1E-10 m^2/s, leading to Péclet numbers much less than 1. Diffusion, therefore, is the dominant transport mechanism. The evolution time of the Cl^- profile cannot be well constrained, but in similar clay-rich low-permeability sequences with similar D_e values, the evolution times were typically between 0.5 and 6.5 Ma (Mazurek et al. 2009). By analogy, this suggests the probability that circulation of groundwater with lower salinity at both upper and lower boundaries (Geissberg Member and Hauptrogenstein Formation units, respectively) of the Effingen Member at these localities was initiated no earlier than the last few millions of years, and diffusive equilibrium through the Effingen Member has still not been established. Diffusion would not, therefore, release radionuclides on a time scale of concern for L/ILW.

4 'Brown Dogger'

The informal term 'Brown Dogger' relates to the suite of generally clay-rich rock units stratigraphically located between the Opalinus Clay and the Malm. In the Geological Atlas of Switzerland, these units are shown in brown colours and occur in the Tabular Jura east of the Aare River and the region Zürich-Nordost-Schaffhausen. The rocks range from claystones to calcareous marls. A comprehensive survey of the available sedimentologic and stratigraphic data base on the 'Brown Dogger' sequence is given in Bläsi et al. (2013) together with an evaluation of the depositional environment in the context of the general basin evolution. Fig. 4-1 presents three litho-stratigraphic profiles of the sequence in WSW-ENE direction (Weiach – Benken – Schlattingen) and in NS direction (Weiach – Triemli/Sonnengarten, Eichberg – Hemmental – Benken), respectively. The rocks of the 'Brown Dogger' are considered as potential host rocks for the geological disposal of L/ILW in the Zürich Nordost and North of Lägern siting areas (see Fig. 1-1) in Northern Switzerland. First investigations of the 'Brown Dogger' as part of the clay-rich sequence of Mesozoic sediments date back to the Sediment Study performed by Nagra in the 1980s (Nagra 1988). Hydraulic testing of portions of the 'Brown Dogger' was performed in the Benken and Weiach boreholes (Nagra 2001; Butler et al. 1989) over a decade ago, and more recently in the Schlattingen-1 borehole (Fig. 4-2).

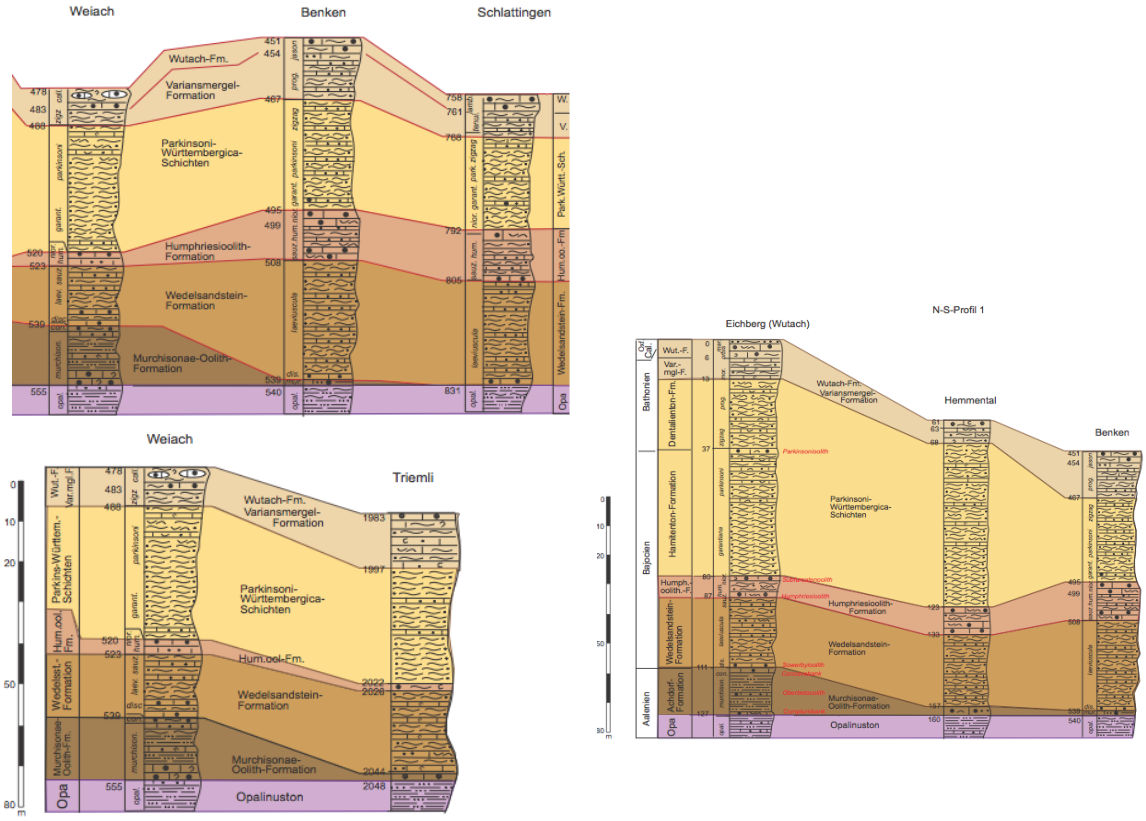

Fig. 4-1: Stratigraphic and lithologic conditions in the clay rock succession of 'Brown Dogger' in northeast Switzerland (modified after Bläsi et al. 2013).

Profiles of the sequence in WSW-ENE direction (Weiach – Benken – Schlattingen) and in NS direction (Weiach – Triemli/Sonnengarten, Eichberg – Hemmental – Benken), respectively.

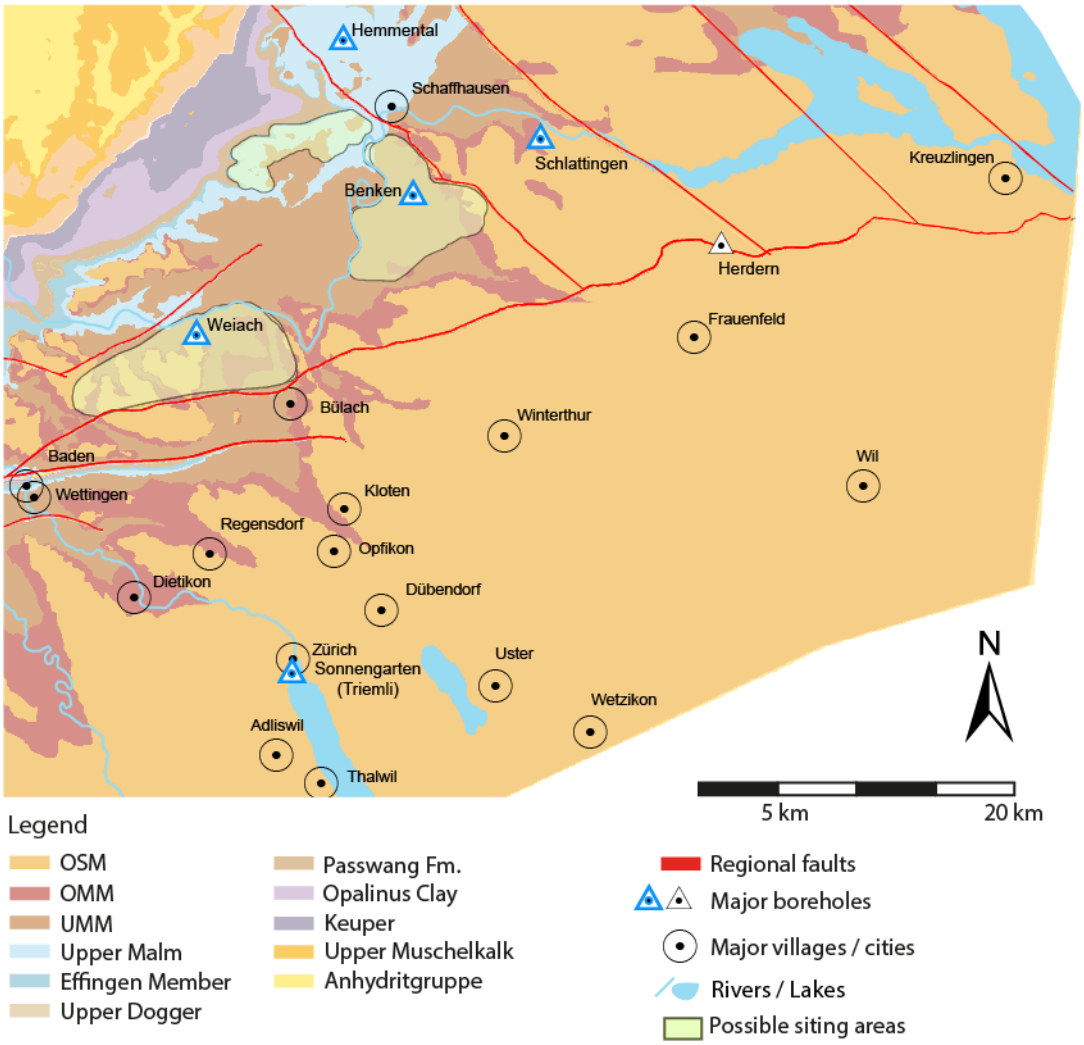

Fig. 4-2: Location of the Zürich Nordost and North of Lägern siting areas and other siting areas for geological disposal of L/ILW in Switzerland.

4.1 Geologic Setting

The Zürich Nordost was selected as a potential siting area for L&ILW because of the absence of known tectonic features and the presence of suitable host rock formations, namely the Opalinus Clay and the 'Brown Dogger', at a suitable depth range (Nagra 2008a). In the area of interest, the 'Brown Dogger' is 60 – 130 m thick at depths of 500 – 790 m below the surface (according to Nagra 2010, Appendix 3) and consists of interlayered calcareous marls to claystones. The Zürich Nordost geological siting area extends over 50 km^2, with the 'Brown Dogger' being considered within most of the siting area (Fig. 4-3). The siting area is located in the Tabular Jura at the northern boundary of the Molasse Basin and is tectonically quiet. The host rock is in a stable setting, with a slight dip to the southeast. This allows considerable flexibility in terms of the layout of the disposal caverns and tunnels. At the Benken borehole, the 'Brown Dogger' includes the Wedelsandstein Formation, a 31-m-thick sandy, marly unit with intercalated limestone and a thin sequence of the Murchisonae-Oolith Formation (Fig. 4-1). The 'Brown Dogger' is approximately 89 m thick (451 to 540 m bGL) at the Benken borehole, and is overlain by approximately 14 m of argillaceous to calcareous marls of the Effingen Member and underlain by 112 m of the Opalinus Clay.

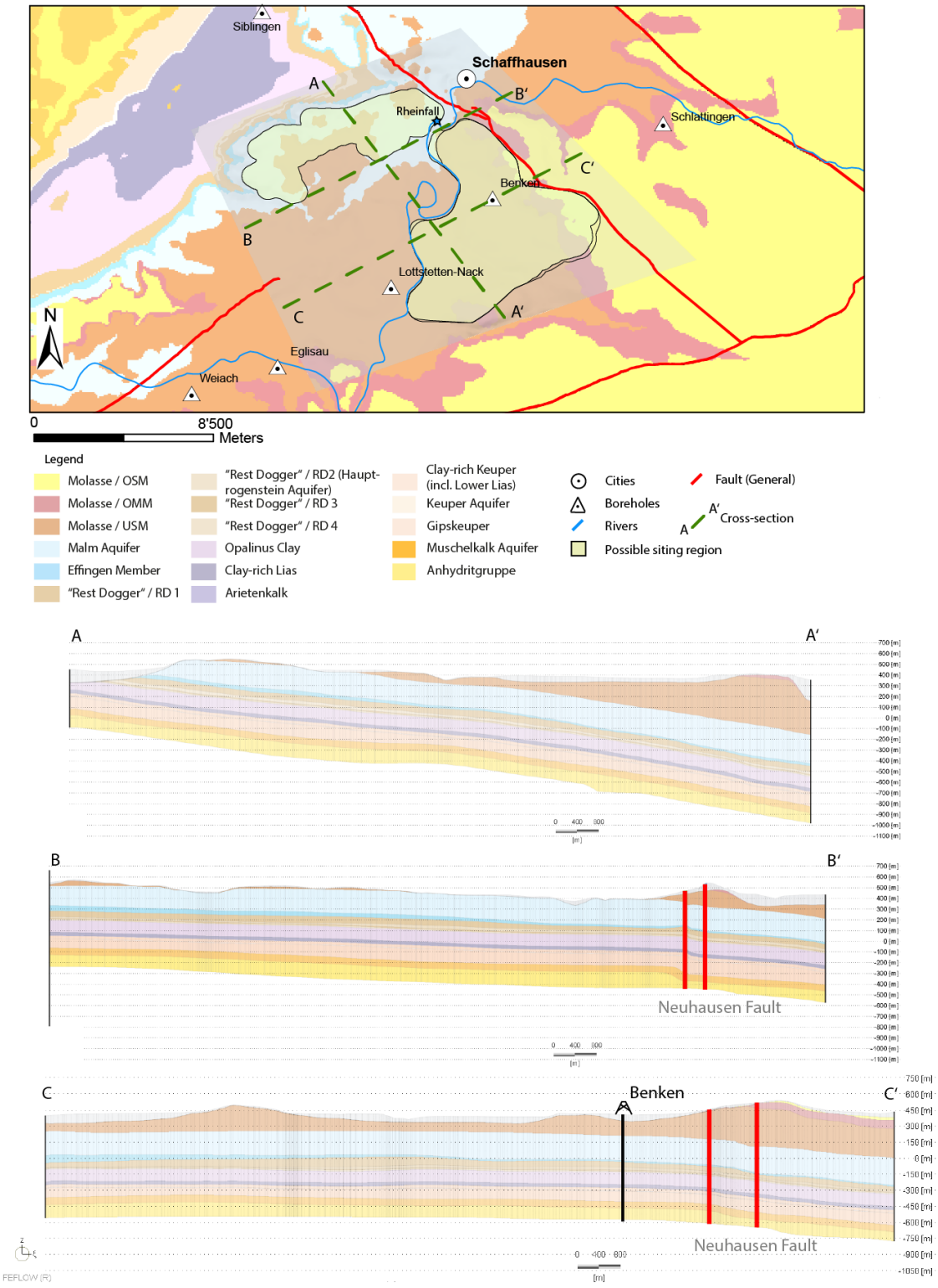

Fig. 4-3: Geological siting area Zürich Nordost for L&ILW.

To the east the siting area is bounded by the NNW-SSE striking Neuhausen fault.

The North of Lägern was selected as a potential siting area for L&ILW because of the absence of known tectonic features and the presence of suitable host rock formations, namely the Opalinus Clay and the 'Brown Dogger', at a suitable depth range (Nagra 2008a). In the area of interest, the 'Brown Dogger' is 60 – 130 m thick at depths of 640 – 850 m below the surface (according to Nagra 2010, Appendix 3). The North of Lägern geological siting area extends over 65 km^2, with the 'Brown Dogger' being considered within most of the siting area (Fig. 4-4). It is located in a region that has partly been tectonically overprinted by the folding of the Jura mountains (precursory folding zone). To the south, the siting area is bound by the Baden-Irchel-Herdern fault (BIH) and to the north by the Ruemi fault. The host rock has areas with largely undisturbed bedding as well as zones with increased tectonic dissection. At the Weiach borehole, the 'Brown Dogger' consists of 76 m of interlayered calcareous marls to claystones from 478.2 to 554.5 m bGL, overlain by approximately 90 m of argillaceous to calcareous marls of the Effingen Member, and underlain by 111 m of the Opalinus Clay.

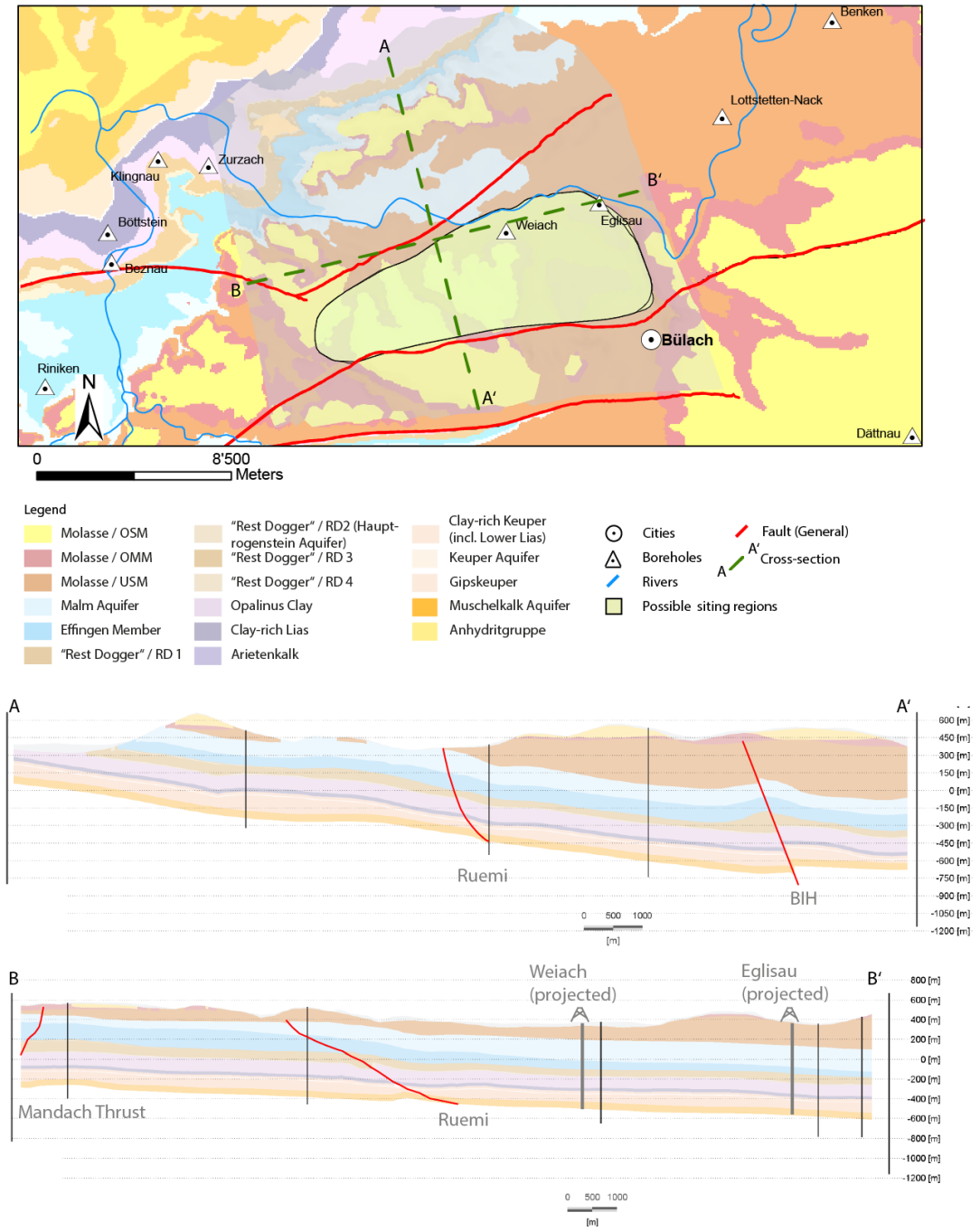

Fig. 4-4: Geological siting area North of Lägern for L&ILW.

The geothermal borehole Schlattingen GTB 1 lies nearly 9 km to the northeast of the Zürich Nordost siting area (Fig. 4-2). The geology at Schlattingen is generally similar to that in the Zürich Nordost siting area, except that units are deeper. Bedding is also offset by a northwest-trending regional fault system (Neuhausen fault) between the Zürich Nordost siting area and Schlattingen-1. The 'Brown Dogger' consists of 84.5 m of interlayered calcareous marls to claystones extending from 757.8 to 842.3 m bGL, overlain by approximately 6 m of limestone and marl of the Birmenstorf Member (absent at Benken and Weiach) and 19 m of calcareous marl of the Effingen Member, and underlain by 107 m of the Opalinus Clay (Fig. 4-5).

4.2 Hydraulic Tests

Hydraulic testing of portions of the 'Brown Dogger' was performed by Nagra in the Weiach borehole in 1983, in the Benken borehole in 1998 – 1999, and in the Schlattingen-1 borehole in 2011. The Weiach and Benken tests have been analyzed and reported previously (Butler et al. 1989; Nagra 2001; Nagra 2002 and references therein), while the final field reporting of the Schlattingen tests has been completed just recently (Reinhardt et al. 2013). The Weiach and Benken test results are summarized below, and the Schlattingen tests and their final field analyses are evaluated in detail. Additional information on 'Brown Dogger' hydraulic heads in the Benken borehole is available from long-term monitoring conducted in multipacker systems installed in the borehole.

4.2.1 Historic Tests at Weiach and Benken Boreholes

In the Weiach borehole, drillstem tests (DSTs) were conducted of the 'Brown Dogger' interval extending from 542.9 to 556.9 m bGL, which included the lower 11.6 m of the Murchisonae-Concava Beds (clay, argillaceous marl, and oolitic sparitic limestone) and the upper 2.4 m of the Opalinus Clay. Butler et al. (1989) reported an estimated average horizontal K of 3E-13 m/s for the interval, assuming that the formation head was at land surface. The observed test response, however, does not support this assumption, and the simulated match to the data is poor. The actual K may be between 1E-14 and 1E-12 m/s, but no more precise estimate can be made, nor can any estimate of formation head be obtained. No tests were conducted in the underlying Opalinus Clay or the overlying Effingen Member.

Numerous hydraulic tests were conducted in the Benken borehole (Nagra 2001). Nagra (2002; see also the references therein) reviewed the final field test analyses, discarded seven for a variety of technical reasons, and reinterpreted seven others. Two of the tests that were judged to be reliable (M4 and MD1) were of intervals that included Malm and 'Brown Dogger' strata (but only 3.37 m of 'Brown Dogger' in the case of M4), while the D2 test included part of the 'Brown Dogger' and the upper part of the Murchisonae Beds considered at Benken to be part of the Opalinus Clay unit. Information on the 'Brown Dogger' tests and other tests relevant to definetion of the low-K buffers above and below the 'Brown Dogger' is given in Tab. 4-1.

The best estimates of K for the two intervals including significant portions of the 'Brown Dogger' ranged from 1.6E-13 to 2.1E-12 m/s, with uncertainty ranges extending from 1.9E-14 to 5.8E-12 m/s (Tab. 4-1). The average K of the D2 test interval is an order of magnitude greater than that of the MD1 interval, perhaps because of the presence of the Wedelsandstein Formation in the D2 interval. Low K was also observed in the lower Malm (test M4, 403.27 to 454.57 m bGL), but not in the M2 interval (379.98 to 394.80 m bGL) or higher intervals. Thus, the low-K buffer above the 'Brown Dogger' extends only into the lower Wohlgeschichtete limestone (~ 400 m bGL) at the Benken borehole. Below the 'Brown Dogger', low K extends through the Opalinus Clay, Lias, and upper Keuper strata until the Stubensandstein is encountered at a depth of 709 m bGL.

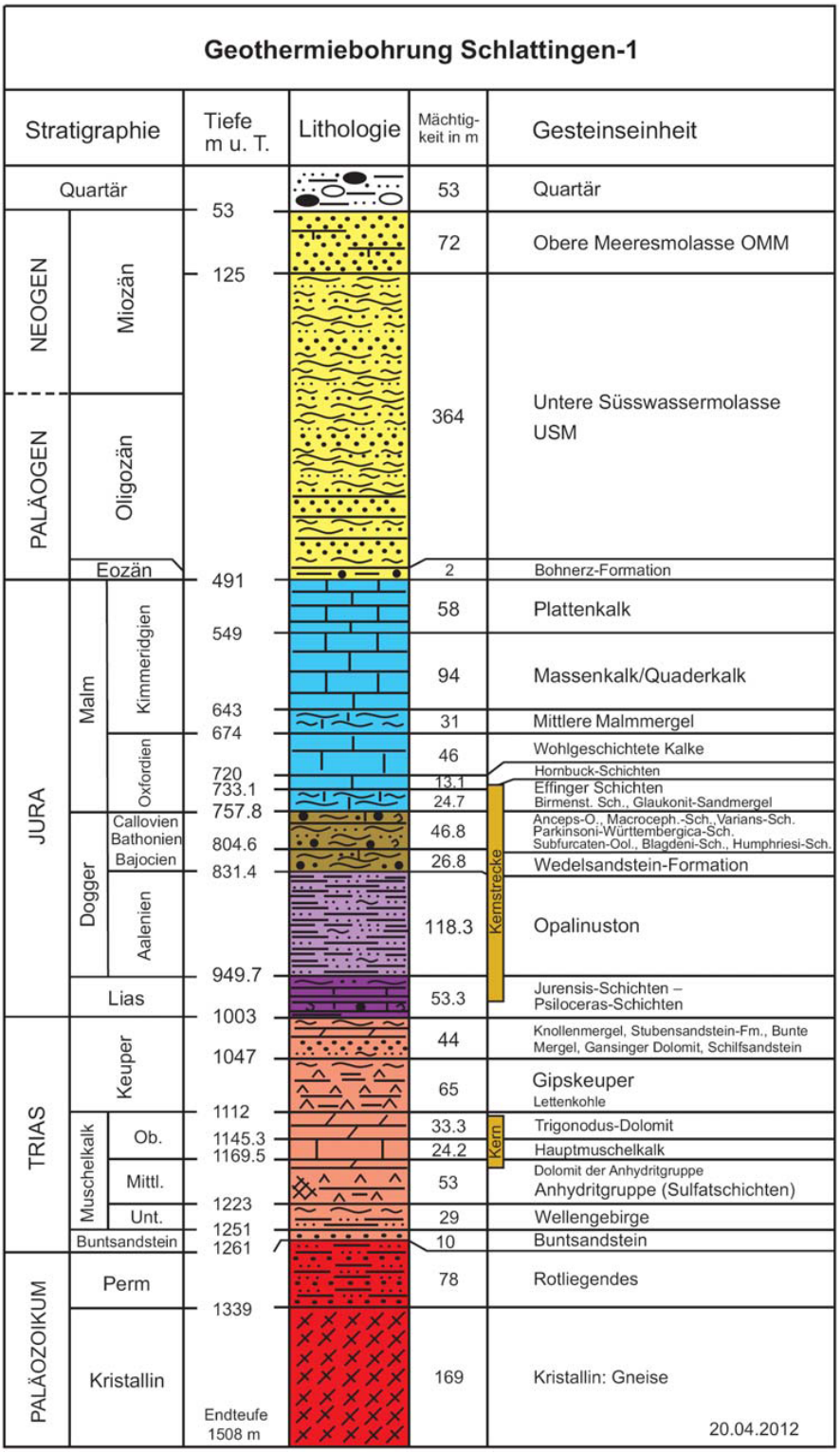

Fig. 4-5: Lithostratigraphical profile of borehole Schlattingen GTB 1 (from Reinhardt et al. 2013).

Tab. 4-1: Benken hydraulic testing results from Nagra (2002; see also the references therein).

Test	Interval Top	Interval Bottom	Strata	K [m/s]			Freshwater Head [m asl]		
	[m bGL[1]]	[m bGL]		Min.	Best est.	Max.	Min.	Best est. [LTM]	Max.
M2	379.98	394.80	Malm: Wohlgeschichtete Kalke	3.4E-10	6.7E-10	3.4E-9	361	393 [< 394]	430
M3	205.28	394.80	Malm: Plattenkalk to Wohlgeschichtete Kalke	4.7E-9	1.1E-8	2.1E-8	359	384	409
M4	403.27	454.57	Malm: Wohlgeschichtete Kalke, Hornbuck, Effingen, Glaukonit-sandmergel; 'Brown Dogger': Anceps, Macrocephalus, Varians	1.2E-14	5.8E-14	7.8E-13	362	388	464
MD1	446.27	497.57	Malm: Effingen, Glaukonitsandmergel; 'Brown Dogger': Anceps, Macrocephalus, Varians, Parkinsoni-Württembergica, Subfurcaten	1.9E-14	1.6E-13	3.9E-13	401	434 [< 400]	501
D2	496.27	547.57	'Brown Dogger': Subfurcaten, Blagdeni, Hum-phriesi, Wedelsandstein Fm; Opalinus Clay	1.0E-12 [1.6E-12]	2.1E-12 [3.4E-12]	5.8E-12 [9.5E-12]	342	380 [< 387]	402
D2-P1[2]	548.8	564.5	Opalinus Clay	-	-	>3.2E-12	-	-	-
O3[3]	544.60	564.50	Opalinus Clay	-	-	>2.5E1-12	-	-	-
O4	566.45	596.50	Opalinus Clay	3.1E-15	1.3E-14	3.1E-14	395	513 [< 381]	535
O5	600.07	603.45	Opalinus Clay	< 1E-15	1.2E-14	3.2E-14	< 390	450 – 650	775
O6	605.13	623.60	Opalinus Clay	4.4E-14	5.8E-14	6.5E-14	400	502	560
O7	623.72	655.70	Dogger to Lias: Opalinus Clay to Jurensis marl	2.0E-14	1.3E-13	1.4E-13	620	691 [< 373]	775
L1	656.78	698.00	Lias to Keuper: Jurensis-mergel, Posidonienschiefer, Numismalis-Amaltheen , Obtusus-Ton, Arietenkalk, Angulaten, Psiloceras, Rhät, Knollenmergel	9.7E-15	4.9E-14	7.3E-13	332	485 [411]	570
K1	698.00	739.22	Keuper: Knollenmergel, Stubensandstein, Bunte Mergel, Gansinger Dol./Hauptstein, Schilfsandstein Fm, Gipskeuper	1.5E-7 [5.4E-7]	7E-7 [2.5E-6]	1.3E-6 [4.7E-6]	459	464 [461]	469

[1] Ground level (GL) at Benken borehole is 404.3 m above sea level (asl).

[2] Bottom hole test D2-P1 terminated prematurely (Nagra 2002). Reliable estimate of upper limit of K-value only.

[3] Test O3 terminated prematurely (Nagra 2002). Reliable estimate of upper limit of K-value only.

K values in brackets represent K if underlined unit is sole contributor to transmissivity. Head values in brackets represent measurements in Baker multipacker long-term monitoring (LTM) system at end of 2011.

Based on the hydraulic test analyses, the Malm and 'Brown Dogger' intervals in the Benken borehole appear to be near hydrostatic equilibrium with freshwater to ground surface, although overpressure is a possibility in the lowermost Malm and uppermost 'Brown Dogger', while the Opalinus Clay intervals appear to be overpressured (Tab. 4-1). However, the uncertainty ranges for the O4, O5, and O6 intervals tested overlap those of the Malm and 'Brown Dogger' intervals, such that those Opalinus Clay intervals cannot be conclusively said to not be in hydrostatic equilibrium with the overlying units. Two intervals in the borehole, the O7 lower Opalinus Clay interval and the K1 Stubensandstein interval, are clearly overpressured relative to a hydrostatic condition, particularly the O7 interval. Why the O7 interval might be so much more highly pressured than the overlying O6 interval or underlying L1 interval cannot be explained unambiguously. The most probable causes for overpressures in the low-permeability intervals of the Opalinus Clay and the clay-rich Lias are borehole closure phenomena associated with the softening of the rock in response to the packer test procedures. On the other hand, test K1 with high conductivity and a head significantly above hydrostatic gives clear evidence for a local aquifer system with artesian conditions. Additional, and in some cases more definitive, information on the hydraulic head of the units penetrated by the Benken borehole has been provided by long-term monitoring, which is discussed in Section 4.2.3.

4.2.2 Schlattingen-1 Tests

Hydraulic tests were conducted in the Schlattingen-1 borehole from February through April 2011. Three test intervals were partially (BD3) or entirely (BD1 and BD2) contained within the 'Brown Dogger', and one interval (M1) extended from the Lower Freshwater Molasse into the Malm limestones. Information about the tests from the final field reports (Reinhardt et al. 2012, 2013) is given in Tab. 4-2, and the tests are discussed in stratigraphically descending order below.

Tab. 4-2: Schlattingen-1 hydraulic testing final field results (Reinhardt et al. 2012, 2013).

Test	**Interval Top**	**Interval Bottom**	**Strata**	**K** [m/s]			**Freshwater Head** [m asl]		
	[m bGL*]	[m bGL]		Min.	Best est.	Max.	Min.	Best est.	Max.
M1	488.00	643.35	Lower Freshwater Molasse, Eocene clay, Malm (Plattenkalk and Massenkalk/Quaderkalk)	1.5E-10	2.6E-10	3.2E-10	400	413	425
BD3	727.00	762.92	Malm: Hornbuck, Effin-gen and Birmenstorf Members; 'Brown Dogger': Anceps, Macro-cephalus, and Varians Beds	3.0E-14	6.2E-14	2.3E-13	421	470	529
BD2	762.00	797.92	'Brown Dogger': Varians, Württembergica, Parkinsoni, Subfurcaten and Blagdeni Beds	1.3E-11	1.3E-11	4.1E-11	429	492	493
BD1	799.25	833.50	'Brown Dogger': Blagdeni Beds, Humphriesi Beds, Wedel-sandstein Fm, Achdorf Fm.	3.3E-10 [4.2E-10]	1.4E-9 [1.8E-9]	1.9E-9 [2.4E-9]	568	606	612

* Ground level (GL) at Schlattingen borehole is 416.6 m above sea level (asl).

K values in brackets represent K if Wedelsandstein Formation is sole contributor to transmissivity.

Test interval M1 (488.00 to 643.35 m bGL) included the lowermost meter of the Lower Freshwater Molasse sandstone, 2 m of Eocene clay, 58 m of Malm/Plattenkalk, and 94 m of Massenkalk/Quaderkalk. The test sequence was appropriate and provided good data. The major uncertainty associated with the testing is the fluid density in the test interval and tubing. The bentonite-based drilling mud was partially circulated out with traced freshwater, but the density and possible variability of the final test-interval fluid is not well known. The numerical analysis of the test in Reinhardt et al. (2012) provides generally reasonable parameter estimates (Tab. 4-2). At present, the only conclusion that can be drawn on head is that it is approximately in hydrostatic equilibrium with a freshwater condition to ground surface; a few meters of underpressure or overpressure are both possible.

Test interval BD3 (727.00 to 762.92 m bGL) included the lower 6.1 m of the Malm Hornbuck limestone, 18.8 m of Effingen Member calcareous marl, 5.9 m of Birmenstorf Member limestone and marl, and 5.1 m of Dogger Anceps, Macrocephalus, and Varians oolitic limestone and silty marl. Inclusion of an SW phase in the testing sequence is questionable given the response observed in the preceding PW phase—the time might have been better spent allowing the PW to recover more fully. The test suffers from the same uncertainty in fluid density described above with respect to test M1. The overall ranges of uncertainty given by Reinhardt et al. (2013) for K and head are unreasonably wide, because they are based on QLR analyses that are not as reliable as the final analysis. K is not likely to differ from the best-estimate value of 6.2E-14 m/s by more than a factor of 2, giving a range of approximately 3E-14 to 1E-13 m/s. A more realistic range for freshwater head is probably from 460 to 485 m asl. Allocation of the interval transmissivity among the stratigraphic units tested is problematic; the limestones might be expected to be more conductive than the marls, but all of the units appear to have K less than 1E-12 m/s.

Test interval BD2 (762.00 to 797.92 m bGL) in the 'Brown Dogger' included 6 m of the oolitic limestone and silty marl of the Varians Beds, 15.5 m of the Württembergica argillaceous marl, 8.4 m of the Parkinsoni oolitic argillaceous marl, 2.1 m of Subfurcaten oolite, and 3.9 m of the Blagdeni oolitic argillaceous marl. The test sequence was appropriate and provided good data. The test suffers from the same uncertainty in fluid density described above with respect to test M1. The numerical analyses of the test in Reinhardt et al. (2013) provide generally reasonable parameter estimates (Tab. 4-2), although the need for a skin in the model is clearly indicated by the mismatch between the data and simulations for all test phases. Reanalysis including a skin could improve on the best-fit parameter estimates, although K would likely not change significantly. The degree of overpressurization of the interval might be estimated more accurately.

Test BD1 was a single-packer test conducted when the bottom of the hole was in the Achdorf Formation (Murchisonae Beds) at a depth of 833.50 m bGL. The test interval was entirely contained in the 'Brown Dogger', and included approximately 5.3 m of the Blagdeni and Humphriesi oolitic argillaceous marls, 26.8 m of argillaceous marls of the Wedelsandstein Formation, and 2.1 m of Achdorf Formation claystone. The interval is clearly overpressured and has appreciable conductivity, as 122 liters of fluid flowed at the surface during the last ~ 200 minutes of the initial COM (compliance) period and the head surpassed the ground surface during all test phases when the SIT was closed.

The BD1 testing sequence involved appropriate phases, altough the PW, SWS, and RWS would ideally have been of longer duration. The SWS was unfortunately disturbed after less than an hour by installation of sucker rods. A C_{tz} of 7.6E-9 Pa^{-1}, which is very high and suggestive of the presence of gas, was estimated from the PW initiation. The presence of gas, and sporadic venting by opening the SIT, would lead to inconsistent behaviour in different test phases,

explaining the difficulties experienced by Reinhardt et al. (2013) in matching the entire test sequence.

Because of inconsistencies observed in the BD1 responses to different test phases, the analysis approach adopted by Reinhardt et al. (2013) was to employ a number of evolving conceptual models as the phases progressed. Different parameters were specified and fit for different test phases, providing a wide range of possible values. The overall test response hints at pressure depletion, suggesting a limited system or the venting of the readily accessible gas. The parameter ranges proposed by Reinhardt et al. (2013) are reasonable, given the major uncertainties remaining in the analyses. In any case, K is relatively high compared to the other 'Brown Dogger' test intervals and freshwater head is well above ground surface.

In conclusion, the only interval tested in the Schlattingen-1 borehole that had an average horizontal K less than 1E-11 m/s was the BD3 interval, which covered the lower 30.8 m of the Malm and the upper 5.1 m of the 'Brown Dogger'. The average horizontal K of the BD3 interval appears to be between 3E-14 and 1E-13 m/s. The BD1 and BD2 intervals covered all but 2.25 m (797.00 to 799.25 m bGL) of the remainder of the 'Brown Dogger', and have average horizontal K values of 1E-11 m/s or greater. The Malm limestones tested in interval M1 had similar K, being between 1E-10 and 4E-10 m/s.

All of the test intervals containing 'Brown Dogger' appear to be overpressured relative to a hydrostatic condition, with the degree of overpressurization probably increasing with depth. The BD1 interval containing the WedelsandsteinFormation appears to be particularly overpressured. Head in the Malm limestones is uncertain, but likely within ~ 10 m of a hydrostatic condition.

A summary of defensible K and freshwater head ranges is given in Tab. 4-3.

Tab. 4-3: Defensible parameter estimates from Schlattingen-1 hydraulic tests: parameter ranges and best estimates [BE].

Test #	**Interval Top**	**Interval Bottom**	**Probable K** [m/s] Range, [BE]	**Probable Fresh-water Head** [m asl] Range, [BE]	**Comments**
	[m bGL*]				
M1	488.00	643.35	1.5E-10 to 3.2E-10 [2.6E-10]	400 to 425 [413]	
BD3	727.00	762.92	3E-14 to 2E-13 [6E-14]	460 to 485 [470]	
BD2	762.00	797.92	1.3E-11 to 4.1E-11 [1.3E-11]	429 to 493 [492]	Head uncertainty could probably be reduced by including skin in analysis
BD1	799.25	833.50	3E-10 to 2E-9 [1E-9]	568 to 612 [606]	Anomalous test responses lead to wide uncertainty in head

* Ground level (GL) at Schlattingen-1 borehole is 416.6 m asl.

4.2.3 Long-Term Monitoring in the Benken Borehole

Subsequent to the hydraulic testing in the Benken borehole, a Westbay multipacker system was installed in the borehole in 1999 to allow long-term monitoring (LTM) of nine intervals (see Nagra 2002 and references therein). Due to concerns about the performance of the Westbay system, it was removed in 2009 and replaced with a 7-packer Baker system that allows monitoring of 8 zones (Fig. 4-6). A preliminary evaluation of the performance of the Baker system was carried out by Baechler et al. (2011), comprising a comparison of the temporal evolution of the long-term monitoring data before and after the removal of the Westbay system. Fig. 4-7 shows the heads measured at the end of 2011 using the Baker multipacker system (black symbols) along with the head estimates derived from the hydraulic test analyses (red lines and symbols). At the end of 2011 (Jäggi & Schwab 2012), heads were stable in the high-K Muschelkalk (400 m; Z8) and Stubensandstein (461 m; Z7; logger failed 29/11/2011) intervals, as well as in the Lias (411 m; Z6; logger began to fail 29/9/2011). Head was approximately 394 m in the Malm Wohlgeschichtete Kalke (Z1) and was declining at a rate of approximately 0.8 m/a, head in the Wedelsandstein Formation (Z3) was approximately 387 m and declining at a rate of approximately 1.8 m/a, head in the 'Brown Dogger' – Varians and Parkinsoni-Württembergica Beds (Z2) was approximately 400 m and declining at a rate of approximately 2.6 m/a, and heads in the two Opalinus Clay intervals were approximately 381 m (Z4), declining at a rate of approximately 6.7 m/a, and 373 m (Z5), declining at a rate of approximately 8.4 m/a. The Rhinefalls near the village of Neuhausen represent a potential discharge area of the Malm aquifer with a local discharge level of 359 m asl. In this context, the hydraulic significance of the Neuhausen fault to the east of Benken may need further consideration as it represents a potential flowpath towards the Rhinefalls.

Thus, the monitoring with the Baker multipacker system confirms the best estimates of head for the Malm (M2), 'Brown Dogger' (Wedelsandstein Formation; D2), and Keuper (Stubensandstein; K1) test intervals listed in Tab. 4-1. With respect to the Malm-Dogger (MD1) test interval, either the Varians-Parkinsoni-Württembergica Z2 monitoring interval has a lower head than other strata contained in the thicker MD1 test interval, or the test analysis has overestimated head; the Z2 interval is clearly not overpressured, but is slightly underpressured. The long-term monitoring does not support the overpressures interpreted for the Opalinus Clay test intervals, but instead shows the Opalinus Clay to be underpressured. With respect to the Lias (L1) test interval, either the Numismalis-Amaltheen-Obtusus-Arietenkalk Z6 monitoring interval has a lower head than other strata contained in the thicker L1 test interval, or the test analysis has overestimated head; the Z6 interval is only slightly, if at all, overpressured.

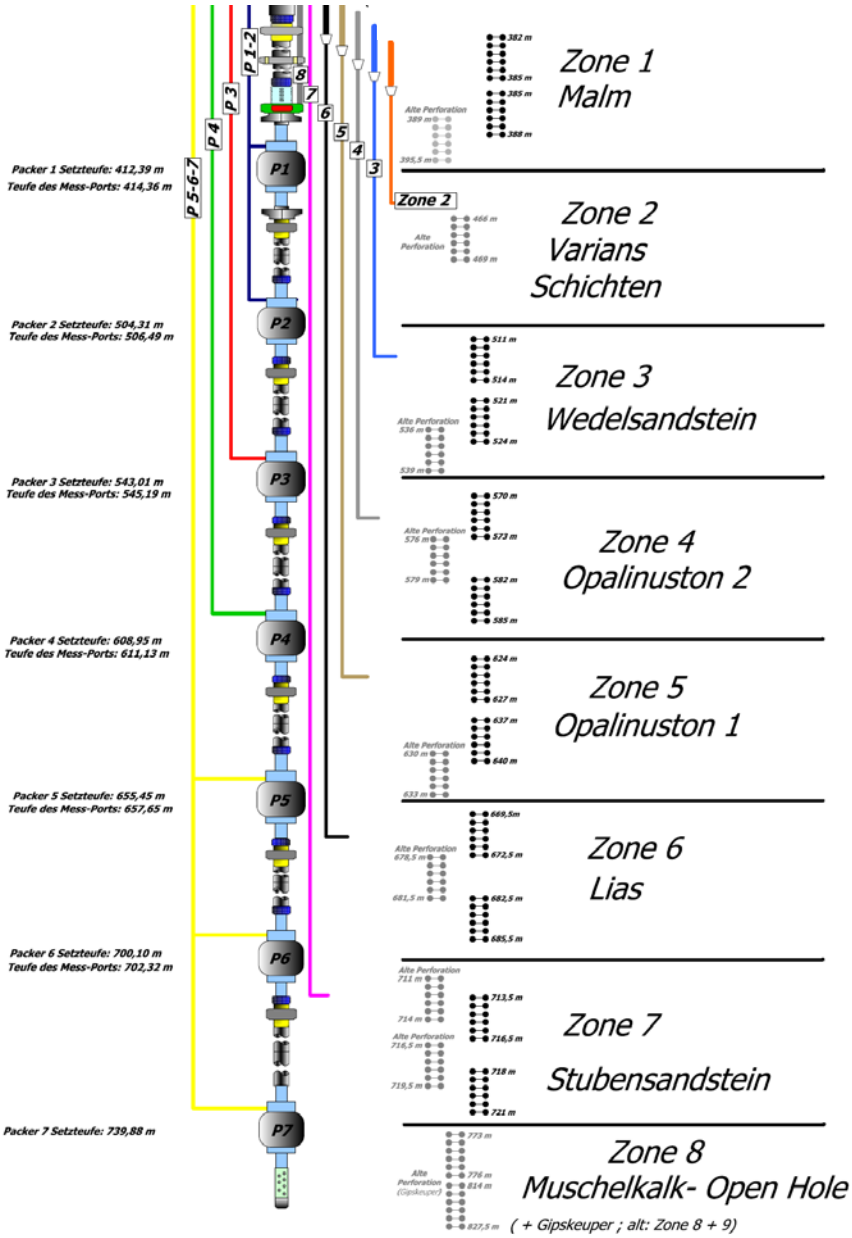

Fig. 4-6: Baker multipacker long-term monitoring system in the Benken borehole.

Packer positions, monitoring intervals and perforation intervals. The "old" perforation intervals correspond to the monitoring intervals of the previous Westbay system, which was removed in 2009.

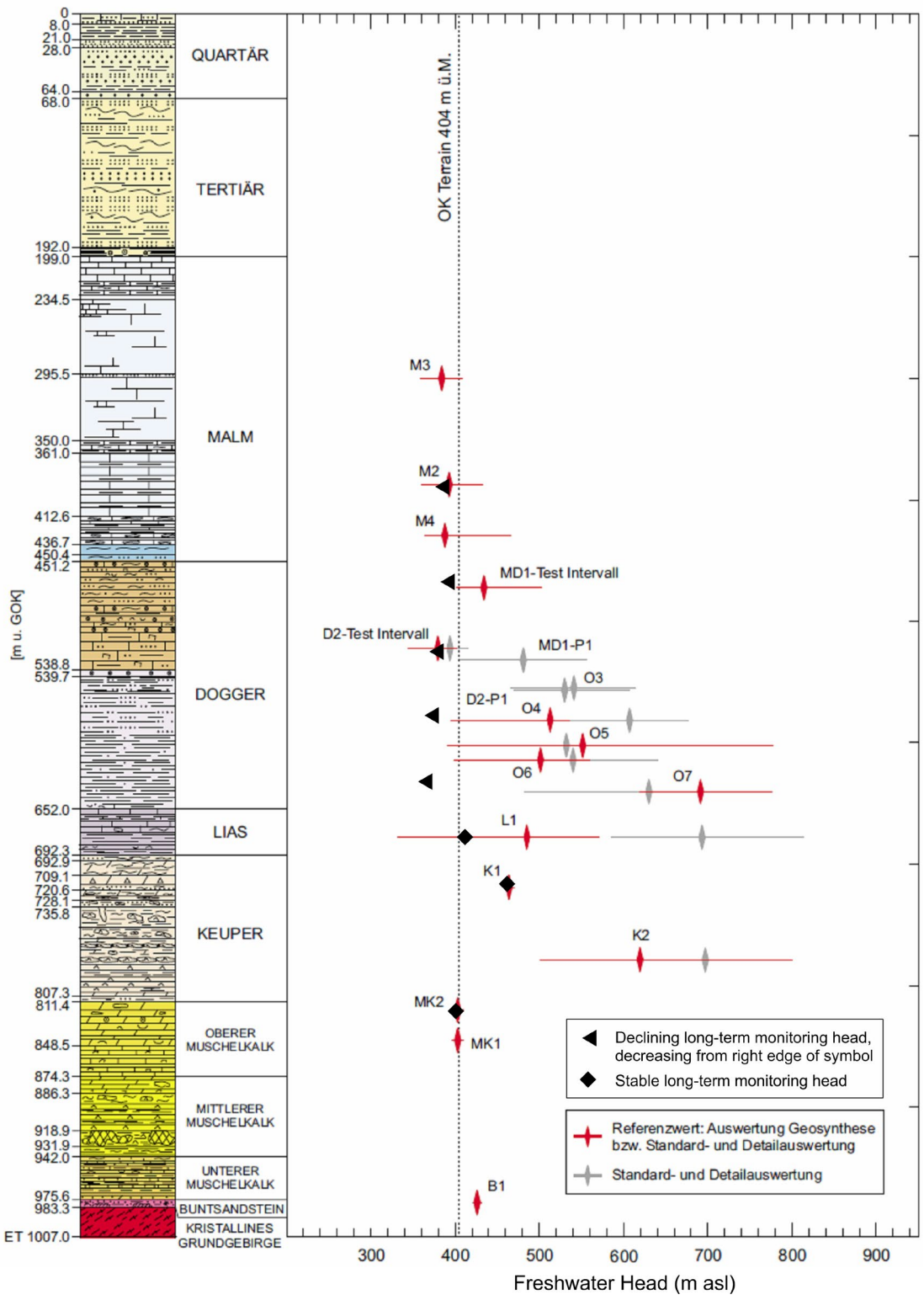

Fig. 4-7: Benken freshwater heads estimated from hydraulic tests and long-term monitoring at end of 2011.

These conclusions depend, of course, on the proper isolation of the intervals being monitored. The Baker packers are installed in perforated casing that is cemented in the borehole. The cement may have sufficient permeability to transmit pressure from one interval to another, leading to erroneous conclusions on interval pressures. If the interval heads ultimately stabilize at different values that will provide evidence that the cement is not providing a leakage pathway. On the other hand, the response of the long-term monitoring system on a pressure perturbation (e.g., removal of the Westbay packer system and substitution by the Baker system) may give evidence for a possible leakage along the cement liner. It would be expected that the monitoring interval highest interval transmissivity controls the pressure recoveries in the adjacent intervals. As shown in Baechler et al. (2011), the pressure recovery after the exchange of the LTM system does not indicate any obvious correlation between the different monitoring intervals. In particular, the Z3/Wedelsandstein recovers to a higher pseudo-static formation pressure than the low-permeability intervals Z4 and Z5, representing the Opalinus Clay formation. This is a clear indication, that the test intervals are properly isolated and leakage along the cement liner is not a major issue. In any case, the long periods required for heads to stabilize provide evidence of low permeability.

Another possible explanation for the discrepancies between heads estimated from the hydraulic testing and those measured by the Baker LTM system is osmotic effects. The discrepancies all occur in low-permeability, clay-rich strata. Neuzil (2000) has shown that if wells are completed in this type of geological environment with the water in the well having a lower total dissolved solids (TDS) concentration than the native pore water, osmosis will cause water to flow from the well into the formation until it is balanced by an equal hydraulic flow from the formation into the well and osmotic equilibrium is obtained. The resulting underpressures in the well will persist until diffusion causes equilibration of TDS between the well and the formation. Osmotic effects seem a less likely explanation of the apparent underpressures the longer the pressures continue to decline. Furthermore, laboratory measurements on core samples have shown that the osmotic efficiency of the Opalinus Clay is fairly low.

Among the possible causes of abnormal formation pressures discussed in Grauls (1999), the compaction disequilibrium (e.g., rebound in response to glacial unloading) and the impact of lateral (tectonic) strain offer the most likely explanations for the observed abnormal pressures in the clay-rich sequences of the Opalinus Clay, the 'Brown Dogger' and the Lias. The hypothesis of compaction disequilibrium also explains the discrepancy between packer testing and longterm monitoring, suggesting that mechanical and chemico-osmotic loading and unloading phenomena associated with the drilling process, packer testing and the subsequent placement of the well casing could lead to long-lasting perturbations of pore pressure around the borehole. In this sense, the evolving underpressures in the Opalinus Clay formation may indicate a glacial rebound phenomenon, similar to the interpretation of the underpressures in the Wellenberg site.

4.2.4 Conclusions on 'Brown Dogger' Hydraulic Conductivity

The hydraulic conductivity of the 'Brown Dogger' appears to show significant spatial variability. At Benken (and probably Weiach), 'Brown Dogger' K appears to be between 2E-14 and 6E-12 m/s, whereas at Schlattingen-1, it appears to be between 3E-14 and 2E-9 m/s. The interval from the lower Malm ("Wohlgeschichtete Kalke" limestone in Benken, Hornbuck Beds in Schlattingen-1) to the Varians Beds in the upper 'Brown Dogger' has a best-estimate K of 6E-14 m/s in both boreholes. The intervals containing most of the 'Brown Dogger' above the Wedelsandstein Formation have higher, and different, average K's: 1.6E-13 m/s (Benken test MD1) and 1.3E-11 m/s (Schlattingen-1 test BD2). Higher 'Brown Dogger' K at Schlattingen compared to Benken persists into the Wedelsandstein Formation. If we assume that the transmissivity in the Benken D2 test interval and in the Schlattingen BD1 test interval is

attributable largely to the Wedelsandstein Formation, the Wedelsandstein K at Benken would be between 1.6E-12 and 9.5E-12 m/s, while at Schlattingen it would be between 4.2E-10 and 2.4E-9 m/s.

With the exception of the Wedelsandstein Formation, little differentiation of hydraulic properties can be made for the stratigraphic units composing the 'Brown Dogger'. The hydraulic testing intervals were too long, encompassing too many units, and were too few in number to allow conclusions to be drawn about the hydraulic properties of the Anceps, Macrocephalus, Varians, Württembergica, Parkinsoni, Subfurcaten, Blagdeni, and Humphriesi Beds individually. Collectively, their K appears to be between 1E-14 and 5E-11 m/s at the Benken and Schlattingen-1 boreholes. It is uncertain, however, how representative the 'Brown Dogger' properties at the Schlattingen-1 borehole are with respect to the Zürich Nordost and North of Lägern siting areas. If only the Benken borehole is considered, upper 'Brown Dogger' K may only range from 1E-14 to 4E-13 m/s.

4.2.5 Conclusions on 'Brown Dogger' Hydraulic Head

At the Benken borehole, estimates of 'Brown Dogger' head from the hydraulic-test analyses seem to present an inconsistent picture. The uppermost 'Brown Dogger' interval (M4) could be underpressured, normally pressured, or overpressured, while the next lower interval (MD1), containing a larger portion of the 'Brown Dogger', appears more likely to be overpressured. In contrast, the interval below containing the Wedelsandstein Formation (D2) appears to clearly be underpressured. The long-term monitoring, however, shows that the Varians beds (Z2) contained within the MD1 test interval are underpressured, not overpressured, while confirming that the Wedelsandstein Formation is underpressured.

According to the terminology of causal mechanisms for overpressures introduced by Grauls (1999), this discrepancy could be explained in several ways. In the clay-rich and low-permeability sequences the overpressures estimated from the hydraulic test analyses could reflect interactions of the clay minerals in contact with the synthetic porewater testing fluid (chemical stresses), borehole closure (compaction disequilibrum caused by the drilling/testing procedures), incomplete temperature equilibration (thermal stresses), or simply analytical error. The lower pressures indicated by the long-term monitoring could reflect compaction dis-equilibrium caused by geological processes (e.g., glacial rebound, uplift) and/or osmotic effects due to natural salinity gradients. Possible leakage through the cement behind the well casing cannot be excluded, but is less likely, because the interval heads ultimately seem to stabilize at different values, suggesting that the cement is not providing a leakage pathway (see also discussion in Chapter 4.2.3). In any case, the long periods required for heads to stabilize provide evidence of low permeability.

The sub-hydrostatic heads in the calcareous sequences of the Wedelsandstein Formation, which were consistently observed during the packer test campaign and in the long-term monitoring system, cannot be explained in a satisfactory way by compaction disequilibrium. Two alternative hypotheses are presented here:

- discrete water conducting features in the calcareous sequences in the Wedelsandstein Formation are well connected with the local discharge areas (e.g., Rhinefalls near Neuhausen; elevation: 360 m asl). The discharge paths could be formed via a connection with the Malm aquifer. Alternatively, the Neuhausen Fault could act as a regional hydraulic feature which allows along-flow towards its intersection point with the Rhine valley near Neuhausen.

- assuming that the recently observed underpressures in the clay-rich formations of the 'Brown Dogger', Opalinus Clay and Lias can be attributed to the action of post-glacial rebound, it is conceivable that the water-conducting features in the calcareous sequences of the Wedelsandstein Formation simply reflect the actual underpressures in the clay sequences above and below. Notably, this hypothesis would imply that the water-conducting features in the Wedelsandstein Formation are poorly connected to the local / regional aquifer systems, because otherwise, the underpressures would have been dissipated rapidly.

At the Schlattingen-1 borehole, the entire 'Brown Dogger', and especially the Wedelsandstein Formation are overpressured, while the upper Malm limestones are near normally pressured. The generally higher 'Brown Dogger' heads at the Schlattingen-1 borehole together with the elevated hydraulic conductivity of hydraulic test BD1 suggest that the hydraulic head in the carbonate rich sequences of the 'Brown Dogger' (Wedelsandstein Formation) is controlled by the recharge areas to the north with elevations > 650 m asl (Southeastern Black Forrest, east of the valley of river Wuttach). In this context, the Neuhausen Fault to the west and the Randen Fault to the east may act as hydraulic features of regional extent, which allow along-flow but prevent cross-flow (sealing faults), thus separating efficiently the hydraulic regime in the siting area Zürich Nordost from the conditions east of the Neuhausen Fault.

4.3 Hydrochemical Information

Information on 'Brown Dogger' pore water chemistry is available only from the Benken and Weiach boreholes. Isotopic compositions of pore waters from the Benken borehole were determined by applying vacuum-distillation and diffusive-exchange methods to core samples (Rübel & Sonntag, referenced in Nagra 2002). Meier & Mazurek (2011) developed a Cl^- profile for the Weiach borehole from the middle of the Keuper to the top of the Malm strata by applying aqueous extraction techniques to remove salts that had precipitated in core samples.

The data and interpretations of the data from Benken are presented in Gimmi & Waber (2004) and Gimmi et al. (2007). Gimmi & Waber (2004) created profiles of $\delta^{18}O$ and $\delta^{2}H$ (Fig. 4-8), Cl^- (Fig. 4-9), and $\delta^{37}Cl$ (Fig. 4-10) through all the strata sampled in the Benken borehole. From modelling, they concluded that the measured stable water isotope profiles seemed to be influenced mainly by diffusive exchange with the underlying Keuper aquifer; no signature of advective flow could be detected. The evolution time is of the order of 0.5 to 1 Ma, with a possible range of about 0.2 to 2 Ma. Fractionation of Cl isotopes occurs during diffusive transport. Applying Cl^- diffusion coefficients determined by Van Loon & Soler (2004) for the Opalinus Clay at Benken to the entire stratigraphic sequence, Gimmi & Waber (2004) concluded that the observed Cl and $\delta^{37}Cl$ data do not contradict the interpretations made in the analysis of the profiles of stable water isotopes, but they also cannot be used to clearly corroborate those findings. The simulation of the Cl and $\delta^{37}Cl$ data requires additional parameters and boundary and initial conditions, which are unknown and, especially for $\delta^{37}Cl$, not easily inferred from geologic history or from process understanding.

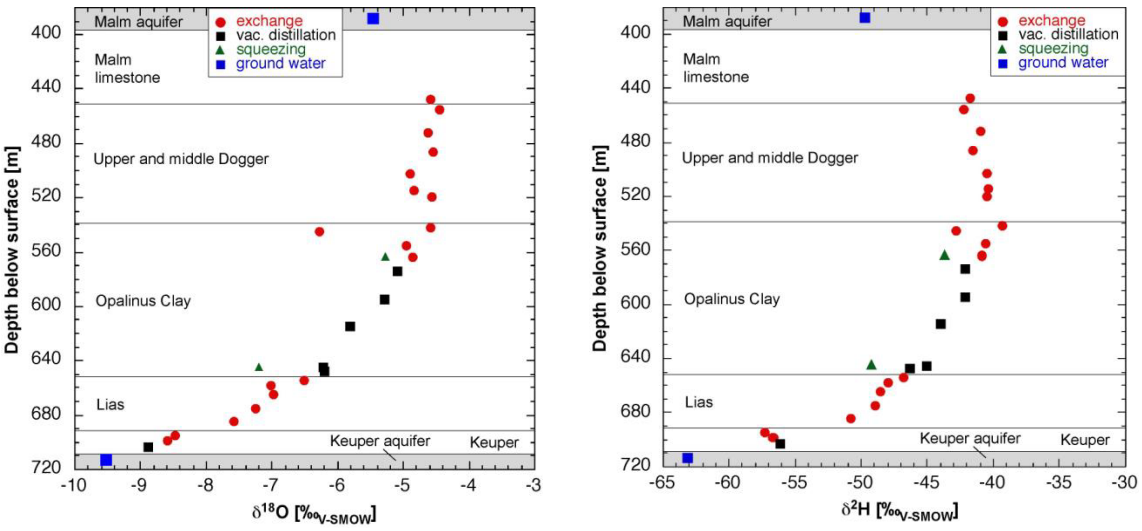

Fig. 4-8: Profiles of $\delta^{18}O$ and $\delta^{2}H$ in the pore water from the Benken borehole (Mazurek et al. 2011).

Data from Rübel & Sonntag and Waber et al., as referenced in Nagra (2002). Opalinus Clay includes the Murchisonae Beds.

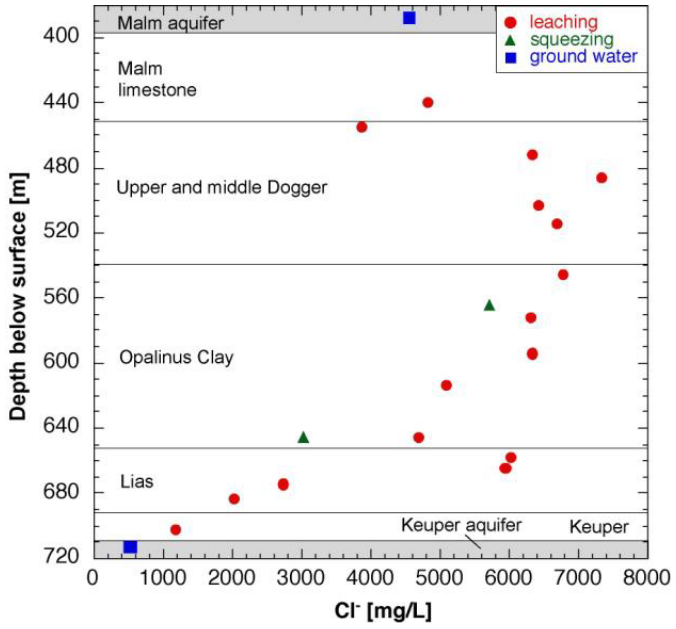

Fig. 4-9: Profile of chloride concentrations of the pore water (mass of chloride per volume of Cl-accessible water) from the Benken borehole (Mazurek et al. 2011).

Data from Gimmi & Waber (2004). Opalinus Clay includes the Murchisonae Beds.

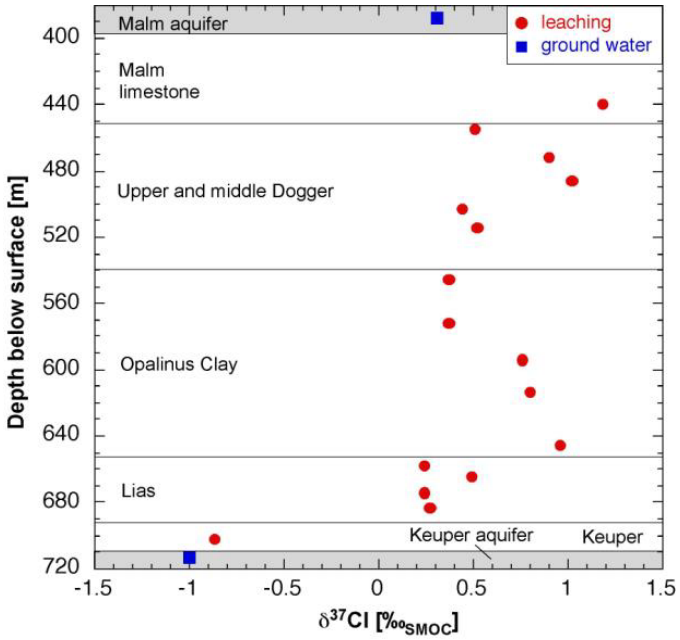

Fig. 4-10: Profile of $\delta^{37}Cl$ in the pore water and groundwater from the Benken borehole (Mazurek et al. 2011).

Data from Gimmi & Waber (2004). Opalinus Clay includes the Murchisonae Beds.

The Weiach Cl^- profile developed by Meier & Mazurek (2011) shows well-defined depth trends (Fig. 4-11). The groundwater sample taken in the Malm fits well with the pore-water data from the underlying units. Cl^- content increases with depth and then remains at 5000 to 6000 mg/L down to the base of the Malm. Cl^- contents decrease in the Opalinus Clay ($\leq$ 4000 mg/L), followed by higher values in the Lias and Keuper. No reliable data are available from the lower part of the Keuper, but the Cl^- content must decrease sharply in order to reach the low value of the Muschelkalk groundwater. The steepness of the profile in this lowermost part tends to suggest that either the freshening within the Muschelkalk aquifer is a geologically young feature, or that diffusion coefficients are very low in the lower Keuper. Some constraints on the times involved could be obtained by transport modelling.

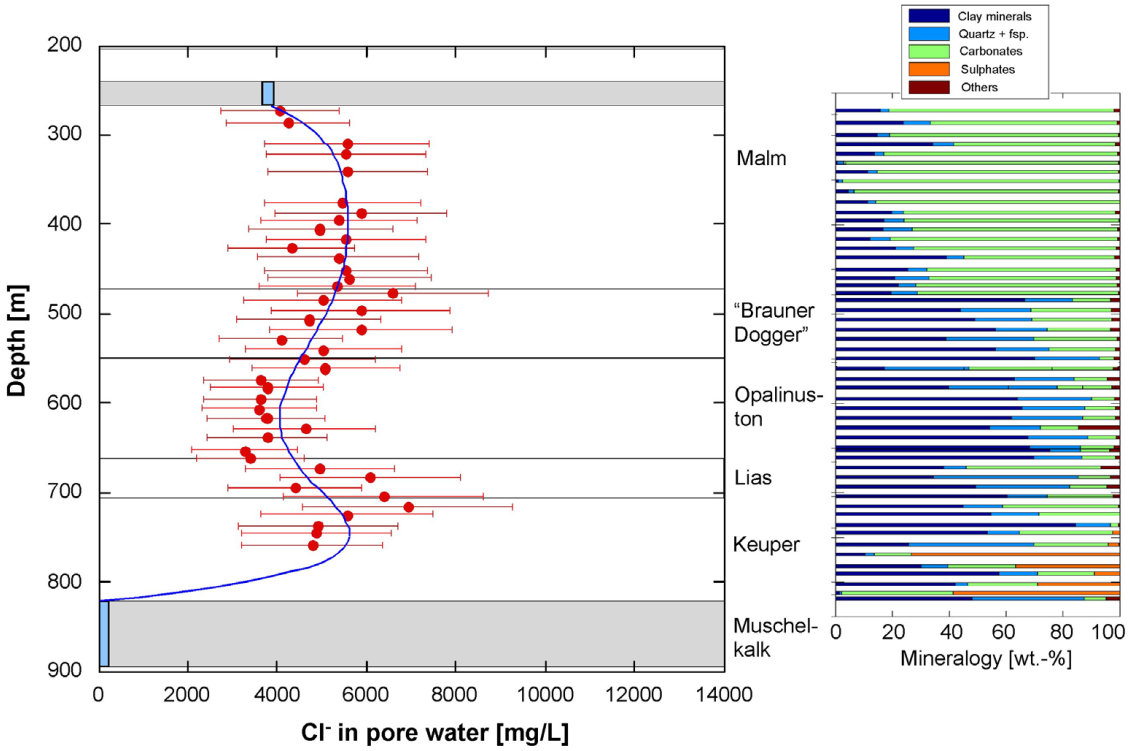

Fig. 4-11: Screened Cl- profile for Weiach using porosity derived from clay-mineral content for the recalculation to pore-water concentrations.

The fraction of anion-accessible porosity was assumed to be 0.5 for rocks with >10 wt.-% clay-mineral content and 1 for ≤ 10 wt.-% clay-mineral content. Only the screened data set is shown, together with a polynomial fit.

4.4 Summary of Results and Conclusions Regarding the Hydraulic Barrier Function of the 'Brown Dogger'

The hydraulic conductivity of the 'Brown Dogger' appears to be generally lower at Benken (and probably Weiach) than at Schlattingen-1. Only test D2 in Benken may indicate a moderate enhancement of the effective K values, if the interval transmissivity (best estimate: ~ 1E-10 m^2/s; see also Tab. 4.1) is attributed to the calcareous sequences of the Wedelsandstein Formation. Given that the Benken borehole lies in the middle of the Zürich Nordost siting area whereas the Schlattingen-1 borehole lies nearly 9 km to the northeast of the siting area across the Neuhausen Fault, the test results from Schlattingen-1 appear to be of minor relevance to the suitability of the 'Brown Dogger' to host a repository for L/ILW in the Zürich Nordost (or North of Lägern) siting area. 'Brown Dogger' K appears to be typically between 2E-14 and 6E-12 m/s at the Benken (and probably Weiach) borehole. For the clay rich sequencies, the K values are comparable with the hydraulic conductivity in the Opalinus Clay (typically ≤ 1E 13 m/s), whereas slightly enhanced K values (typically 1E-11 – 1E-12 m/s) may be expected in the calcareous sequences of the Wedelsandstein Formation. At Schlattingen-1, hydraulic conductivity appears to be between 1E-11 and 2E-9 m/s.

Characterization of the strata above and below the 'Brown Dogger' is also much more complete at Benken that it is at either Weiach or Schlattingen-1. The low-K buffer above the 'Brown Dogger' extends approximately 50 m into the Malm (lower Wohlgeschichtete Kalke) at the Benken borehole. Below the 'Brown Dogger', low K extends 170 m through the Opalinus Clay, Lias, and upper Keuper strata until the Stubensandstein is encountered at a depth of 709 m bGL. At the Weiach borehole in the North of Lägern siting area, the low-K buffer above and below the 'Brown Dogger' probably includes approximately 90 m of overlying argillaceous to calcareous marls of the Effingen Member and 111 m of the underlying Opalinus Clay, along with some thickness of Lias and upper Keuper strata. At Schlattingen-1, little can be said other than that low K extends above the 'Brown Dogger' through at least the lower 31 m of the Malm.

The 'Brown Dogger' at the Benken borehole is, according to long-term monitoring, slightly underpressured, whereas at the Schlattingen-1 borehole, the entire 'Brown Dogger', and especially the Wedelsandstein Formation, is overpressured. Possible causes for the abnormal pressures are discussed in greater detail in Chapter 4.2.5. The generally higher 'Brown Dogger' heads at the Schlattingen-1 borehole may indicate that the borehole is in a different hydrogeological regime, controlled by the recharge areas in the Black Forest, whereas the heads of the calcareous sequences of the Wedelsandstein Formation in the Benken borehole may be governed by the local discharge conditions. In this context, the Rhinefalls via the Neuhausen Fault (discharge level: 360 m asl) and the outcrops near Bad Zurzach (discharge level: 330 m asl) are considered as potential discharge areas. On the other hand, the abnormal pressures in the clay-rich sequences of the 'Brown Dogger', both overpressures and underpressures, are clear indicators for the excellent hydraulic barrier function of the host rock in vertical direction, confirming that hydraulic conductivities are so low that vertical advection is insignificant. It can be concluded that only the calcareous sequences of the 'Brown Dogger' (e.g., Wedelstandstein Formation) may represent potential pathways for lateral advection towards the local discharge areas. The relevance of these hypothetic pathways is limited due to the low overall transmissivity of the carbonate rich sequencies in the 'Brown Dogger' and due to the moderate lateral head gradients in the siting regions.

Consistent with the measured low K of the 'Brown Dogger', stable water isotope data suggest that vertical solute transport through the entire low-K Malm-to-Keuper sequence at Benken is dominated by diffusion, with no evidence of advection. The evolution time of the stable isotope profiles is of the order of 0.5 to 1 Ma, with a possible range of about 0.2 to 2 Mio years. Diffusion would not, therefore, release radionuclides from a repository in the 'Brown Dogger'on a time scale of concern for L/ILW.

5 Opalinus Clay

In the central and eastern part of Northern Switzerland, the Opalinus Clay has a thickness of 80 to 140 m and consists of a monotonous sequence of dark grey, silty, micaceous clays which were deposited 180 Ma ago in a shallow marine environment (Aalenian age). In the Zürich Nordost siting region, the uppermost sequences of the Aalenian, the so-called Murchisonae Beds, are accounted as part of the host rock formation. The Opalinus Clay has been classified as a moderately overconsolidated claystone that has been formed by a complex burial and compaction history with two distinct periods of subsidence. In the Molasse Basin, the formation reached a burial depth of about 1000 m during the Cretaceous. A period of uplift of the area in the mid-Tertiary was followed by subsidence in the late Tertiary, when the Opalinus Clay reached its greatest burial depth of about 1700 m below the surface. From about 10 Ma ago, alpine uplift and erosion brought the Opalinus Clay progressively up to its present burial depth. In its burial history, the Opalinus Clay in the central and eastern part of Northern Switzerland has experienced maximum temperatures in the range of 75 to 90°C.

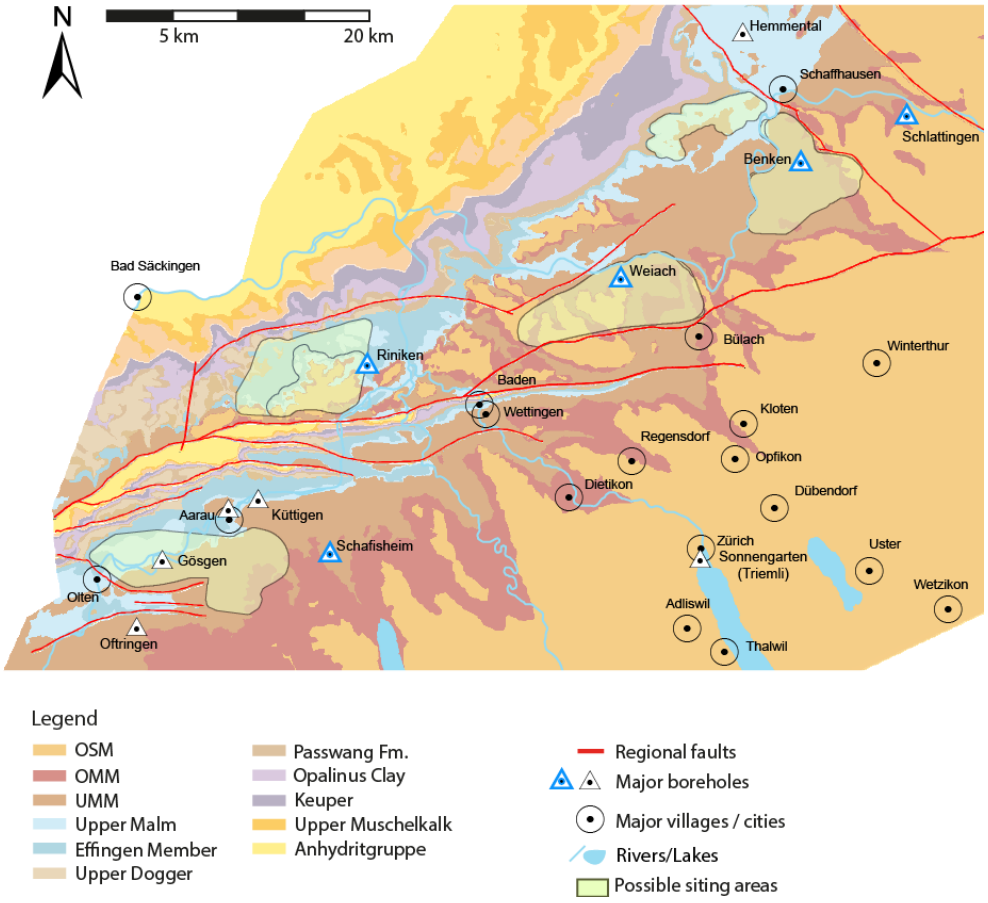

Fig. 5-1: Locations of the siting areas for geological disposal of L/ILW and/or HLW in Switzerland.

Adapted from Nagra (2008)[2]. Locations of Opalinus Clay boreholes discussed herein are shown in blue.

[2] The nomenclature of the potential siting areas has recently been updated: Zürcher Weinland → Zürich Nordost, Nördlich Lägern → North of Lägern, Bözberg → Jura Ost.

The Opalinus Clay is being considered as a potential host rock for the geological disposal of L/ILW in the Jura-Südfuss and Südranden siting areas, and for the disposal of both L/ILW and HLW in the Jura Ost, North of Lägern, and Zürich Nordost siting areas in Northern Switzerland (see Fig. 1-1). First investigations of the Opalinus Clay date back to the Sediment Study performed by Nagra in the 1980s (Nagra 1988). Hydraulic testing of portions of the Opalinus Clay was performed in the Riniken borehole at the eastern margin of the Jura Ost siting area (Belanger et al. 1989), in the Schafisheim borehole northeast of the Jura-Südfuss siting area (Moe et al. 1990), and in the Benken borehole in the Zürich Nordost siting area (Nagra 2001) over a decade ago (Fig. 5-1). Nagra (2002) provides a comprehensive synthesis of the hydrogeological investigations of the Opalinus Clay carried out in the Benken borehole in 1998 and 1999.

5.1 Geologic Setting

The Opalinus Clay is considered a potential host rock for the geological disposal of L/ILW and/or HLW in five siting areas in the eastern Tabular Jura and in the eastern sub Jurassic zone: Jura-Südfuss (L/ILW), Südranden (L/ILW), Jura Ost (L/ILW and HLW), North of Lägern (L/ILW and HLW), and Zürich Nordost (L/ILW and HLW). The Jura-Südfuss siting area lies close to the Folded Jura at the northern boundary of the Molasse Basin, and is therefore partly subject to strong tectonic stress, which is expressed visibly in some of the regional structures. The siting area was selected because of the absence of known tectonic features and the presence of a suitable host rock, the Opalinus Clay. The Opalinus Clay is between 65 and 105 m thick, and occurs at a depth of 490 to 700 m below ground surface in the siting area (according to Nagra 2010, Appendix 3). The Jura-Südfuss geological siting area extends over 65 km^2, with the Opalinus Clay being considered within a subarea within the western portion of the overall siting area (Fig. 3-1 and Fig. 5-1, respectively).

The Südranden siting area lies beneath a range of hills in the Tabular Jura area and has a simple geologic setting. The Opalinus Clay host rock shows undisturbed bedding, with no indication of any zones with increased tectonic dissection. In the area of interest, the Opalinus Clay is 70 - 130 m thick at depths of 310 – 410 m below the surface (according to Nagra 2010, Appendix 3), and dips slightly to the south in the siting area. The Südranden geological siting area extends over 24 km^2, with the Opalinus Clay being considered within almost the entire siting area (Fig. 4-3).

The Jura-Ost siting area lies in a region that has partly been tectonically overprinted by the folding of the Jura mountains (precursory folding zone). For this reason, the Opalinus Clay host rock has areas with largely undisturbed bedding as well as zones with tectonic elements that occur mainly in the marginal zones of the siting area. The Jura-Ost geological siting area for L/ILW extends over 60 km^2, with the Opalinus Clay being considered for waste disposal within most of the siting area (Fig. 5-2). The Opalinus Clay is between 85 and 130 m thick, and occurs at a depth of 300 to 510 m below ground surface in the L/ILW siting area. The HLW siting area occupies only the southeastern 27 km^2 of the L/ILW siting area, within which waste disposal is considered within a still smaller area (Fig. 5-4). The Opalinus Clay is between 100 and 120 m thick, and occurs at a depth of 450 to 550 m below ground surface in the HLW siting area (according to Nagra 2010, Appendix 3).

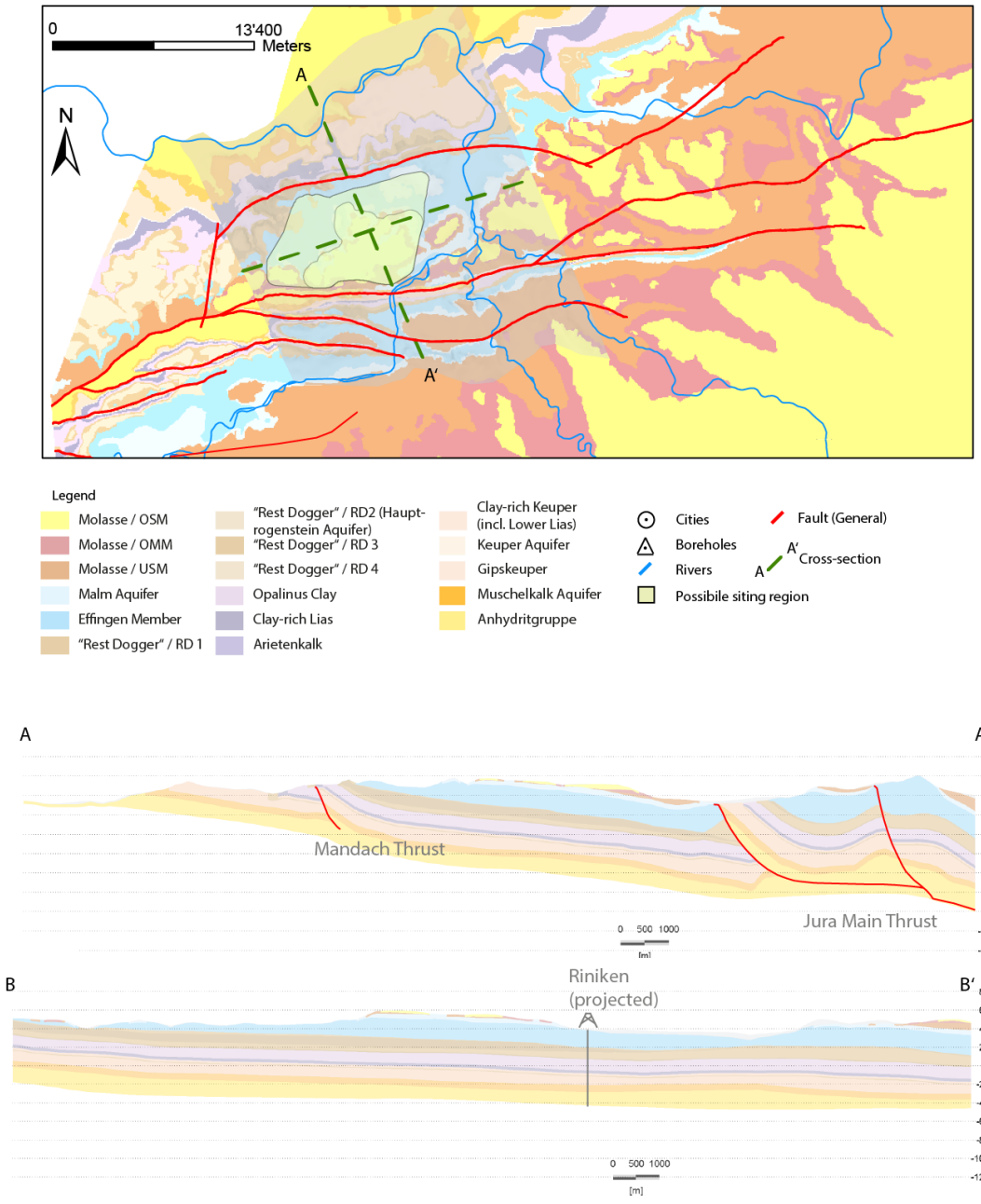

Fig. 5-2: Geological siting area Jura Ost for L/ILW.

The Zürich Nordost siting area is located in the Tabular Jura at the northern boundary of the Molasse Basin and is tectonically quiet. The Zürich Nordost geological siting area extends over 50 km^2, with the Opalinus Clay being considered within most of the siting area (Fig. 4-3). The host rock is in a stable setting, with a slight dip to the southeast. In the siting area, the Opalinus Clay is 90 to 130 m thick at depths of 570 to 860 m bGL. The Zürich Nordost siting areas for L/ILW and HLW (Fig. 4-3) are almost identical. In the Zürich Nordost siting area, the potential host rock for waste disposal includes not only the Opalinus Clay, but also the overlying Murchisonae Beds. The underlying "Toniger Lias" is exhibits a hydraulic conductivity which is in the same order of magnitude as the Opalinus Clay.

The North of Lägern siting area lies in a region that has partly been tectonically overprinted by the folding of the Jura mountains (precursory folding zone). For this reason, the Opalinus Clay

host rock has areas with largely undisturbed bedding as well as zones with increased tectonic dissection. The Opalinus Clay is approximately 90 – 130 m thick, and occurs at a depth of 700 to 910 m below ground surface in the siting area (according to Nagra 2010, Appendix 3). The North of Lägern geological siting area extends over 65 km^2, with the Opalinus Clay being considered for L/ILW disposal within a northeastern subarea, and for HLW disposal within eastern and western subareas within the overall siting area (Fig. 4-4).

5.2 Hydraulic Tests

Hydraulic tests have been performed in the Opalinus Clay in the Riniken (Belanger et al. 1989), Schafisheim (Moe et al. 1990), and Benken (Nagra 2001) boreholes. As discussed in Section 3.2.1, a test was conducted in the Weiach borehole of the interval extending from 542.9 to 556.9 m bGL, which included the lower 11.6 m of the Murchisonae-Concava Beds (clay, argillaceous marl, and oolitic sparitic limestone) and the upper 2.4 m of the Opalinus Clay (Butler et al. 1989). While the hydraulic conductivity of the interval appears to be low (1E-14 to 1E-12 m/s) no defensible estimates of either K or head can be made.

5.2.1 Tests Performed

The three Riniken tests and two of the Schafisheim tests (1015.2D and 1065.6D) were reanalyzed in the context of the geosynthesis project (Nagra 2002; see also references therein). Three of the Opalinus Clay tests (O1, O2, and O3) conducted in the Benken borehole were discarded in Nagra (2002) for a variety of technical reasons, and reinterpreted the other four tests. The analytical results of the reanalyses for the Riniken and Schafisheim boreholes and for the Benken borehole are presented in Tab. 5-1, along with the results from Moe et al. (1990) for Schafisheim tests 1003.2D and 1042.8D.

At the Riniken borehole, Opalinus Clay K appears to be approximately 1E-13 m/s, with an uncertainty range from 2E-14 to 5E-13 m/s. The best estimates of head from the three Opalinus Clay test intervals show an apparent increase in head with depth, from near normally pressured to overpressured. But the estimates for the upper two Opalinus Clay test intervals have uncertainty ranges that extend from underpressured to overpressured conditions, preventing any firm conclusion on vertical hydraulic gradients from being drawn. The lowest test interval, which includes all of the Lias strata in addition to the lowermost 17.5 m of Opalinus Clay, appears to be significantly overpressured, but the analysis cannot be considered reliable without additional sensitivity studies. If the overpressure is real, it may be associated with Lias limestones (e.g., the Arientenkalk and/or Angulaten) rather than with the Opalinus Clay.

With regard to the Schafisheim tests, Opalinus Clay K values between 8E-14 and 1E-12 m/s can be considered as estimates only; Moe et al. (1990) report that the test results may have been affected by drilling mud invasion. The head estimates obtained from the test reanalyses (see Nagra 2002) are considered highly uncertain, covering a wide range between underpressured and overpressured conditions.

The tests of the Opalinus Clay performed in the Benken borehole were carefully reanalyzed (Nagra 2002 and references therein), and provide the most reliable estimates of Opalinus Clay properties. Best-estimate K values range from 1.2E-14 to 1.3E-13 m/s, with uncertainty ranging from less than 1E-15 to 1.4E-13 m/s. Best estimates of head all indicate overpressured conditions, although the uncertainty ranges for three of the four tests extend to normally pressured conditions. The lowermost Opalinus Clay (interval O7) is clearly significantly overpressured.

Tab. 5-1: Opalinus Clay hydraulic testing results.

Test	Interval Top [m bGL][1]	Interval Bottom [m bGL]	Strata	K [m/s]			Freshwater Head [m asl]		
				Min.	Best est.	Max.	Min.	Best est.	Max.
Riniken 368.2S	338.65	397.70	Opalinus Clay	2E-14	1E-13	3E-13	300	380	440
Riniken 413.9S	397.70	430.10	Opalinus Clay	2E-14	8E-14	3E-13	350	400	500
Riniken 461.8S	433.42	490.20	Opalinus Clay (17.51 m) / Lias (37.57 m)/ Upper Keuper (1.70 m)	5E-14	9E-14	5E-13	730	830	930
Schafisheim 1003.2D	989.30	1017.16	Dogger / Opalinus Clay	1E-13	N.D.	5E-13	N.D.	N.D.	N.D.
Schafisheim 1015.2D	1001.30	1029.16	Opalinus Clay	1E-13	2E-13	5E-13	-260	220	760
Schafisheim 1042.8D	1028.88	1056.74	Opalinus Clay	8E-14	N.D.	2E-13	N.D.	N.D.	N.D.
Schafisheim 1065.6D	1051.70	1079.56	Opalinus Clay	2E-13	4E-13	1E-12	-300	100	500
D2-P1[2]	548.8	564.5	Opalinus Clay	-	-	>3.2E-12	-	-	-
O3[3]	544.60	564.50	Opalinus Clay	-	-	>2.5E-12	-	-	-
Benken O4	566.45	596.50	Opalinus Clay	3.1E-15	1.3E-14	3.1E-14	395	513 [< 381]	535
Benken O5	600.07	603.45	Opalinus Clay	< 1E-15	1.2E-14	3.2E-14	< 390	450 – 650	775
Benken O6	605.13	623.60	Opalinus Clay	4.4E-14	5.8E-14	6.5E-14	400	502	560
Benken O7	623.72	655.70	Opalinus Clay (28.32 m) / Jurensismergel (3.66 m)	2.0E-14	1.3E-13	1.4E-13	620	691 [< 373]	775

[1] Ground level (GL) at Riniken borehole is 385.07 m above sea level (asl), GL at Schafisheim borehole is 421.20 m asl, and GL at Benken borehole is 404.3 m asl.

[2] Bottom hole test D2-P1 terminated prematurely (Nagra 2002). Reliable estimate of upper limit of K-value only.

[3] Test O3 terminated prematurely (Nagra 2002). Reliable estimate of upper limit of K-value only.

N.D.: not determined.

Head values in brackets represent measurements in Baker multipacker long-term monitoring (LTM) system at end of 2011 (Jäggi & Schwab 2012).

5.2.2 Long-Term Monitoring in the Benken Borehole

The long-term monitoring performed in the Benken borehole is discussed in Section 4.2.3. With respect to the Opalinus Clay, the long-term monitoring does not support the overpressures estimated from the hydraulic test analyses; the two Opalinus Clay intervals monitored are instead underpressured. At the end of 2011, head in the Z4 interval (Fig. 4-5) was 381 m and declining at a rate of 6.7 m/a, and head in the Z5 interval was 373 m and declining at a rate of 8.4 m/a (Fig. 4-6). Considering that the Z4 and Z5 intervals showed the lowest heads in the borehole at the end of 2011, and were continuing to decline at the fastest rates, leakage between

intervals behind the casing cannot be an explanation for the Opalinus Clay underpressures. Osmotic effects, as discussed in Section 4.2.2, are a possible but not very likely cause of the underpressures. More likely is the assumption of a compaction disequilibrium according to the terminology introduced by Grauls (1999). Unloading phenomena associated with the drilling process and the subsequent placement of the well casing are beliefed to be the cause of the overpressures which very observed during packer testing; a detailed discussion of such "borehole closure" phenomena is given in Nagra (2002). The underpressures observed in the longterm monitoring system may originate from geological processes such as glacial undloading or even tectonic uplift. A further discussion of the origin of abnormal pressures in the clay-rich sequences is found in Chapter 4.2.3 and 4.2.5, respectively.

5.2.3 Conclusions on Opalinus Clay Hydraulic Conductivity

Hydraulic testing of portions of the Opalinus Clay was performed in the Riniken borehole at the eastern margin of the Jura Ost siting area (Belanger et al. 1989), in the Schafisheim borehole northeast of the Jura-Südfuss siting area (Moe et al. 1990), and in the Benken borehole in the Zürich Nordost siting area (Nagra 2001). The hydraulic tests performed in these boreholes show that the Opalinus Clay has hydraulic conductivity between 1E-14 and 4E-13 m/s, with uncertainty ranging from less than 1E-15 to 1E-12 m/s. The highest K values, and also probably the least reliable, are from the Schafisheim borehole where the Opalinus Clay is deepest. At the Benken borehole, the potential host rock is divided into five Opalinus Clay facies plus the Murchisonae layers, differentiated primarily on the basis of differing amounts of clay, quartz, and carbonate. Differences among the hydraulic properties of these six units cannot be determined from the limited data available.

No hydraulic testing of the Opalinus Clay has been performed within the Südranden or North of Lägern siting areas. The Opalinus Clay is shallower in the Südranden siting area (310 – 410 m bGL) than in the nearby Zürich Nordost siting area (570 – 860 m bGL), but is expected to have similar properties in the two areas. The Opalinus Clay is at a similar depth in the North of Lägern siting area (700 – 910 m bGL) as in the Zürich Nordost siting area, and is expected to have similar hydraulic properties in the two areas.

5.2.4 Conclusions on Opalinus Clay Hydraulic Head

(Apparent) inconsistencies were faced in the characterization of the hydraulic head in the Opalinus Clay. At the Riniken borehole in the Jura Ost siting region, two test intervals have uncertainty ranges that extend from underpressured to overpressured conditions. The lowest test interval appears to be significantly overpressured, but the analysis cannot be considered reliable without additional sensitivity studies, and the estimated head could be associated with Lias limestones in the test interval rather than with the Opalinus Clay. At the Schafisheim borehole near the Jura-Südfuss siting region, the head estimates are considered highly uncertain, covering a wide range between underpressured and overpressured conditions. At the Benken borehole in the Zürich Nordost siting region, best estimates of head from the hydraulic-test analyses all indicate overpressured conditions, although the uncertainty ranges for three of the four tests extend to normally pressured conditions. The lowermost Opalinus Clay (interval O7) appears to be significantly overpressured; however, Nagra (2002) suggests the estimated head values should be treated with caution because borehole breakouts may have occurred during the hydraulic test. The long-term monitoring performed in the Benken borehole (Section 4.2.3), however, does not support the overpressures interpreted for the Opalinus Clay and Lias test intervals, but instead shows the Opalinus Clay to be underpressured and the Lias to be near

normally pressured. Fig. 4-6 shows that the overlying 'Brown Dogger' and Malm units have similar underpressures as the Opalinus Clay.

As discussed in Section 5.2.2, the underpressures in the Opalinus Clay shown by the long-term monitoring in Benken cannot be the result of leakage between intervals behind the well casing, because the Opalinus Clay heads are lower than any other heads in the borehole, and are declining at faster rates than any other heads. Furthermore, osmotic effects are an unlikely explanation, because pressures are declining over nearly three years without some evidence that osmotic equilibrium was being approached. In the experiment reported by Neuzil (2000), osmotically induced underpressures had begun to reduce, not continue to increase, after less than 500 days. The overpressures inferred from the hydraulic tests are, therefore, a result of drilling and testing perturbations. Nagra (2002) suggested that interactions of the clay minerals in contact with the synthetic porewater testing fluid (chemico-osmotic disequilibrium), incomplete temperature equilibration (thermal disequilibrium), borehole closure (compaction disequilibrium) and/or analytical error could lead to erroneous estimated heads. The most likely explanation for the overpressures during packer testing is the assumption of a drilling-induced compaction disequilibrium. Such a short-term pressure perturbation is consistent with the hypothesis of long-ranging pressure perturbations due a geological compaction disequilibrium (e.g., glacial unloading, uplift), as supported by the observed underpressures in the longterm monitoring programme. In any case, the long periods required for heads to stabilize provide evidence of low permeability.

No information on the head distribution through the Opalinus Clay in the Südranden or North of Lägern siting areas is available.

5.3 Hydrochemical Information

Opalinus Clay water chemistry information is available only from the Benken and Weiach boreholes, as discussed in Section 4.3. The data and interpretations of the data from Benken are presented in Gimmi & Waber (2004) and Gimmi et al. (2007). Gimmi & Waber (2004) created profiles of $\delta^{18}O$ and $\delta^{2}H$ (Fig. 4-5), Cl^- (Fig. 4-6), and $\delta^{37}Cl$ (Fig. 4-7) through all the strata sampled in the Benken borehole. From modelling, they concluded that the measured stable water isotope profiles seemed to be influenced mainly by diffusive exchange with the underlying Keuper aquifer; no signature of advective flow could be detected. The evolution time is of the order of 0.5 to 1 Ma, with a possible range of about 0.2 to 2 Ma (Fig. 5-3).

Van Loon & Soler (2004) used through-diffusion experiments to measure effective diffusion coefficients (D_e) and diffusion-accessible porosities for tritiated water (HTO), $^{36}Cl^-$, $^{125}I^-$, and $^{22}Na^+$ through Opalinus Clay core from the Benken borehole and the Mont Terri Underground Rock Laboratory. The Opalinus Clay occurs between 200 and 300 m below ground at Mont Terri, similar to its depth in the Südranden siting region. They found that diffusion parallel to bedding was a factor of 4 to 6 larger than diffusion perpendicular to bedding. The best estimate of D_e parallel to bedding for $^{36}Cl^-$ in the samples from Benken was 3.4E-12 m^2/s, while the best-estimate value perpendicular to bedding was 6.7E-13 m^2/s. For the samples from Mont Terri, the values were 1.6E-11 m^2/s (parallel) and 4.1E-12 m^2/s (perpendicular). The differences between locations are attributed to the smaller pore diameter and lower ionic strength of the pore water at Benken relative to that at Mont Terri.

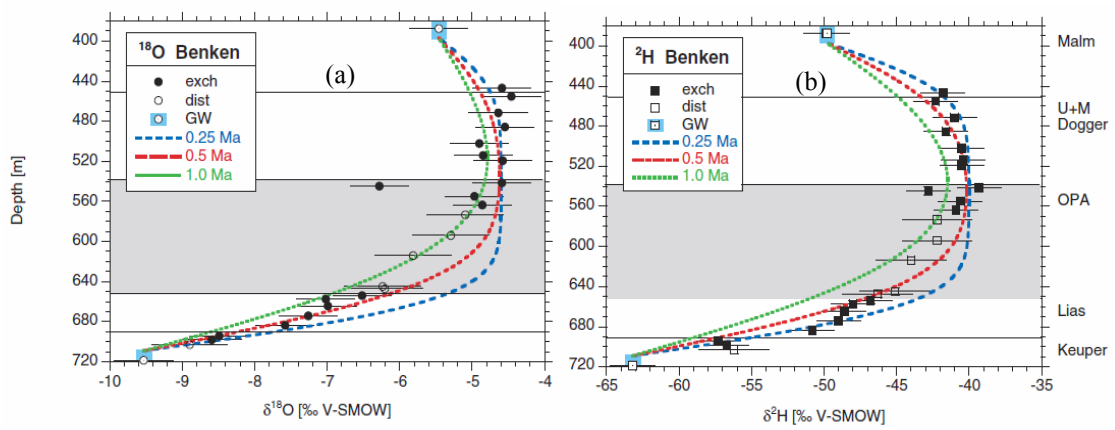

Fig. 5-3: Effect of variation of evolution time on the calculated profiles for $\delta^{18}O$ (a) and $\delta^{2}H$ (b) for the base-case model (Gimmi & Waber 2004).

The curves for 0.5 Ma correspond to the best fits for the combined data sets, shown in Fig. 3-5. The evolution times t were estimated from $\xi = (D_p\ t)^{0.5}$ with the laboratory diffusion coefficient D_p for HTO at 40°C, which represents approximately the relevant *in situ* temperature.

5.4 Summary of Results and Conclusions Regarding the Hydraulic Barrier Function of the Opalinus Clay

The physical properties of the Opalinus Clay combine to make it an effective barrier to radionuclide transport. Firstly, the clay minerals will sorb most cationic radionuclides, so only transport of nonsorbing radionuclides is of concern. Transport may occur through advection and/or diffusion, but both processes are limited in the Opalinus Clay by the controlling parameters (primarily hydraulic conductivity and diffusion coefficient).

The hydraulic conductivity of the Opalinus Clay is low at Riniken, Schafisheim, and Benken (and probably Weiach), ranging from approximately 1E-15 to 1E-12 m/s. No measurements of Opalinus Clay K have been made within the Südranden or Jura Ost siting regions, but K is expected to be low in those areas as well because of lithological similarities to the Opalinus Clay where it has been tested.

Characterization of the strata above and below the Opalinus Clay is much more complete at Benken that it is at Riniken, Weiach, or Schafisheim. The low-K buffer above the Opalinus Clay/Murchisonae Beds extends approximately 140 m through the 'Brown Dogger' and Effingen Member into the Malm (lower Wohlgeschichtete Kalke) at the Benken borehole. Below the Opalinus Clay, low K extends 57 m through the Lias and upper Keuper strata until the Stubensandstein is encountered at a depth of 709 m bGL. At the Weiach borehole in the North of Lägern siting area, the low-K buffer above the Opalinus Clay probably extends at least 77 m through the 'Brown Dogger', and probably extends some distance higher into the Malm. Below the Opalinus Clay, low-K strata extend approximately 50 m through the Lias strata to high K in the Keuper. At Schafisheim, the low-K buffer above the Opalinus Clay probably extends at least 83 m to the Hauptrogenstein Formation. Below the Opalinus Clay, low-K strata extend approximately 32 m through the Lias strata to slightly higher K in the Keuper Gansingen dolomite.

The hydraulic head in the Opalinus Clay is strongly affected by hydro-mechanical coupled processes and thus may vary in the different siting regions according to the local stress conditions. Long-term monitoring in the Benken borehole suggests that the Opalinus Clay may be underpressured by some tens of meters. The abnormal heads in the Opalinus Clay are a strong indicator for the excellent hydraulic barrier function of the host rock, confirming that hydraulic conductivities are so low that vertical advection is insignificant.

Consistent with the measured low K of the Opalinus Clay, stable water isotope data suggest that vertical solute transport through the entire low-K Malm-to-Keuper sequence at Benken is dominated by diffusion, with no evidence of advection. Estimated Cl^- D_p values for the Opalinus Clay are in the order of 1E-10 m^2/s, leading to Péclet numbers much less than 1. Diffusion, therefore, is the dominant transport mechanism.The evolution time of the stable isotope profiles is of the order of 0.5 to 1 Ma, with a possible range of about 0.2 to 2 Ma. Diffusion would not, therefore, release significant quantities of radionuclides from a repository in the Opalinus Clay for hundreds of thousands of years.

6 Helvetic Marls

The Helvetic Marls are being considered as a potential host rock for the geological disposal of L/ILW in the Wellenberg siting area in central Switzerland (Figs. 1-1 and 6-1). The term "Helvetic Marls" here refers to the Lower Cretaceous Palfris Formation and Vitznau Marls as well as the Tertiary Globigerina Marls and Shimberg Shales. The Palfris Formation consists of dark, silty-fine sandy, shaly clay marls, sometimes with isolated light limestone and lime marl beds and sometimes with such beds as interstratifications (limestone bed sequences). The Vitznau Marls consist of a clay-rich limestone/marl interstratification, with an upward transition into sand-rich limestones and marls. The Palfris Formation and Vitznau Marls form part of the base of the Drusberg nappe in Canton Nidwalden. The Globigerina Marls are dark, mica-bearing, silty clay marls, sometimes with lime marls. The Schimberg Shales are made up of grey, fine-sandy clay and lime marls. The Globigerina Marls and Schimberg Shales are the uppermost Tertiary formations of the Axen nappe.

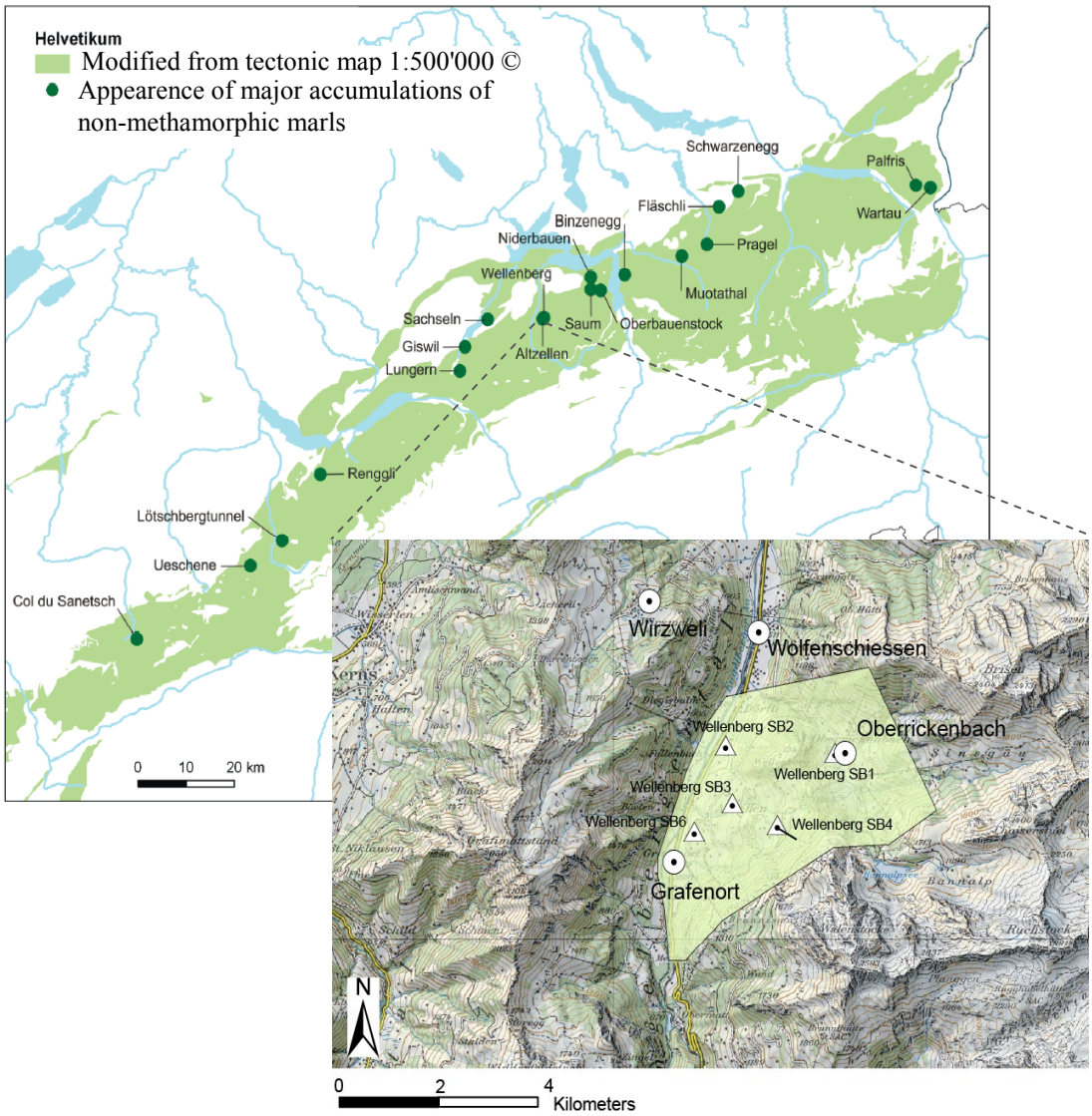

Fig. 6-1: The Helvetic Marls in Central Switzerland with the location of the Wellenberg (WLB) siting area.

Seven deep boreholes were drilled to investigate conditions at Wellenberg from 1990 to 1995 (Fig. 6-1). Hydraulic testing of portions of the Helvetic Marls was performed in all seven of the boreholes. Nagra (1997) provides an overall synthesis of all of the investigations undertaken in the Wellenberg siting area. Nagra (1997) and the references therein provide a comprehensive synthesis of the hydrogeological investigations of the Helvetic Marls carried out in the Wellenberg boreholes from 1990 to 1995.

6.1 Geologic Setting

The Wellenberg siting area in central Switzerland is located in the contact zone between the Drusberg and Axen nappes (Fig. 6-2), which were created by overthrusting during the Alpine orogeny. The Drusberg nappe is composed of Cretaceous and Cenozoic sediments and the Axen nappe of Jurassic, Cretaceous, and also Cenozoic sediments. Both tectonic units lie on top of a stack of Parautochthonous and Autochthonous sediments of Triassic and Jurassic age, themselves forming the cover of the crystalline basement of the Aar Massif. The marl-shale aquitard consists of Lower Cretaceous sediments of the Drusberg nappe (Palfris Formation and Vitznau marls, formerly designated as Valanginian Marls) and of minor amounts of Tertiary sediments of the Axen nappe (Globigerina Marls and Schimberg Shales), together with interhelvetic mélanges, which appear within the above formations or between them. In addition to the tectonic activities producing these nappes and associated disturbances, the area was also affected by valley cutting, notably through glacial erosion. Due to tectonic accumulation, the marl formations have a vertical thickness of more than 1000 m within the Wellenberg siting area. The Wellenberg geological siting area extends over 6 km^2, with the Helvetic Marls being considered within the entire siting area (Fig. 6-2).

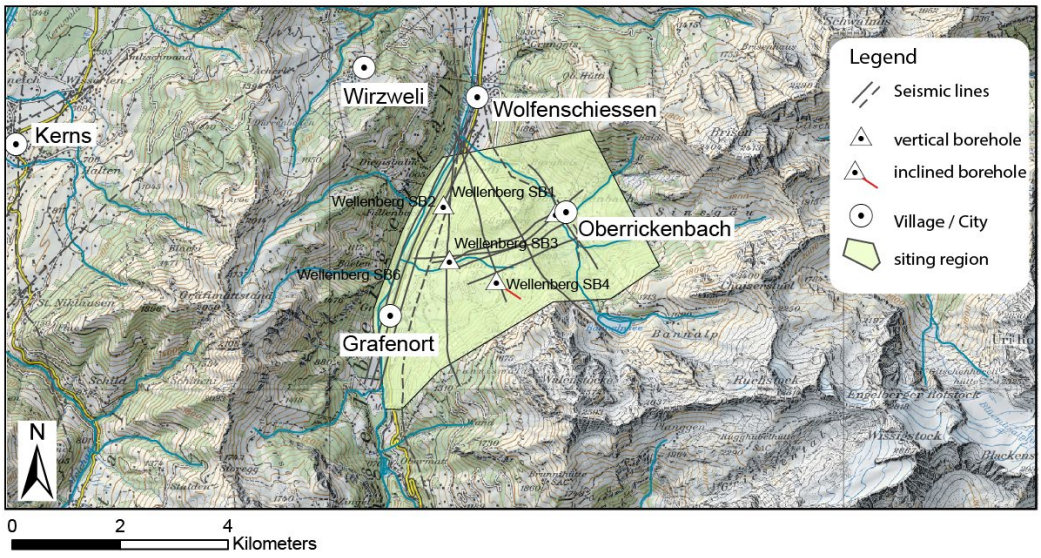

Fig. 6-2: Geological siting area Wellenberg for L/ILW.
Geological profile and map (Boisson 2005).

6.2 Hydraulic Tests

Hydraulic testing of portions of the Helvetic Marls was performed by Nagra in the SB1, SB2, SB3, SB4, and SB6 boreholes from 1990 to 1993, and in the SB4a/v and SB4a/s boreholes in 1994 and 1995. The locations of the boreholes are given in Fig. 6-1. Various levels of analysis were applied to the tests, as described in Nagra (1997). Fluid logging was also performed in the boreholes to identify and localize the major inflow locations along the boreholes. By integrating the fluid logging data with the hydraulic testing data, it has been confirmed that groundwater flow in all tested geological formations occurs mainly through discrete water-conducting features (WCFs) that correspond to joints, fissures, and fractures. Under conditions such as these in which only a small part of a packed-off test interval is hydraulically active, comparing transmissivity (T) among test intervals is more meaningful than comparing hydraulic conductivity (K) values obtained by simply dividing the T values by the interval thicknesses. Fig. 6-3 shows the final T profiles in the seven tested boreholes as defined in Nagra (1997). The symbols show T values at discrete WCFs separated by blank zones where flow was below the detection limit of the fluid logging. T of WCFs in the Palfris and Tertiary formations appears to decrease with depth to values of 1E-10 m^2/s or lower.

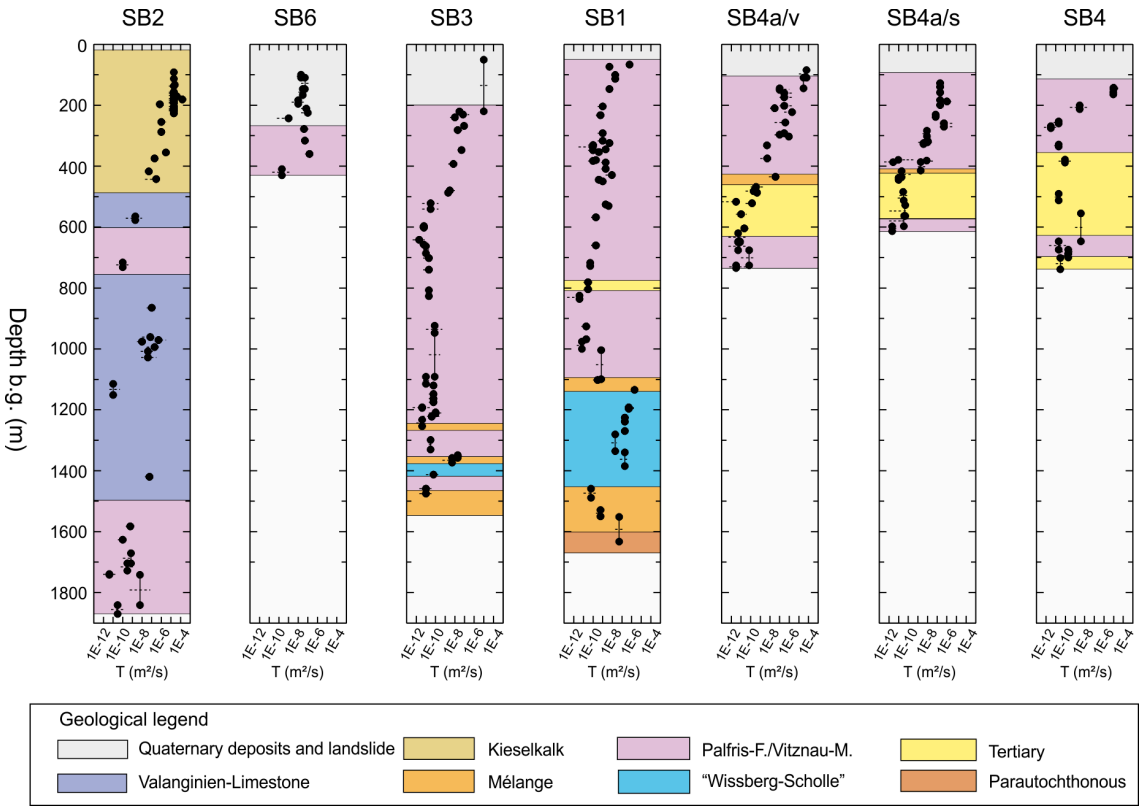

Fig. 6-3: Profile of WCF transmissivity in boreholes SB1 through SB6.

From packer tests conducted of intervals where fluid logging showed no WCFs were present, the K of the sound host rock was found to vary between 1E-14 and 1E-11 m/s, with an average value of roughly 1E-13 m/s.

Hydraulic head estimates were derived from hydraulic test analyses and from long-term monitoring, and assigned to the locations of the WCFs detected by fluid logging. Fig. 6-4 shows the head profiles for the seven boreholes. The hydraulic heads in the host rock range from hydrostatic to artesian in the upper section to very low values immediately below the level of the Engelberg valley. The latter c1early lie below the local and regional exfiltration areas and almost reach sea level values in boreholes SB1 and SB2. The consistent form of head profiles indicates the presence of an underpressure zone (UPZ) in the central part of the host rock. Distinct underpressures are seen in portions of the Palfris and Tertiary strata, returning to near normal or even overpressured conditions with greater depth. SB2 shows no underpressures due to its proximity to the highly permeable formations of the Drusberg nappe.

Modelling studies by Vinard et al. (2001) showed that the UPZ could be attributed to slow dissipation of pressure disequilibrium caused by mechanical unloading of the strata following the glacial retreat at the end of the last ice age. Alternatively, Diamond (1998) has proposed that the underpressures resulted from porosity being created by nappe folding under hydrodynamically closed conditions (compaction disequilibrium / lateral [tectonic] stress; according to Grauls 1999), which would mean that the underpressures have existed for ~ 20 Ma. Whether the underpressures were created 20 Ma or 20 Ka ago, the fact that they persist today further confirms the low K of the host rock.

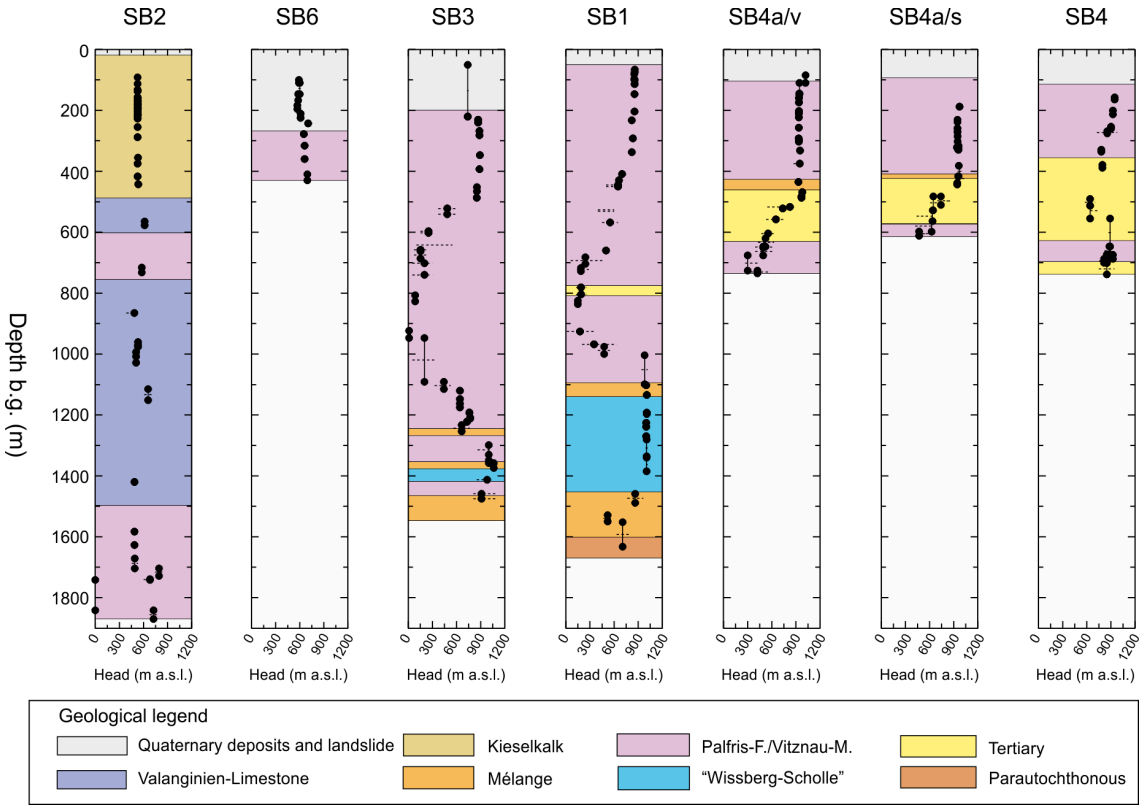

Fig. 6-4: Profile of WCF hydraulic head in boreholes SB1 through SB6.

Methane gas was frequently observed during the hydraulic packer tests conducted in the Palfris and Tertiary strata. The gas typically evolved from solution during fluid-withdrawal events. A classification scheme was developed with four categories to summarize and assess the evidence for gas in each test interval (see Nagra 1997 and references therein). The categories are:

- Category 1: No gas evolved during major withdrawal tests
- Category 2: No clear (quantitative) observation of gas
- Category 3: Minor gas flow rates observed
- Category 4: Major gas flow rates observed

The results of the categorization are shown in Fig. 6-5. Only a few tests in the Palfris Formation indicate a free gas phase (12 of 141 tests in category 4). Clustering of category 4 tests at certain depths is not observed. Major gas flow rates are observed only in the southern part of the host rock (SB4, SB4a/v, SB4a/s). A quarter of all tests indicate that single-phase conditions are most likely under natural pressure conditions (27 of 141 tests in category 1, 7 tests in category 3). No depth-dependence of category 1 and 3 tests is observed. The majority of tests did not provide conclusive evidence on the *in situ* phase conditions in the host rock (primarily because the tests were not designed to provide that information).

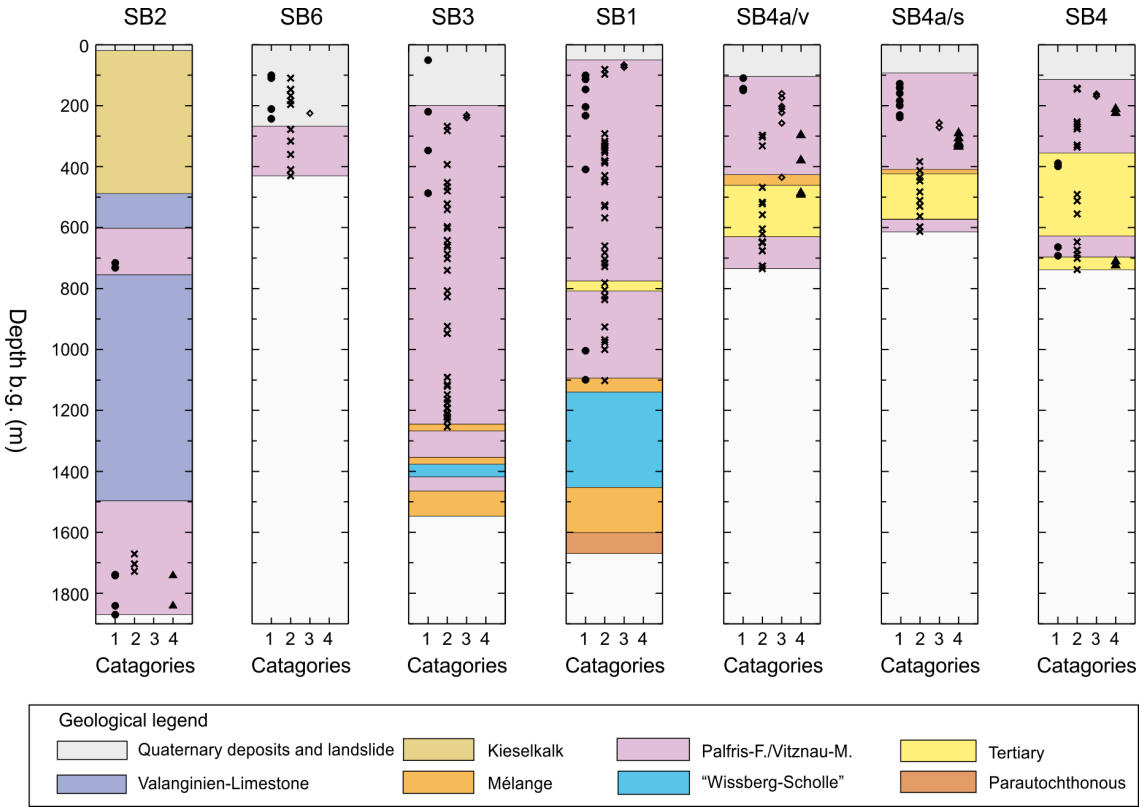

Fig. 6-5: Profile of gas categorization in boreholes SB1 through SB6.

Based on the results of the categorization, it appears unlikely that a continuous two-phase flow system exists on the large scale within the WCFs of the host rock because of the lack of any correspondence between depth and category. Even in the southern portion of the siting area, no correlation is observed between the gas categories along the boreholes SB4, SB4a/v, and SB4a/s. Therefore, two-phase flow conditions probably occur, at most, on a local scale.

6.3 Hydrochemical Information

A detailed presentation of the hydrochemical characteristics of the Helvetic Marls at Wellenberg can be found in Nagra (1997) and an overview in Pearson et al. (1998). A brief summary of key characteristics from Vomvoris et al. (1998) is presented below.

The chemical and isotopic compositions of the deep groundwaters sampled at Wellenberg indicate that they represent three different groundwater systems: (1) groundwaters within the host rock formation, (2) groundwaters below the host rock formation in the "Äquivalent der Wissberg-Firrenband Schuppe" (Lower Na-HCO_3 type), and (3) groundwaters in the geological formations stratigraphically above the host rock formations which occur today north of the host rock formations and were encountered in borehole SB2 (not discussed further because of SB2's location in the valley of the Engelberger Aa). The groundwaters of these three systems have chemical and isotopic compositions that indicate evolution mainly within the geological formations from which they were sampled. The hydrochemical conceptualization is shown schematically in Fig. 6-6.

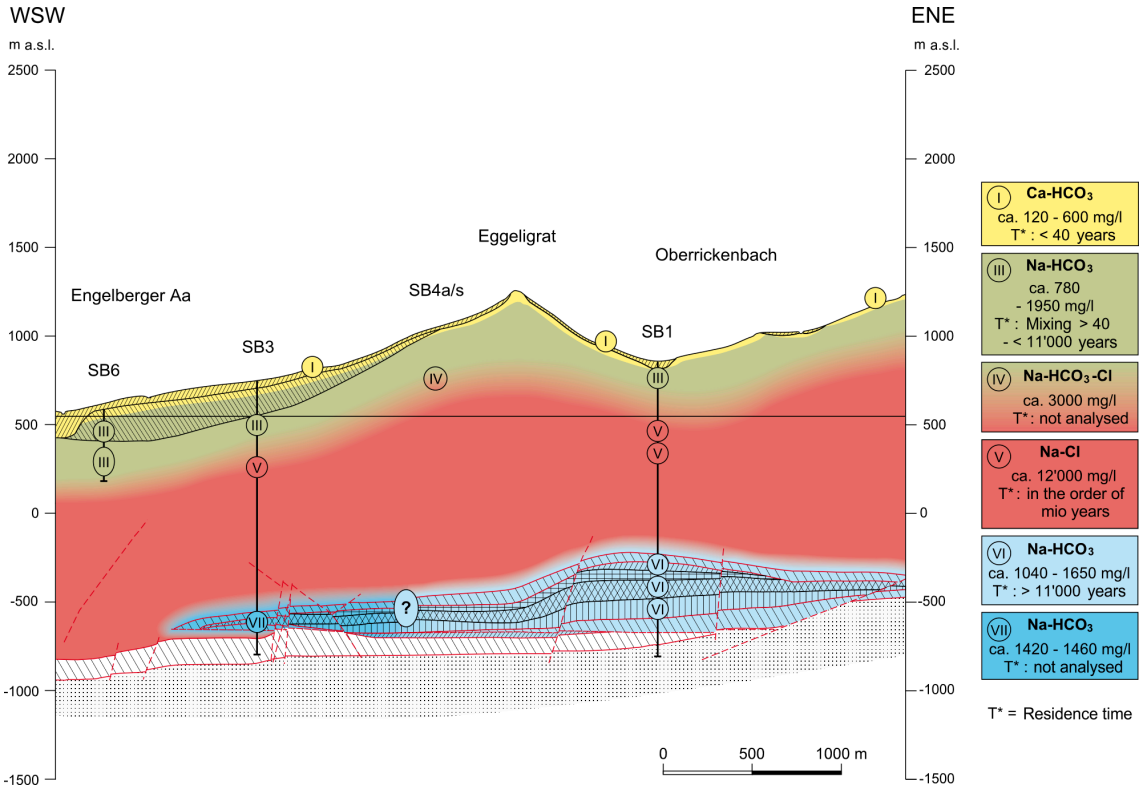

Fig. 6-6: Hydrochemistry at Wellenberg.

The Upper Na-HCO_3 (Type III and Type IV in Fig. 5-6) groundwaters within the host rock formations can be explained as the product of infiltrating superficial Ca-HCO_3 (Type 1) groundwaters replacing connate Na-Cl (Type V) groundwater and reacting with the formation minerals. Geochemical evolution of these groundwaters with the rock from which they were sampled is consistent with the measured chemical and isotopic properties of the groundwaters and the rocks. There is need for neither large groundwater movement nore for mixing with other known (or presently unknown) groundwater types. The only exception is the Upper Na-HCO_3

groundwater sampled in borehole SB6 at the bottom of the Engelberger Aa valley. There, measureable influences exist of groundwaters that evolved in the Kieselkalk on the western flank of the valley.

The Lower Na-HCO_3 (Type VI in Fig. 6-6) groundwaters from the "Äquivalent der Wissberg-Firrenband-Schuppe" must have evolved differently from the Upper Na-HCO_3 groundwaters or any other groundwater at Wellenberg. The chemical and isotopic composition of these groundwaters indicate evolution mainly in rocks similar to the ones found in the Nordhelvetischer Flysch. Mixing with Na-Cl groundwater can be excluded, based on the chemical and isotopic composition of the Lower Na-HCO_3 groundwaters and the fact that marls of the Palfris Formation act as a confining layer for these groundwaters.

The hypothetical repository location would be primarily in the region of the Na-Cl Type V water, which is thought to be residual from the last stages of Alpine metamorphism of the marl. The residence time of this water is on the order of millions of years, showing that it has little potential to transport radionuclides. The repository would also be near the region of the Na-HCO_3-Cl Type IV water, where some infiltrating Ca-HCO_3 (Type 1) groundwater has mixed with the connate Na-Cl (Type V) groundwater.

A through-diffusion experiment was performed on one core sample from the Palfris Formation, providing a D_e estimate perpendicular to bedding for tritium of 2E-12 m^2/s (Boisson 2005). The D_e for Cl^- is likely lower than that for tritium because of anion exclusion effects, as was found to be the case by Van Loon and Soler (2004) for the Opalinus Clay.

6.4 Summary of Results and Conclusions Regarding the Hydraulic Barrier Function of the Helvetic Marls

Hydraulic testing shows that discrete water-conducting features provide the primary permeable pathways through the Helvetic marls. T of WCFs in the Palfris and Tertiary formations appears to decrease with depth to values of 1E-10 m^2/s or lower. The K of the sound host rock was found to vary between 1E-14 and 1E-11 m/s, with an average value of roughly 1E-13 m/s. Head profiles indicate the presence of an underpressure zone (UPZ) in the central part of the host rock. Modelling studies by Vinard et al. (2001) showed that the UPZ could be attributed to slow dissipation of pressure disequilibrium caused by mechanical unloading of the strata following the glacial retreat at the end of the last ice age, whereas Diamond (1998) relates the UPZ to nappe folding $\sim$ 20 Ma ago. Hydrochemical information shows the presence of Na-Cl water below depths of a few hundred meters in the Helvetic marls with residence times on the order of millions of years.

Both the head and water chemistry data show the WCFs are restricted in their extent and/or lack interconnection, and that the overall hydraulic conductivity of the Helvetic marls is low-underpressure conditions have apparently persisted at least since the last glacial period, and pore waters millions of years old have not been flushed by younger fluids. Advection through the marls is, therefore, insignificant on the time scale of concern for an L/ILW repository. Cationic radionuclides would largely be sorbed by the clays in the marls, and nonsorbing radionuclides would be transported only slowly by diffusion. Therefore, the Helvetic marls would provide an effective barrier to the migration of radionuclides from an L/ILW repository.

7 Integration and Comparison

7.1 Evaluation of Recent Nagra Hydraulic Testing and Analysis

The hydraulic testing performed in the Gösgen, Küttigen, Oftringen, and Schlattingen-1 boreholes to date has been limited by the short periods of time available to Nagra for the testing. In most cases, Nagra used the time available effectively, but in some instances, nonproductive test phases (e.g., slug tests) were initiated despite clear evidence from the preceding PSR or other tests that such a test phase would be unproductive. In other cases, too many test phases were attempted during the limited time available with the result that many of the phases were uninterpretable. When testing low-permeability formations, a standardized testing protocol should be applied that gives the initial test phase (after the PSR) a high likelihood of success regardless of the conditions encountered, and then provides options for later phases (if any) based on the results of the first phase. Pulse-withdrawal tests represent the preferred initial phase because they: (1) draw water from the formation into the borehole rather than forcing particulate-bearing borehole fluid into the formation; (2) provide an immediate measurement of Ctz that is both necessary for test analysis and provides evidence on the presence/absence of gas and other unusual conditions; (3) will be concluded quickly if K is high, providing information to define, and leaving time to perform, subsequent test phases; and (4) can be continued for as long as necessary (up to the total time available) to obtain a reliable analysis if K is low.

In many cases, the procedure used to initiate pulse tests (creating a pressure difference between the test interval and test tubing, and opening and closing the SIT) was non-ideal, creating undesirable pressure transients and introducing uncertainty into the calculation of C_{tz}, a key parameter in the analysis of tests in low-permeability formations. In addition, C_{tz} values, which should be made as low as possible to maximize the formation response observed, were generally high (> 1E-9 Pa^{-1}), perhaps because packer-inflation pressures were too low.

The numerical packer test simulator nSIGHTS was used for most of the analyses. The software is a very powerful tool for packer test interpretation, but its capabilities were not adequately used. Thus, optimizations were directed towards fitting simulations only to the Cartesian pressure record, sacrificing the better diagnostic and fitting capabilities of the derivatives for each test phase. nSIGHTS allows specification of composite fits that can include all types of diagnostic data formats, such as log-log pressure change and derivatives, Ramey A, B, and C with derivatives, and Horner plots, in combination with the Cartesian record. By optimizing on a composite fit, a better overall match to the data is achieved with better constraints on the fitting parameters. Fitting is also enhanced by including specific storage as a fitting parameter rather than specifying a value for it based on measurement of constitutive properties. Specific storage (and formation pressure) should not be restricted to "plausible" ranges based on preconceived notions about the system being tested. Specific storage is not well estimated from a single-well test under the best of conditions because it is tightly correlated with skin properties and the manner in which skin is represented in the model. The objective of the modelling is usually to estimate K and static formation pressure of the undisturbed formation, not specific storage. If the model needs to set specific storage at an "unrealistic" value to compensate for short-comings in the model implementation of skin, it should not be prevented from doing so. A full-blown perturbation analysis could have been performed for each test to evaluate correlations among, and uncertainties associated with, all fitting parameters. This should entail a minimum of 500 perturbations, with multiple iterations likely (note, a complete analysis of a test, including perturbations, should take no more than two days).

7.2 Comparison to Hydraulic Testing Programmes at Other Sites

The recent hydraulic testing of the Malm and Dogger strata performed by Nagra in the Gösgen, Küttigen, Oftringen, and Schlattingen-1 boreholes is qualitatively similar to testing of the Callovian and Oxfordian strata in the vicinity of Andra's Bure URL in France and to the testing of the Silurian and Ordovician sedimentary sequence at the NWMO's Bruce nuclear site in Canada. The Nagra and Andra testing programs are similar in most respects, in large part because they tend to use the same testing contractors and equipment suppliers. Recognizing that the recent testing was necessarily performed under an accelerated time frame and was not as comprehensive as it would have been had Nagra had full control of the schedule, some comparisons to the testing programs at the French and Canadian sites may still be of value.

The basic testing equipment and procedures used for the Nagra tests were similar to those used by Nagra for other testing at Benken and Wellenberg, although Nagra's full normal testing procedure could not be implemented because of externally driven time constraints. The equipment and procedures used are also similar to those used by Andra and the NWMO. Single- or double-packer test tools are used to isolate intervals for testing, while pressures are measured in the bottom of the hole, in the test interval, in the tubing above the shut-in tool, and in the annulus between the tubing and borehole wall. Pulse tests are the favored type of test where hydraulic conductivity is less than approximately 1E-10 m/s.

From an equipment standpoint, what most distinguishes the NWMO tests from the Nagra and Andra tests is the method of pulse initiation. Nagra and Andra either remove water from or add water to the tubing above the closed shut-in tool to create a pressure difference between the tubing and the test interval. They then open and close the shut-in tool to create a nearly instantaneous pressure change in the test interval (although procedure-induced transients are evident in the data from many of the tests). By measuring the pressure (or water level) change that occurs in the tubing, they are able to calculate the compressibility of the test interval. This calculation is not possible, however, if anything prevents the measurement of pressure (or water level) in the tubing, or if the tubing is charged with gas to initiate a pulse injection. NWMO, on the other hand, includes a hydraulically actuated piston in the tool string below the SIT (Roberts et al. 2011). The pistons can be made in any size, and are designed to produce a pulse of between 500 and 900 kPa given the known test-interval dimensions. The piston is configured as either fully extended or fully retracted before the interval is shut in, depending on whether the first test is to be a pulse withdrawal or pulse injection, respectively. Compared to the Nagra/ Andra method of pulse initiation, the piston method produces a cleaner, more consistent pulse signal from which test-zone compressibility can always be accurately calculated. The piston can also be used at the end of any test sequence or phase to measure the test-zone compressibility.

Another difference between the NWMO and Nagra tests is the packer-inflation pressures chosen. NWMO always inflated packers to 15 to 16 MPa above hydrostatic pressure, which was at least 6 MPa above the highest interval pressure reached in the deepest intervals, and more for shallower intervals. In contrast, Nagra inflated packers to only 1.5 MPa above the hydrostatic pressure at Gösgen and Küttigen, to 3.5 MPa above hydrostatic at Oftringen, and to less than 5 MPa above hydrostatic at Schlattingen-1 except for the M1 test during which the packers were inflated to 10 MPa above hydrostatic. This difference in packer-inflation pressures may explain why C_{tz} values from Nagra tests were typically higher than those from NWMO tests. In the testing performed by the NWMO at the Bruce site, the majority of C_{tz} values were less than 1E-9 Pa^{-1}, within a factor of two of the compressibility of water. Tests that had C_{tz} values greater than 1E-9 Pa^{-1} were examined closely for evidence of gas (Roberts et al. 2011). Of the 26 tests conducted by Nagra at Gösgen, Küttigen, Oftringen, and Schlattingen-1, only 8 had C_{tz} values less than 1E-9 Pa^{-1}. The high Nagra C_{tz} values may be related to the packers being

more compliant at lower inflation pressures, the possible presence of gas, and also, in the cases of Gösgen and Küttigen, to shallow test depths where the confining pressure on the rock is low.

Nagra employs a tiered approach to test analysis, beginning with Quick Look Reports (QLRs) begun in the field when a test is underway. QLRs typically include attempts to match the test data to analytical solutions and examination of the data in a variety of diagnostic plot formats. An analysis code such as nSIGHTS may be used at this stage to find an optimized match to the entire Cartesian data record from the test. A QLR report is prepared and evaluated, and then a decision is made as to whether to proceed to a “Standard” or “Detailed” analysis. A “Standard” analysis involves inverse parameter estimate and residual analysis, while a “Detailed” analysis also includes a multi-component objective function in parameter estimation, perturbation analysis, and an evaluation of the role of non-fitting parameters in the hydraulic parameter estimation.

In contrast, NWMO has simply decided that all tests will be analyzed in detail, and structures the entire analysis process accordingly. Only steps that lead directly to a final detailed nSIGHTS analysis are taken. NWMO begins real-time analyses using nSIGHTS within an hour of test initiation. Successive iterations are performed as more data become available to make sure test objectives have been met before the test phase is terminated. Results of each phase are used to predict the response expected in the next phase. A full baseline analysis of the entire testing sequence is completed within hours of test termination. These real-time analyses include the entire borehole pressure history, which is updated with every change in test interval. After all tests are completed in a borehole, the only analyses that remain to be performed are the perturbation analyses used to identify the global minimum in the solution space and quantify parameter correlations and uncertainty. The perturbation analyses typically take no more than two days per test interval. A single report is prepared on only the final analysis results. Nagra might consider adopting more of the NWMO approach to test analysis as a more cost- and time-effective method than their current tiered approach.

7.3 Comparison to Other Radioactive Waste Repository Sites

The four rock types being considered by Nagra in six siting regions for the potential disposal of L/ILW and/or HLW can be compared to the potential host rocks and sites being considered for radioactive waste disposal in other countries.

From a quantitative standpoint, the estimated K values for the Effingen Member (1E-15 to 1E-12 m/s) are comparable to those estimated for the argillaceous Ordovician strata at the Bruce nuclear site, which for the most part range from approximately 3E-15 to 2E-12 m/s (Roberts et al. 2011), and to those estimated for the Callovo-Oxfordian argillite in the Meuse/Haute Marne area, which range from approximately 1E-14 to 1E-12 m/s (Andra 2005). The calcareous sequences of the Effingen Member (Gerstenhübel Beds) may exhibit higher effective K values up to 5E-10 m/s, because the rigid limestones are prone to brittle failure, associated with discrete water-conducting features. K's estimated for the Opalinus Clay in the Benken and other boreholes range from less than 1E-15 to 1E-12 m/s (Nagra 2002). A moderate dependence of the K values on porosity is observed, which is explained by the compaction behavior of the rock (Fig. 7-1). As a consequence, the hydraulic conductivity of the Opalinus Clay decreases with overburden depth, whereas the corresponding lateral variability is exceptionally low due to the high clay content of the rock. While the 'Brown Dogger' K values at the Benken borehole fall in a similar range as those of the Opalinus Clay, 'Brown Dogger' K at the Schlattingen-1 borehole appears to be between 1E-11 and 2E-9 m/s. The calcareous sequences of the Wedelsandstein Formation may bear discrete water-conducting features with enhanced transmissivity. The matrix K of the sound Helvetic marl host rock was found to vary between 1E-14 and 1E-11 m/s,

with an average value of roughly 1E-13 m/s. Discrete water-conducting features within the Helvetic marl have higher K. At the intended repository level (200 m below the local discharge area) these water-conducting features appear to lack the connectivity that would make them of hydraulic significance. Host rock K's in the six siting regions, therefore, are similar to those at other sedimentary sites selected worldwide for radioactive waste repositories.

With respect to hydraulic head, the four potential host rocks considered by Nagra are similar to other potential argillaceous host rocks in that they are not in hydrostatic equilibrium with the underlying and overlying formations. Although head conditions in the Effingen Member are not well defined, portions of the unit are clearly underpressured at Gösgen and Oftringen, while portions are overpressured at Küttigen. Possible causes for the anormal pressures in the Effingen Member are dynamic transfers (two-phase flow), compaction disequilibrium (e.g., glacial unloading) and lateral strains (tectonics). At the Benken borehole, the 'Brown Dogger' appears from long-term monitoring to be underpressured, while at the Schlattingen-1 borehole it is overpressured. Both, underpressures in Benken and overpressures in Schlattingen can be interpreted as gravity driven flow, associated with the regional discharge and recharge levels. The hydraulic head of the Opalinus Clay has not been well characterized at any location. At the Benken borehole where it has been studied most thoroughly, the Opalinus Clay appears from hydraulic testing to be overpressured, but from long-term monitoring to be underpressured. Both phenomena can be explained by compaction disequilibrium: while the drilling and packer testing procedures may have induced short-term pressure perturbations (pore water over-pressures), geological processes such as glacial unloading may have caused long-term perturbations in the opposite sense (underpressure). In any case, abnormal pressures as a consequence of compaction disequilibrium are a clear indicator for very low hydraulic conductivity. Heads in the Helvetic marls at Wellenberg are variable, but an underpressured zone is a prominent feature of the host rock at the potential repository location. In comparison, much of the Ordovician strata at the Bruce nuclear site are underpressured (Roberts et al. 2011), while the Callovo-Oxfordian argillite in the Meuse/Haute Marne area is overpressured relative to the underlying and overlying formations (Andra 2005). At all the sites, the absence of a hydrostatic equilibrium condition is taken as evidence of low permeability in the host rock.

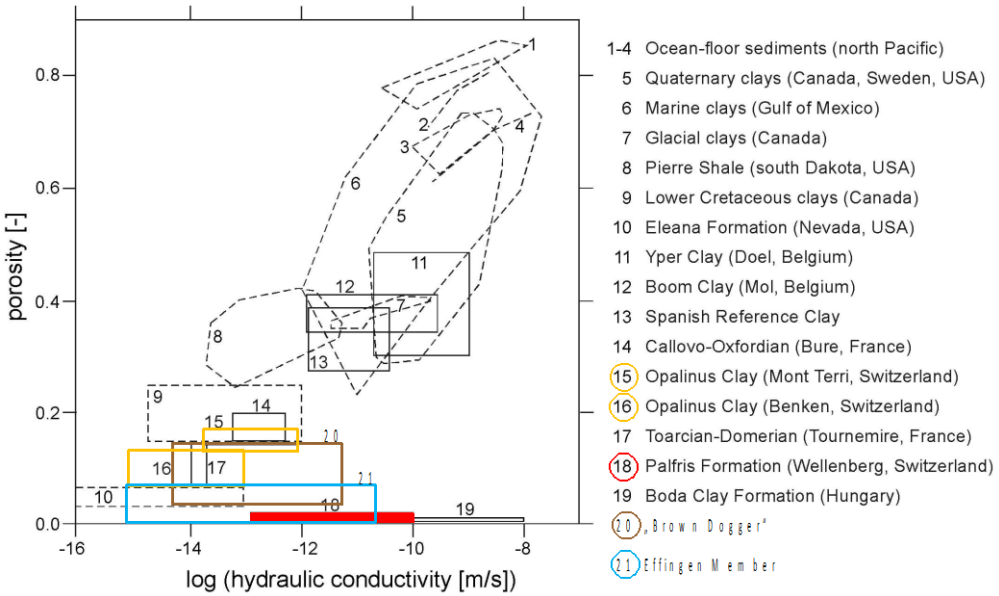

Fig. 7-1: Hydraulic conductivity of argillaceous formations as a function of porosity.

Dashed areas 1-10 represent laboratory-measured values normal to bedding reported by Neuzil (1994). Other areas represent values measured *in situ*, presumably parallel to bedding. From NWMO (2011), modified from Mazurek et al. (2008).

In the area under consideration for disposal of L&ILW in the Jura-Südfuss siting area, the Effingen Member is 220 to 240 m thick, wheras the thickness of the Opalinus Clay sequence in the western part of the siting area is not very well-defined (estimate 65 – 105 m). The low-K section including the 'Brown Dogger' and Opalinus Clay in the North of Lägern siting area is at least 344 m thick. The low-K section at Benken in the Zürich Nordost siting area is 312 m thick. In the Jura Ost siting area, the low-K sequence including the Opalinus Clay could be up to 208 m thick, extending from the Keuper Stubensandstein to the Hauptrogenstein Formation. The Helvetic Marl formations have a vertical thickness of more than 1000 m within the Wellenberg siting area. In comparison, the low-K Ordovician sequence at the Bruce site is 400 m thick and the low-K section at Bure is 256 m thick. Thus, the thicknesses of the low-K sequences in the six siting regions are adequate to provide a reasonable buffer between a repository and underlying and overlying aquifers, and are comparable to those at those other sedimentary sites beging considered for radioactive waste disposal.

Cl^- D_e values perpendicular to bedding from samples of the Effingen Member and Opalinus Clay range from approximately 7E-13 to 3E-12 m^2/s, and the value from the Palfris Formation likely falls within the same range. Estimates of D_e are available from the 'Brown Dogger' (van Loon 2013), indicating typical Cl^- D_e values perpendicular to bedding of ~2E-12 m^2/s for samples, recovered from the clay-rich and calcareous sequences, respectively. These values are similar to those from other argillaceous strata with low anion-accessible porosities, such as the Couche Silteuse at Marcoule, the Toarcian-Domerian at Tournemire, the Callovo-Oxfordian at Bure, and Michigan Basin Ordovician shales (Fig. 7-2; Mazurek et al. 2011).

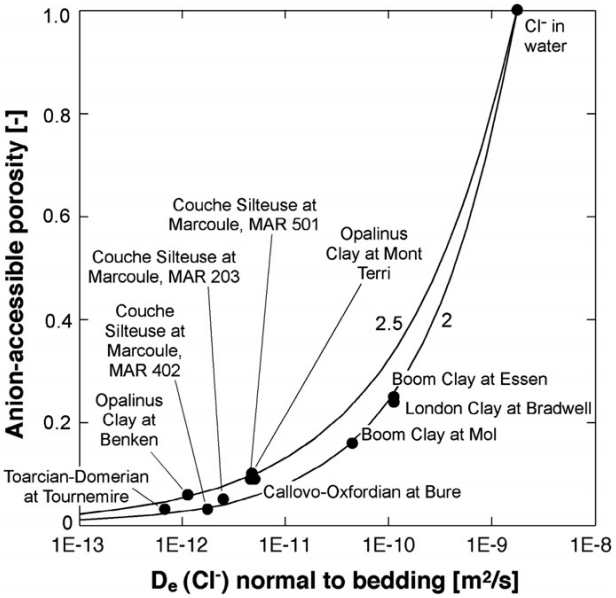

Fig. 7-2: Effective diffusion coefficients normal to bedding for Cl- in clays and shales as a function of anion-accessible porosity.

Curves represent Archie's law relationships, and numbers indicate the empiric exponents. From Mazurek et al. (2011).

Cl^- and/or stable isotope profiles have been defined at the Effingen Member boreholes as well as for the low-K sequences in the Zürich Nordost and North of Lägern siting regions. These profiles are generally arcuate in nature, showing disequilibrium with concentrations in overlying and underlying aquifers. Similar arcuate profiles are seen for $\delta^{18}O$ at Bure (Andra 2005), for $\delta^{18}O$ and Cl^- at the Bruce site (NWMO 2011), and for Cl^- in the low-K argillaceous strata at Mont Terri and Marcoule. At all of these locations, the profiles are explained as resulting from out-diffusion of Cl^- and/or ^{18}O from the argillaceous strata to underlying and overlying aquifers with lower salinity over periods of hundreds of thousands to millions of years (Andra 2005, NWMO 2011, Mazurek et al. 2011). Considering the similarities in diffusion coefficients and low-K sequence thicknesses between the siting regions and these other areas studied, diffusive equilibration times at the siting regions are likely to be of a similar magnitude.

7.4 Information from Other Types of Studies

In addition to radioactive waste programmes, low-permeability environments have been studied in the context of oil and gas reservoirs, carbon sequestration, compressed air energy storage, and hydrodynamics of sedimentary basins, among others. Most of these projects are focused on either the exploitation of resources that have already been trapped within the geologic environment, or on disposal or storage of materials where their isolation can be assured. These other types of studies contribute to our overall understanding of low-permeability environments and of the behaviors/performance to be expected from specific sites.

Oil and gas reservoirs are typically formed when a relatively permeable unit is overlain by a low-permeability layer or caprock that traps the oil and gas in the permeable unit. These reservoirs have typically been confined for millions of years. In its definition of "cap rock", the Schlumberger Oilfield Glossary (www.glossary.oilfield.slb.com) states *"The permeability of a cap rock capable of retaining fluids through geologic time is ~ 10^{-6} – 10^{-8} darcies."* The corresponding K range for freshwater is approximately 1E-13 to 1E-11 m/s. By this definition, the potential host rocks under consideration by Nagra would qualify as caprocks.

Carbon sequestration involves the injection of pressurized, liquid CO_2 into a permeable formation at depth that is overlain by low-permeability strata that will prevent the CO_2 from escaping over at least 5 to 10 ka. While this time scale may be relatively short for radioactive waste, actual performance at a carbon sequestration site may in fact reach 100 ka or 1 Ma scales. At the Krechba CO_2 sequestration site in Algeria, caprock permeability is 1E-23 to 1E-19 m^2, equivalent to hydraulic conductivity of approximately 1E-16 to 1E-12 m/s (Armitage et al. 2011).

A number of studies have examined the role of low permeability on the creation and maintenance of abnormal pressures in sedimentary basins (e.g., Bredehoeft & Hanshaw 1968; Corbet & Bethke 1992; Neuzil 1993; Jiao & Zheng 1998). Corbet & Bethke (1992) concluded that underpressures observed in the western Canada sedimentary basin were only possible if the permeability of the Cretaceous shales was on the order of 1E-22 m^2 (K of 1E-15 m/s). Neuzil (1993) concluded that underpressures observed in the Pierre Shale on the margin of the Williston Basin required local K to be between 1E-14 and 1E-13 m/s. Jiao & Zheng (1998) found that underpressures induced by erosional unloading in two reservoirs in Oklahoma, USA, required the K of shale formations to be 4E-14 to 5E-14 m/s. Thus, studies of anomalous pressures in sedimentary basins confirm that the abnormal pressures observed in the Swiss siting regions are consistent with the measured K's, and support the conclusion that flow through these systems is insignificant even on a geologic time scale.

8 References

Albert, W. & Bläsi, H.R. 2008: NOK EW-Bohrung Oftringen: Geologische, mineralogische und bohrlochgeophysikalische Untersuchungen (Rohdatenbericht). Nagra Arbeitsbericht NAB 08-02. Nagra, Wettingen, Switzerland.

Albert, W. & Schwab, K. 2013: Analyse des Tonmineralgehalts anhand von Bohrlochmessungen in Bohrungen der Nordschweiz. Nagra Arbeitsbericht NAB 12-56. Nagra, Wettingen, Switzerland.

Albert, W., Bläsi, H.R. & Weber, H.P. 2009: Geologische und geophysikalische Untersuchungen in Bohrungen am Standort Gösgen/Niederamt. Unpubl. Nagra Project Report. Nagra, Wettingen, Switzerland.

Albert, W., Bläsi, H.R., Koroleva, M. & Weber, H.P. 2007: EP-05 EWS Küttigen: Geologische, mineralogische und bohrlochgeophysikalische Untersuchungen (Rohdatenbericht). Nagra Arbeitsbericht NAB 07-15. Nagra, Wettingen, Switzerland.

Andra 2005: Dossier 2005 Argile, Référentiel du site de Meuse/Haute-Marne, Tome 1: Le site de Meuse/Haute-Marne: histoire géologique et état actuel. Andra, Châtenay-Malabry, France.

Armitage, P.J., Faulkner, D.R., Worden, R.H., Aplin, A.C., Butcher, A.R. & Iliffe, J. 2011: Experimental measurement of, and controls on, permeability and permeability anisotropy of caprocks from the CO_2 storage project at the Krechba Field, Algeria. Journal of Geophysical Research 116, B12208, doi:10.1029/2011JB008385.

Baechler, S., Croisé, J., Enachescu, C., Ebeling, K., Frieg, B., Jäggi, K. & Schwarz, R. 2009: Hydraulische Untersuchungen in Piezobohrungen am Standort Gösgen/Niederamt. Unpubl. Nagra Project Report. Nagra, Wettingen, Switzerland.

Baechler, S., Croisé, J. & Schwarz, R. 2011: Analysis of Benken Longterm-Monitoring Data. Nagra Arbeitsbericht NAB 11-27. Nagra, Wettingen, Switzerland.

Balderer, W. 1990: Hydrogeologische Charakterisierung der Grundwasservorkommen innerhalb der Molasse in der Nordostschweiz aufgrund von hydrochemischen und Isotopenuntersuchungen. Steirische Beiträge zur Hydrogeologie 41, 35-104.

Belanger, D.W., Cauffman, T.L., Lolcama, J.L., Longsine, D.E. & Pickens, J.F. 1989: Interpretation of Hydraulic Testing in the Sediments of the Riniken Borehole. Nagra Technical Report NTB 87-17. Nagra, Wettingen, Switzerland.

Bläsi, H.R., Deplazes, G., Schnellmann, M. & Traber, D. 2013: Sedimentologie und Stratigraphie des 'Braunen Doggers' und seiner westlichen Äquivalente. Nagra Arbeitsbericht NAB 12-51. Nagra, Wettingen, Switzerland.

Boisson, J.-Y.(ed.) 2005: Clay Club Catalogue of Characteristics of Argillaceous Rocks. NEA No. 4436, OECD 2005. ISBN 92-64-01067-X. Nuclear Energy Agency, Issy-les-Moulineaux, France.

Bredehoeft, J.D. & Hanshaw, B. 1968: On the maintenance of anomalous fluid pressures, I, Thick sedimentary sequences. Geological Society of America Bulletin 79/9, 1097-1106.

Butler, G.A., Cauffman, T.L., Lolcama, J.L., Longsine, D.E. & McNeish, J.A. 1989: Interpretation of Hydraulic Testing at the Weiach Borehole. Nagra Technical Report NTB 87-20. Nagra, Wettingen, Switzerland.

Corbet, T.F. & Bethke, C.M. 1992: Disequilibrium Fluid Pressures and Groundwater Flow in the Western Canada Sedimentary Basin. Journal of Geophysical Research 97/B5, 7203-7217.

Diamond, L.W. 1998: Underpressured paleofluids and future fluid flow in the host rocks of a planned radioactive waste repository. *In*: Arehart, G.B. & Hulston, J.R. (eds.): Proceedings of the 9th International Symposium on Water-Rock Interaction, 769-772. A.A. Balkema, Rotterdam, The Netherlands.

Deplazes, G., Bläsi, H.R., Schnellmann, M. & Traber, D. 2013: Sedimentologie und Stratigraphie der Effinger Schichten. Nagra Arbeitsbericht NAB 13-16. Nagra, Wettingen, Switzerland.

Enachescu, C., Rohs, S. & Böhner, J. 2010: Borehole Gösgen SB 2 – Hydraulic Packer Testing. Unpubl. Nagra Project Report. Nagra, Wettingen, Switzerland.

Enachescu, C., Rohs, S. & Böhner, J. 2007: Küttigen Borehole 2 Hydraulic Packer Testing. Nagra Arbeitsbericht NAB 07-18. Nagra, Wettingen, Switzerland.

ENSI 2011: Stellungnahme zu NTB 10-01 Beurteilung der geologischen Unterlagen für die provisorischen Sicherheitsanalysen in Etappe 2 SGT. ENSI Report 33/115. ENSI, Brugg, Switzerland.

Fisch, H.R., Rösli, U., Reinhardt, S., Yeatman, B., Senger, R. & Dale, T. 2008: Oftringen Borehole – Hydraulic Packer Testing. Nagra Arbeitsbericht NAB 08-15. Nagra, Wettingen, Switzerland.

Gimmi, T. & Waber, H.N. 2004: Modelling of Tracer Profiles in Pore Water of Argillaceous Rocks in the Benken Borehole: Stable Water Isotopes, Chloride, and Chlorine Isotopes. Nagra Technical Report NTB 04-05. Nagra, Wettingen, Switzerland.

Gimmi, T., Waber, H.N., Gautschi, A. & Rübel, A. 2007: Stable water isotopes in pore water of Jurassic argillaceous rocks as tracers for solute transport over large spatial and temporal scales. Water Resources Research 43, W04410, doi:10.1029/2005WR004774.

Gmünder, Ch., Jordan, P. & Becker, J.K. 2013a: Documentation of the Nagra 3D geological model 2012.1. Nagra Arbeitsbericht NAB 13-28. Nagra, Wettingen, Switzerland

Gmünder, Ch., Malaguerra, F., Nusch, S. & Traber, D. 2013b: Regional Hydrogeological Model of Northern Switzerland. Nagra Arbeitsbericht NAB 13-23. Nagra, Wettingen, Switzerland

Grauls, D. 1999: Overpressures: Causal mechanisms, conventional and hydromechanical approaches. Oil&Gas Science and Technology – Rev. IFP 54, 667-678.

Gygi, R.A. 1969: Zur Stratigraphie der Oxford-Stufe (oberes Jura-System) der Nordschweiz und des süddeutschen Grenzgebietes. Beiträge zur Geologischen Karte der Schweiz 136.

Gygi, R.A. 2000a: Annotated index of lithostratigraphic units currently used in the Upper Jurassic of northern Switzerland. Eclogae Geol. Helv. 93/3, 125-146.

Gygi, R.A. 2000b: Integrated stratigraphy of the Oxfordian and Kimmeridgian (Late Jurassic) in northern Switzerland and adjacent southern Germany. Denkschriften der Schweizerischen Akademie der Naturwissenschaften, vol. 104. Birkhäuser, Basel.

Heidbach, O., Hergert, T. & Reiter, K. 2013: Sensitivity studies on the local stress field in the candidate siting region Nördlich Lägern. Nagra Arbeitsbericht NAB 13-88. Nagra, Wettingen, Switzerland.

Jäggi, K. & Schwab, M. 2012: OPA: Sondierbohrung Benken Langzeitbeobachtung 2011 Dokumentation der Messdaten. Nagra Arbeitsbericht NAB 12-18. Nagra, Wettingen, Switzerland.

Jiao, J.J. & Zheng, C. 1998: Abnormal fluid pressures caused by deposition and erosion of sedimentary basins. Journal of Hydrology 204, 124-137.

Klump, S., Waber, H.N., Koroleva, M., Eichinger, L., Lorenz, G., Albert, W., Frieg, B. & Gautschi, A. 2008: EWS-Bohrung Küttigen – Synthese der geologischen und hydrogeologischen Untersuchungen. Nagra Arbeitsbericht NAB 08-12. Nagra, Wettingen, Switzerland.

Luo, J., Monninkhoff, B. & Becker, J. 2013a: Hydrogeological model Zürich Nordost and Südranden – Modelling and Interpretation. Nagra Arbeitsbericht NAB 13-24. Nagra, Wettingen, Switzerland.

Luo, J., Monninkhoff, B. & Becker, J. 2013b: Hydrogeological model Nördlich Lägern – Modelling and Interpretation. Nagra Arbeitsbericht NAB 13-25. Nagra, Wettingen, Switzerland.

Luo, J., Monninkhoff, B. & Becker, J. 2013c: Hydrogeological model Jura Ost – Modelling and Interpretation. Nagra Arbeitsbericht NAB 13-26. Nagra, Wettingen, Switzerland.

Luo, J., Monninkhoff, B. & Becker, J. 2013d: Hydrogeological model Jura Südfuss – Modelling and Interpretation. Nagra Arbeitsbericht NAB 13-27. Nagra, Wettingen, Switzerland.

Lusczynski, N.J. 1961: Head and flow of groundwater of variable density. Journal of Geophysical Research 66, 4247-4256.

Madritsch, H. & Hammer, P. (2012): Characterisation of Cenozoic brittle deformation of potential geological siting regions for radioactive waste repositories in Northern Switzerland based on structural geological analysis of field outcrops. Nagra Arbeitsbericht NAB 12-41. Nagra, Wettingen, Switzerland.

Mazurek, M., Alt-Epping, P., Bath, A., Gimmi, T., Waber, H.N., Buschaert, S., De Cannière, P., De Craen, M., Gautschi, A., Savoye, S., Vinsot, A., Wemaere, I., & Wouters, L. 2011: Natural tracer profiles across argillaceous formations. Applied Geochemistry 26/7, 1035-1064.

Mazurek, M., Alt-Epping, P., Bath, A., Gimmi, T. & Waber, H.N. 2009: Natural tracer profiles across argillaceous formations: The CLAYTRAC project. OECD/NEA report 6253. Nuclear Energy Agency, Paris, France, 358 pp.

Mazurek, M., Gautschi, A., Marschall, P., Vigneron, G., Lebon, P. & Delay, J. 2008: Transferability of geoscientific information from various sources (study sites, underground rock laboratories, natural analogues) to support safety cases for radioactive waste repositories in argillaceous formations. Physics and Chemistry of the Earth 33, S95-S105.

Mazurek, M., Waber, H.N., Mäder, U.K., de Haller, A. & Koroleva, M. 2013: Geochemical Synthesis for the Effingen Member in Boreholes at Oftringen, Gösgen and Küttigen. Nagra Technical Report NTB 12-07. Nagra, Wettingen, Switzerland.

Meier, D. & Mazurek, M. 2011: Ancillary rock and pore water studies on drillcores from northern Switzerland. Nagra Arbeitsbericht NAB 10-21. Nagra, Wettingen, Switzerland.

Moe, H., McNeish, J.A. McCord, J.P. & Andrews, R.W. 1990: Interpretation of Hydraulic Testing at the Schafisheim Borehole. Nagra Technical Report 89-09. Nagra, Wettingen, Switzerland.

Nagra 2010: Beurteilung der geologischen Unterlagen für die provisorischen Sicherheitsanalysen in SGT Etappe 2. Nagra Technischer Bericht NTB 10-01. Nagra, Wettingen, Switzerland.

Nagra 2009: The Nagra Research, Development and Demonstration (RD&D) Plan for the Disopsal of Radioactive Waste in Switzerland. Nagra Technical Report NTB 09-06. Nagra, Wettingen, Switzerland.

Nagra 2008a: Vorschlag geologischer Standortgebiete für das SMA- und das HAA-Lager. Darlegung der Anforderungen, des Vorgehens und der Ergebnisse. Nagra Technischer Bericht NTB 08-03. Nagra, Wettingen, Switzerland.

Nagra 2008b: Vorschlag geologischer Standortgebiete für das SMA- und das HAA-Lager, Geologische Grundlagen, Beilagenband. Nagra Technischer Bericht NTB 08-04. Nagra, Wettingen, Switzerland.

Nagra 2002: Projekt Opalinuston, Synthese der geowissenschaftlichen Untersuchungsergebnisse. Nagra Technischer Bericht NTB 02-03. Nagra, Wettingen, Switzerland.

Nagra 2001: Sondierbohrung Benken Untersuchungsbericht. Nagra Technischer Bericht NTB 00-01. Nagra, Wettingen, Switzerland.

Nagra 1997: Geosynthese Wellenberg 1996, Ergebnisse der Untersuchungsphasen I und II. Nagra Technischer Bericht NTB 96-01. Nagra, Wettingen, Switzerland.

Nagra 1988: Sedimentstudie – Zwischenbericht 1988: Möglichkeiten zur Endlagerung langlebiger radioaktiver Abfälle in den Sedimenten der Schweiz. Nagra Technischer Bericht NTB 88-25. Nagra, Wettingen, Switzerland.

Neuzil, C.E. 2000: Osmotic generation of 'anomalous' fluid pressures in geological environments. Nature 403, 182-184.

Neuzil, C.E. 1994: How permeable are clays and shales? Water Resources Research 30/2, 145-150.

Neuzil, C.E. 1993: Low Fluid Pressure Within the Pierre Shale: A Transient Response to Erosion. Water Resources Research 29/7, 2007-2020.

Nuclear Waste Management Organization (NWMO) 2011: OPG's Deep Geologic Repository for Low & Intermediate Level Waste, Geosynthesis. NWMO DGR-TR-2011-11. NWMO, Toronto, Canada.

Papafotiou, A. & Senger, R.K. 2013: Thermo-hydraulic modelling of the candidate siting area Nördlich Lägern. Nagra Arbeitsbericht NAB 13-56. Nagra, Wettingen, Switzerland.

Pearson, F.J., Waber, H.N. & Scholtis, A. 1998: Modeling the Chemical Evolution of Porewater in the Palfris Marl, Wellenberg, Central Switzerland. Scientific Basis for Nuclear Waste Management XXI, MRS Symposium Proceedings 506, 789-796, doi:10.1557/ PROC-506-789.

Ramey, H.J., Jr., Agarwal, R.G. & Martin, I. 1975: Analysis of 'slug test' or DST flow period data. Journal of Canadian Petroleum Technology 14/3, 37-47.

Reinhardt, S, Rösli, U. & Senger, R. 2012: Schlattingen Borehole SLA-1 Hydraulic Packer Testing – Malm. Unpubl. Nagra Project Report. Nagra, Wettingen, Switzerland.

Reinhardt, S, Rösli, U. & Senger, R. 2013: Schlattingen Borehole SLA-1 Hydraulic Packer Testing – 'Brauner Dogger'. Unpubl. Nagra Project Report. Nagra, Wettingen, Switzerland.

Roberts, R., Chace, D., Beauheim, R. & Avis, J. 2011: Analysis of Straddle-Packer Tests in DGR Boreholes. Technical Report TR-08-32 for the Nuclear Waste Management Organization, Geofirma Engineering Ltd., Ottawa, Canada.

Schmassmann, H. 1990: Hydrochemische Synthese Nordschweiz: Tertiär- und Malm-Aquifere. Nagra Technischer Bericht NTB 88-07. Nagra, Wettingen, Switzerland.

Senger, R.K., Papafotiou, A. & Marschall, P. 2013: Gas related property distributions in the proposed host rock formations of the candidate siting regions in Northern Switzerland and in the Helvetic Marls. Nagra Arbeitsbericht Nagra 13-83. Nagra, Wettingen, Switzerland.

Swiss Federal Office of Energy (SFOE) 2008: Sectoral Plan for Deep Geological Repositories, Conceptual Part. Swiss Federal Office of Energy, Bern, Switzerland.

Traber, D. & Blaser, P. 2013: Gesteinsparameter der Wirtgesteine Opalinuston, 'Brauner Dogger', Effinger Schichten und Helvetische Mergel als Grundlage für die Sorptionsdatenbank. Nagra Arbeitsbericht NAB 12-39. Nagra, Wettingen, Switzerland.

Van Loon, L.R. 2013: Effective Diffusion Coefficients and Porosity Values for Argillaceous Host Rocks: Measured and Estimated Values for Provisional Safety Analyses for SGT-E2. Nagra Tech. Rep. NTB 12-03. Nagra, Wettingen, Switzerland.

Van Loon, L.R. & Soler, J.M. 2004: Diffusion of HTO, $^{36}Cl^-$, $^{125}I^-$ and $^{22}Na^+$ in Opalinus Clay: Effect of Confining Pressure, Sample Orientation, Sample Depth and Temperature. PSI Report No. 04-03, Paul Scherrer Institut, Villigen, Switzerland.

Vinard, P., Bobet, A. & Einstein, H.H. 2001: Generation and evolution of hydraulic underpressures at Wellenberg, Switzerland. Journal of Geophysical Research 106/B12, 30593-30605, doi: 10.1029/2001JB000327.

Vomvoris, S., Scholtis, A., Waber, H.N., Pearson, F.J., Voborny, O., Schindler, M. & Vinard, P. 1998: Lessons Learned from the Use of Hydrochemical Data for the Evaluation of the Groundwater-Flow Models Developed within the Swiss L/ILW Programme. Use of Hydrogeochemical Information in Testing Groundwater Flow Models, Workshop Proceedings, Borgholm, Sweden, 1-3 September 1997. Paris, France: OECD NEA, 107-115.

Waber, H.N. (ed.) 2008: Borehole Oftringen: Mineralogy, Porosimetry, Geochemistry, Pore Water Chemistry. Nagra Arbeitsbericht NAB 08-18. Nagra, Wettingen, Switzerland.

Waber, H.N., Pearson, F.J., Aeschbach-Hertig, W., Eichinger, L., Lehmann, B.E. & Loosli, H.H. 2002: Sondierbohrung Benken: Hydrochemical and hydroisotopic characterisation of groundwaters. Unpubl. Nagra Internal Report. Nagra, Wettingen, Switzerland.